RUTHENIUM(II) POLYAZA-CAVITY COMPLEXES AS STRUCTURAL AND PHOTOCHEMICAL PROBES OF ELECTRON TRANSFER REACTIVITY

GRAHAM DE LISLE YEARWOOD

A THESIS SUBMITTED FOR THE DEGREE OF DOCTOR OF PHILOSOPHY

CITY UNIVERSITY, LONDON

The Department of Chemistry

October 1990

CONTENTS

ABSTRACT

A ruthenium(II) *bis* (triflate) (CTf) is used to synthesise polyaza-cavity ruthenium species. Ligands, formally derived from phenanthroline are coordinated to give mixed ligand complexes. Isolated as hexafluorophosphate salts, these complexes are characterised by elemental analysis, proton N.M.R., infra-red, FAB-mass spectrometry and uv/visible absorption spectroscopy. In an attempt to investigate the tuning of the excited state potential of these complexes, luminescence photochemical data are ~~is~~ presented. Results for the mononuclear metallo-complexes indicate substituents to *tris* (1,10-phenanthroline) co-ordination spheres merely alter non-radiative decay rates. Tuning of the excited state is only observed upon alteration of the ligator's magnitude of d level splitting.

Dinuclear complexes are shown to possess exciting characteristics required for tailored excited state species.

Proton N.M.R. is used to illustrate the presence of diastereomers for the complex, *tetrakis* (1,10-phenanthroline)[-3,6-*bis* (2'-pyridyl)-1,2,4,5-tetrazine]diruthenium(II) *tetrakis* (hexafluorophosphate), C28. Dramatic solvent sensitivity is also demonstrated by the luminescent C28.

Distance dependence of electron transfer is investigated by derivatisation of sperm whale myoglobin with polyaza-cavity ruthenium complexes.

Analysis of the conjugate obtained with *bis* (1,10-

phenanthroline)[4-(*p* -chlorosulphonyl) phenyl-1,10-phenanthroline] ruthenium(II), C27, gives the through space electron transfer rate, k_{et}, as 3.0×10^6 s^{-1}. Assuming the distance between the ruthenium(II)and iron(III) centres to be 25(±2 Å), the coupling coefficient, β, is found to be between 0.8 and 1.0. This was lower than expected for a protein matrix, suggesting a coupling enhancement effect.

A new metallo-protein is prepared by affinity labelling of chymotrypsin with a ruthenated L-phenylalanine chloromethylketone derivative, C24. Perturbation of the semi-synthetic system's excited state is tentatively ascribed to the presence of disulphide bonds in the inner-sphere.

Milestones in the analysis of long-distance electron transfer are reviewed. Also presented are pertinent considerations regarding luminescence observed at ruthenium(II) centres.

ACKNOWLEDGEMENTS

I wish to express my gratitude to Professor R. S. Davidson for his conception of this project and his encouragement and support throughout this work. I am also grateful to the S.E.R.C. for the award of a Quota research grant to fund this project.

It is a pleasure to record thanks to my colleagues Jeff Abrahams, Dr. Stuart Blinko, Dave Chapple, Steve Collins, Paul Crick, Dr. Maggie Dewar, Phil Duncanson, Trev Gilby, Dr. Martin Hilchenbach and Dr. Martin Walker. Their encouragement in times of trouble and ability to celebrate in times of success was greatly appreciated.

I extend my sincere gratitude to the technical staff at the Department of Chemistry for their excellent services, especially Paul Hemming, Ron Jacobs, Anthony Murphy and Adrian Taylor.

I would also like to thank Dr. Alan Osborne for his help with n.m.r. and Dr. Max Muir for taking my attempts at structures and turning them into diagrams!

I am indebted to Lorna Midgelow for her support and her help in typing the final edit of this thesis.

There is one debt of gratitude that will be hardest of all to repay and that is to my parents. Their unfailing support throughout the long course of my education will always be a reminder to me of their love and affection.

G. De L. Yearwood
October 1990

To my parents.

for love

laughter

and life.

Ah Love! could you and I with Fate conspire
To grasp this sorry Scheme of Things entire,
Would we not shatter it to bits-and then
Re-mold it nearer to the Heart's Desire!

Rubáiyát

NOTES

1. The paragraph beginning * C,M,L,H... on page 13 relates to Figure 1.2 (p 11)

2. Ligand composition of ruthenium complexes identified in the text with the legend C(number), is described in Table 4.1 (p 125).

3. Proton assignments indicating proximity to hetero-ligand (Section 5.1) are intuitive.

1.0 INTRODUCTION

Most of us have, at some stage, been drafted to participate in the endless battle to tame the most important biological process on earth. As lawnmowers are extracted from their winter hibernation, it marks the unruly spring growth of grass. For the majority of people this is the most obvious sign of the power of photosynthesis: the ability of green plants (and other living cells) to harness the energy of the sun's light.

Photosynthesis has come a long way in the 3,000 million years or so of evolution! However, the way in which modern plants absorb sunlight, use its energy to promote chemical

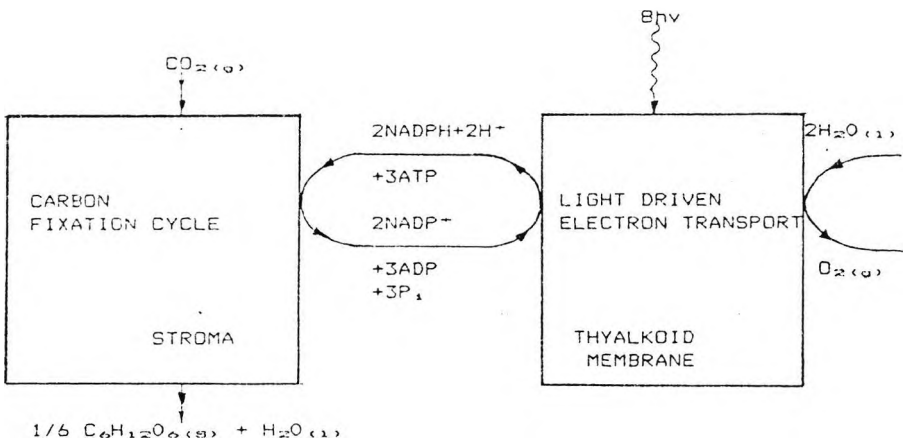

Where:-

NADP⁺ = Oxidised form of nicotinamide adenine dinucleotide phosphate
ATP = adenosine triphosphate
P_i = inorganic phosphate

Figure 1.1 The separation of the half reaction in the chloroplast of the photosynthetic plant cell. The dark reaction (left) and the light driven reactions (right) are shown.

reactions and excrete oxygen into their surroundings is the same (as far as we know) as that of the earliest forms of life. We can glimpse its essential features in the membranes of the cells of green plants, algae and photosynthetic bacteria (Figure 1.1)[2]. In all cases, a network of "light harvesting" pigments collects light and channels it to the "reaction centre" where energy conversion occurs.

The detailed structure of the molecular machine - the reaction centre (Figure 1.2)[3] - that carries out this crucial early event of photosynthesis was revealed by Johann

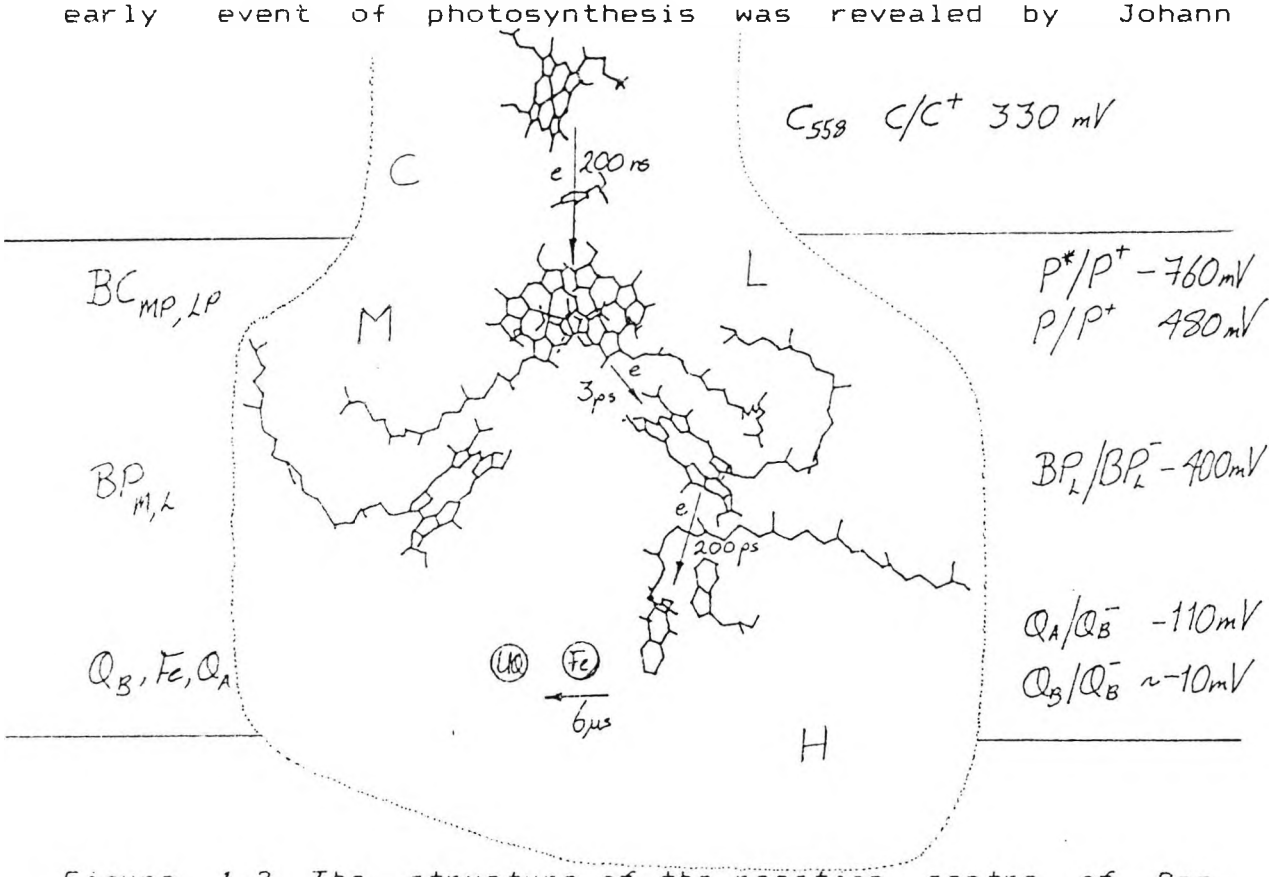

Figure 1.2 The structure of the reaction centre of Rps. viridis showing the cofactor system, the outline of the protein sub units (C,M,L,H), the E.T. half times, and redox potentials of defined intermediates. Note the intercalating tyrosine (YL162) and the gap bridging tryptophan M250. It is felt that these may facilitate E.T. by mediating electronic coupling between the widely spaced donors and acceptors. The two voyeur chlorophyll molecules have been omitted for clarity.*

Deisenhofer, Harmut Michel and Robert Huber of the Max Plank Institute for Biochemistry at Martinsried[4] in a report that won them the 1988 Nobel Prize for chemistry.

In a technical *tour de force*, they made X-ray diffraction studies of crystals obtained from the photosynthetic membranes of purple bacteria. Though protein crystallography has been done for some time, their studies were the first of a membrane protein, which is intrinsically more difficult to crystallise than water-soluble proteins like haemoglobin.

The studies revealed a structure that fits the Identikit picture of a reaction centre that had been put together from indirect evidence[5,6]. It shows four chlorophyll molecules, two phaeophytin molecules, a quinone molecule and an iron atom held in a very precise symmetrical arrangement by three large protein molecules (Table 1.1 and Figure 1.2.1)[3,7]. These proteins are plugged through the cell

---

Table 1.1 Reaction Centre Vital Statistics and "Construction Principles".

1. It is about 130Å in length and has an elliptical cross-section of 70 and 30Å respectively. The total molecular weight is approx. 125,000, about 125X that of $Ru(phen)_3(PF_6)_2$.

2. Dye-like molecules with overlapping -orbitals appear in dimers rather than in single crystal-like configurations. Absorbing in the visible spectral region, they are present at a dilute conentration and surrounded by non-absorbing (and space filling) proteins.

3. The systems are very complex, having sub-systems with sub-picosecond E.T., nanosecond lifetimes, and microsecond to millisecond metastable states. The latter state stores chemical or electrical energy before the allowing the systems to return to their G.S. after the light source has been extinguished.

---

membrane and folded around and between the other molecules, even including a quinone-shaped hole for a second quinone molecule. The relative positions and orientations of these molecules reflect the individual steps of electron transfer in the reaction centre.

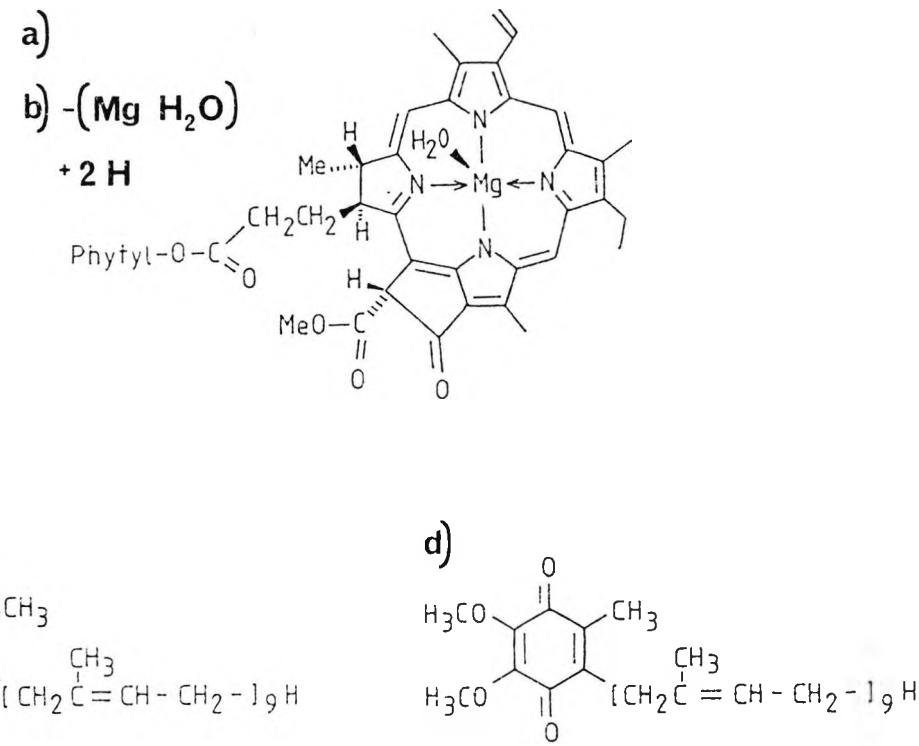

Figure 1.2.1 Cofactors in the reaction centre of the purple bacteria:
a) BC = (as special pair) the primary electron donor
b) BP = BC without magnesium
c) Q_A = the primary electron acceptor
d) Q_B = the secondary electron acceptor

** C,M,L,H the four subunits of the reaction centre from Rps. viridis the cytochrome c subunit (C) with four hemes (only H3 shown) displaying one of the redox potentials (c558) is located on the periplasmic side of the membane; the L- and M-subunits are integrated in the membrane, their polypeptide chains span this membrane with five α-helices each; they bind the bacteriochlorophyll-b (BChl-b or BC), bacteriopheophytin-b (BPh-b or BP), menaquinone-9 (QA), ubiquinone-9 (UQ or QB) and Fe2+ cofactors.*
The subscripts P,A,M,L indicate pair, accessory M- and L-subunits respectively.
The H- subunit is located on the cytoplasmic side, and its N-terminal α-helical segment (H) spans the membrane.

So the first and fundamental step of energy conversion in photosynthesis is the movement of an electron from a sandwich-like pair of chlorophyll molecules to the adjacent phaeophytin. This takes a few picoseconds (millionths of a millionth of a second). The electron moves to one quinone in just 200ps, resulting in virtual stabilisation of the charge separation, allowing subsequent processes to occur at a more leisurely pace (on to a second quinone in 6μs and through the electron transport chain to ATP synthesis and reduction of NADP).

What is still puzzling, is that the chromophores involved in these primary electron transfer steps seem rather widely separated, by distances of approximately 10Å. Furthermore, there is no evidence that they are connected by molecular "wires" for electrons to flow through. The active components are rigidly embedded in a non-polar region of the transmembrane protein matrix. Charge separation, therefore, must occur by electron tunnelling between components[8,9].

Employed in this project, is an approach to chemical synthesis to elucidate the electronic-tunnelling process, an approach that could be described as molecular engineering. In this spirit, the ~~the~~ compound synthesised is considered as a device fulfilling a physico-chemical function: that of a rectifier for converting electromagnetic waves into a d.c. voltage.

Synthesis of donor-insulator-acceptor species (DIAS's) is now being performed in many laboratories (with rigid

carbon-carbon bond systems[18-19], aliphatic[17-21] and aromatic[17] spacers as mediating structures). An important pioneering contribution has come from Mike Paddon-Row[20,21] (Table 1.2 and Figure 1.3), who has made a beautiful series of variable length DIAS's with complete distance and

Table 1.2 Lifetime ( ) of donor (dimethoxynaphthalene) fluorescence (detected at 360nm) and calculated rates of photoinduced, intramolecular electron $k_{(et)}$ for $I_{(n)}$ (n=8, 10, 12), in various solvents at 24°C.

	$I_{(8)}$		$I_{(10)}$		$I_{(12)}$	
Solvent	τ /ps	k_{et} /$10^8 s^{-1}$	τ /ps	k_{et} /$10^8 s^{-1}$	τ /ps	k_{et} /$10^8 s^{-1}$
Cyclohexane	48	210	5400	-	5400	-
Benzene	19	520	135	72	1030	7.3
Di-n-butylether	21	470	270	35	1920	3.1
Diethylether	21	470	190	51	1740	3.7
Ethylacetate	22	450	115	85	1160	6.3
Tetrahydrofuran	15	670	80	120	650	13.0
Acetonitrile	33	300	380	24	2710	1.6

orientational rigidity. Molecular components which closely resemble those found in nature cannot fail to bring a certain romance to the field, as is the case in the work of Alvin Joran[25-27] (Table 1.3 and Figure 1.4). The most renowned of such compounds are the three component assemblies of Thomas Moore[28], being composed of carotene, porphyrin and quinone residues (Table 1.4 and Figure 1.5).

From a synthetic point of view, oligopeptides could be a useful moiety to employ, allowing ready separation variation

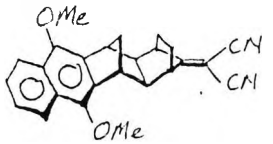

R_{tb}/Å	R_c/Å	R_e/Å
6.1	7.0	4.6

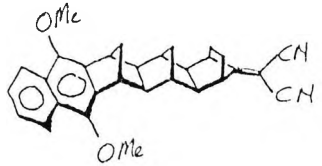

9.2	9.0	6.8

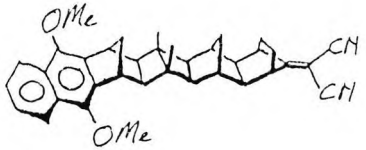

12.3	11.4	9.4

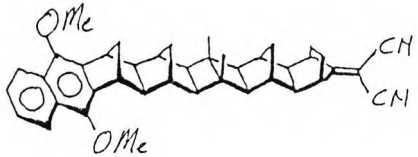

15.4	13.3	11.5

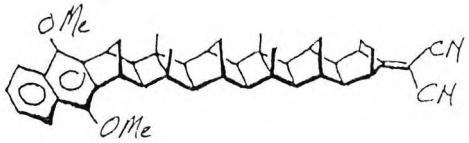

18.5	14.9	13.5

Figure 1.3 Structure of the Paddon-Row donor-acceptor assemblies; the bridge is a rigid norbonyl type non-conjugated hydrocarbon; and Rtb, Rc, and Re are the through-bond, centre to centre, and edge to edge distances between donor and acceptor respectively.

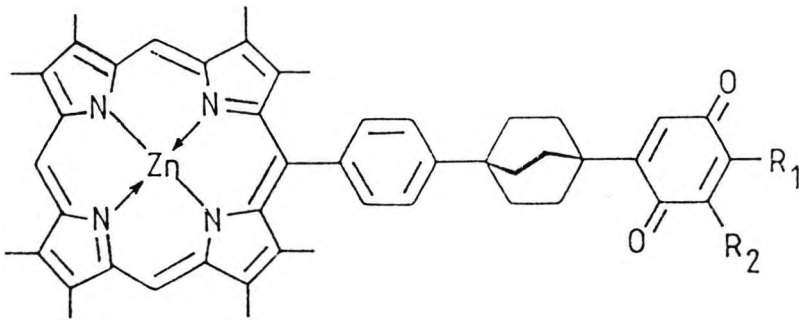

Figure 1.4 The series of zinc meso-phenyloctamethylporphyrins coupled to differently substituted quinones via a bicyclo [2.2.2.] octane spacer, synthesised by Joran et al[27-29]. These were used to study the exothermicity effects at fixed distance and solvent.

Table 1.3 Results for E.T. from porphyrin excited singlet to the substituted quinones (the compound 5 was a mixture of 3- and 4- chlorobenzoquinone isomers). The minor component with longer lifetime is assigned to the porphyrin-hydroquinone species.

R_1	R_2	Solvent*	τ /ns	k_{et} /$10^9 s^{-1}$	$-\Delta G^\circ_{r-et}$ /eV
Me	Me	1a	0.801,1.722(9:1)	0.57	0.50
Me	H	2a	0.443,1.161(20:1)	1.58	0.58
H	H	3a	0.076,1.490(71:1)	12.50	0.67
Br	H	4a	0.075,1.362(50:1)	12.70	0.83
Cl	H	5a	0.082,1.549(200:1)	11.50	0.84
Cl	Cl	6a	0.055,1.894(167:1)	17.50	0.96
CN	H	7a	0.114,1.520(1:2)	8.09	1.07
		1b	0.594,1.488(7:1)	1.08	0.76
		2b	0.384,1.591(16:1)	2.00	0.84
		3b	0.092,1.537(11:1)	10.30	0.93
		4b	0.090,1.611(20:1)	10.50	1.09
		5b	0.099,1.661(77:1)	9.50	1.10
		6b	0.062,1.629(42:1)	15.50	1.22
		7b	0.236,1.717(2:3)	3.63	1.33
		1c	0.679,1.798(4:1)	0.84	0.82
		2c	0.448,1.295(7:1)	1.60	0.90
		3c	0.118,1.467(20:1)	7.85	0.99
		4c	0.121,1.512(8:1)	7.64	1.15
		5c	0.132,1.576(25:1)	6.95	1.16
		6c	0.085,1.445(23:1)	11.10	1.28
		7c	0.302,1.811(1:1)	2.68	1.39
		1d	0.829,1.569(2:1)	0.59	0.84
		2d	0.617,1.430(6:1)	1.01	0.92
		3d	0.178,1.601(20:1)	5.00	1.01
		4d	0.178,1.513(5:1)	5.00	1.17
		5d	0.215,1.491(2:1)	4.03	1.18
		6d	0.121,1.283(24:1)	7.65	1.30
		7d	0.335,1.660(1:1)	2.37	1.41

* Solvent a, benzene; b, 2-methyltetrahydrofuran; c, butyronitrile; d, acetonitrile.

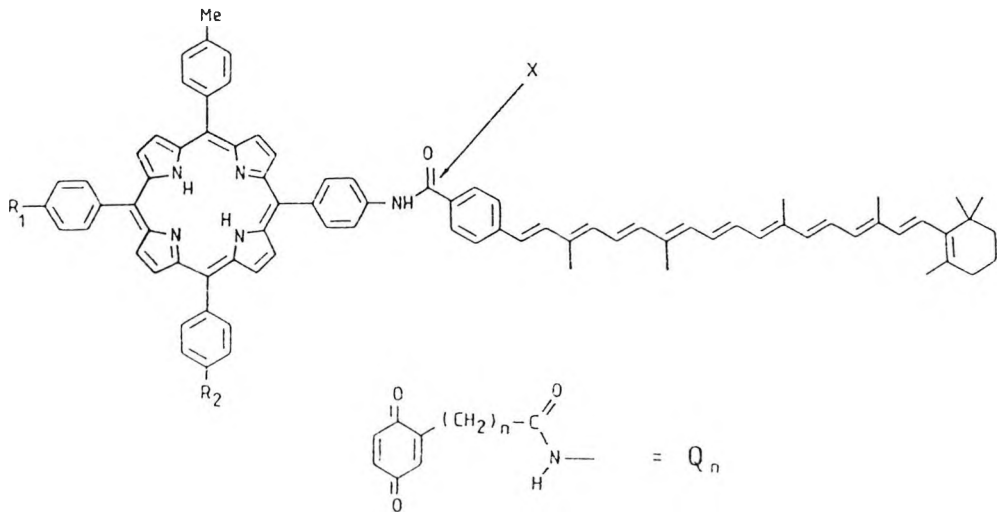

Figure 1.5 The structure of the Moore et al[28] . amphipathic triads; excitation of these species, (C-P-Q), initiates a two step electron transfer to yield C·⁺P-Q·⁻. Nanosecond transient absorption spectroscopic studies were performed on a series of such triads. This revealed that charge recombination did not occur in a single step but rather via a two step E.T. involving an intermediate C -P·⁺-Q·⁻ species, formed via a temperature dependent pathway.

Table 1.4 Quantum Yield and Lifetime (τ) of C·⁺-P-Q·⁻ at different temperatures in CH_2Cl_2.

Molecule	R_1	R_2	x	τ /ns (295 K)	rel. Quantum Yield (295 K)	(220 K)
1	Q_1	Me	-	298	1.00	2.50
2	Q_2	Me	-	283	1.44	3.09
3	Q_3	Me	-	315	0.65	1.04
4	Q_4	Me	-	335	0.56	0.48
5	Me	Q_2	-	285	1.47	3.20
6	Q_1	Me	$-CH_2-$	1010	-	-

in such a DIAS. Isied *et al.* [29] have illustrated the usefulness of such systems through the use of oligo(L-proline) as mediating ligand in intramolecular E.T. reactions. Our strategy to enter this field, was to use a sterically constrained poly-peptide of 1-

aminocyclohexanecarboxylic acid[59] as a spacer group, and with a quinone moiety as the acceptor. The donor would be provided by a ruthenium trisphenanthroline derivative.

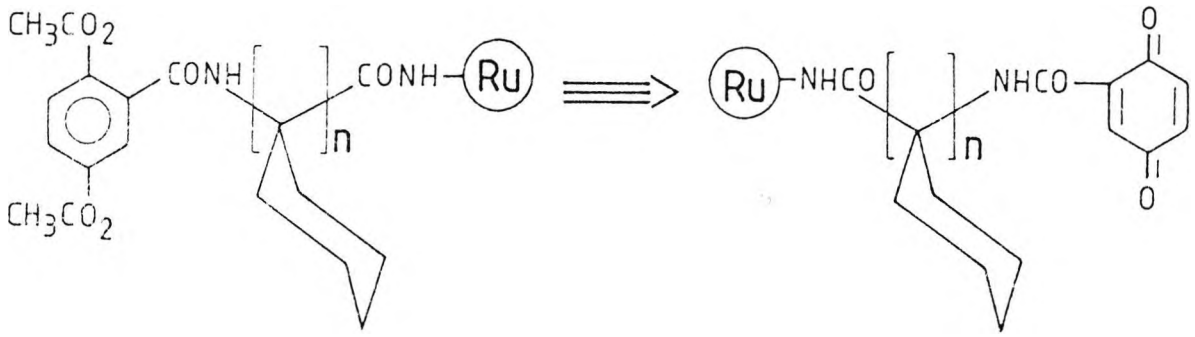

Illustrative example depicting synthon manipulation to yield a DIAS's. In this strategy the bridging moiety is a stereochemically constrained polypeptide.

Here it is possible to alter the free energy of the electron transfer over a considerable range by manipulations in both the quinone and complex moieties whilst avoiding major perturbations of the electronic structure. At very negative free energies, the electron transfer rate is predicted to diminish, and this approach would be expected to allow us to investigate this region, a source of continuous controversy for 33 years since Marcus[61] derived his relationship. Also, it would be interesting to compare reactivity in such a system with those where α-amino-acids preserve an α-H.

However, the rigid DIAS's are significant far beyond simply being humble imitations of the wonderfully complex

machinery of natural photosynthetic compounds. With them it is possible to test general theories of long distance electron-transfer and microscopic ion - solvent interactions far more rigorously. The results will not be limited to systems of chemical interest but will be relevant to any process in which electron tunnelling is important[7,32-39].

As has been indicated, in natural electron transport systems, a network of single bonds rarely link redox sites. Thus a model for "through-space" electron transfer is important, and also one which will explain the high degree of specificity of binding site required of natural redox partners. Few experiments have addressed these points in a systematic manner[39-37].

A strategy here could proceed by introduction of an electron transfer donor site into a structurally characterised metalloprotein[39,37-44]. Stephen Isied and Greg Worosila[37] selected Horse heart cytochrome c[43] as a first target for derivatisation experiments with aquopentaamine-ruthenium(II) [$a_5Ru(OH_2)^{2+}$, $a = NH_3$] (See below, Figure 1.6)[37]. This complex covalently bonds to surface histidines of proteins under mild conditions, the "ruthenated" protein being purified by ion- exchange chromatography. Spectroscopic measurements[40] and electrochemical data[41] confirmed that the conformation and the heme were virtually the same as that of the native protein. In this system, the product is actually the fully oxidised $a_5Ru(His-33)^{3+}$-Cyt c-Fe^{3+}, necessitating that the mixed valence species required to observe reduction

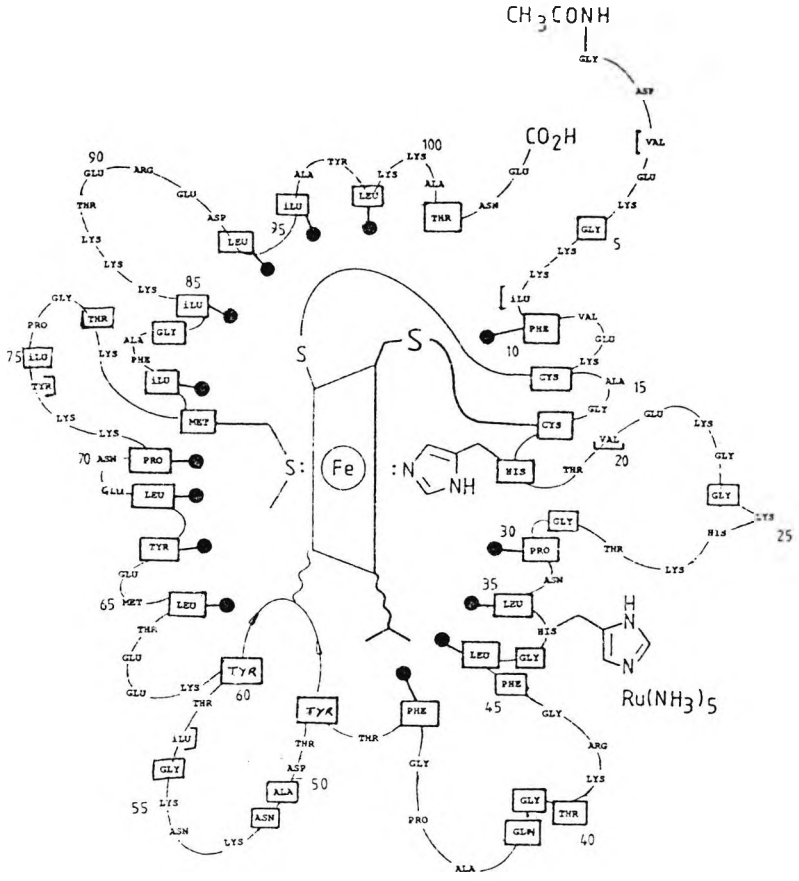

Figure 1.6 Heme packing diagram of the Isied et al. ruthenium modified horse heart cytochrome c. Heavy squares indicate side chains that inside the interior of the molecule. Black dots mark residues whose side chains pack against the heme. The driving force for E.T. in this system is ~0.1 eV.

of the heme must be generated under the reaction conditions [by flash photolysis[35,39] in the presence of $Ru(bipy)_3^{2+}$ or pulse radiolysis[35,39]]. The intramolecular rate constants extracted from the two types of experiments for the long range (Ru^{2+}-->Fe^{3+}) electron transfer were not substantially different ($30s^{-1}$ and $80s^{-1}$ respectively) but are much slower than the rates of 10^6 to $10^9 s^{-1}$ observed in rigid DIAS's[16,17]. Ruling out the 70Å through-bond route, they

concluded that the electron transfer from Ru^{2+} to Fe^{3+} was most likely forced to occur through the 12A "space".

Harry Gray[50] extended this work on ruthenated sperm whale myoglobin (Mb). Unlike cytochrome c, the heme in Mb is high spin in both the ferrous and ferric states and a water ligand is lost when $Mb(Fe)^{3+}$ is reduced to $Mb(Fe)^{2+}$. Of the four singly modified proteins a_5Ru(His-12)Mb, a_5Ru(His-48)Mb, a_5Ru(His-81)Mb and a_5Ru(His-116)Mb (Figure 1.7)[51] prepared

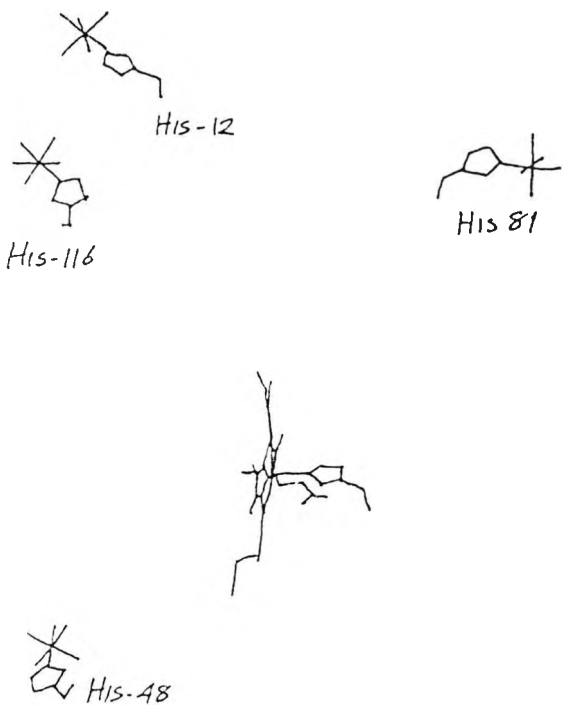

Figure 1.7 View of the heme and the surface histidines that are modified in the four ruthenated myoglobins.

and fully characterised, the shortest Ru-Fe electron transfer distance is in a_5Ru(His-48)Mb (13.3A)(Figure 1.7.1)[50,51].

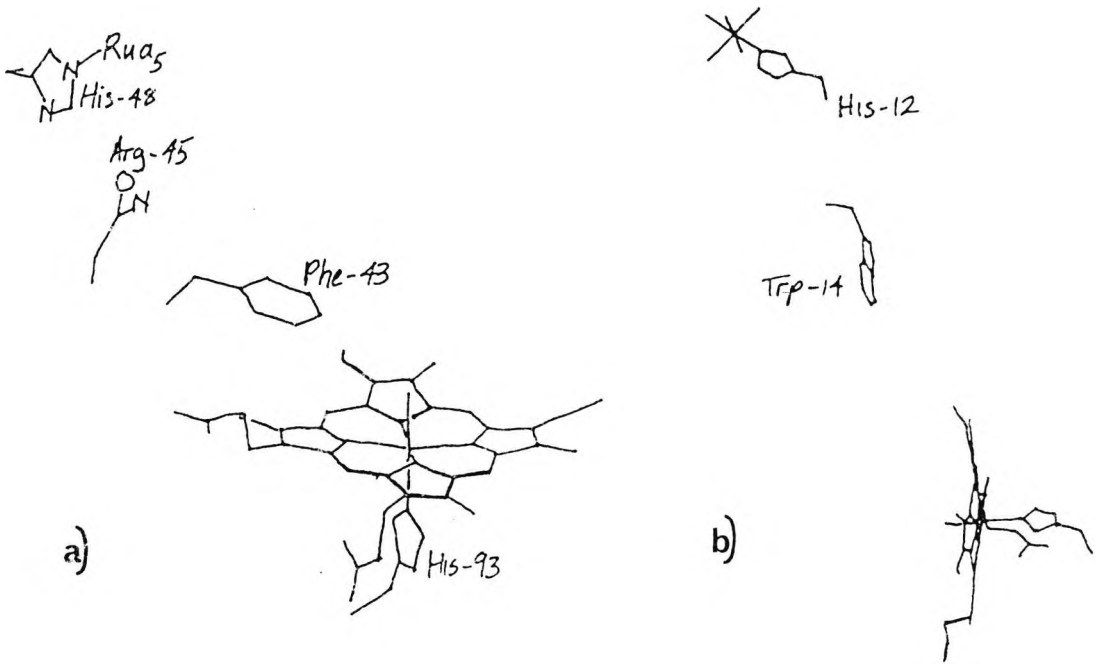

Figure 1.7.1 View of selected parts of the molecular skeleton of sperm whale myoglobin (a) with a$_5$Ru^{3+}bonded to the imidazole of His-48 and (b) the tryptophan-14 between the porphyrin and a$_5$Ru(His-12)$^{3+}$

They obtained an (Ru^{2+}-->Fe^{3+}) electron transfer rate constant of 0.019s^{-1}, which was strongly temperature dependent. Based on the thermodynamic and kinetic data for long-range electron transfer in a$_5$Ru(His-48)Mb, the reorganisation energy of the Mb high-spin heme was calculated to be 0.87eV, which, as expected, was much larger than for the low spin heme in cytochrome c[47,48], in accord with earlier studies on Mb[47].

Gray *et al.* [55] went on to modify surface histidine in bacterial protein Pseudomonas aeruginosa azurin (a blue copper electron transfer protein). Schemes 1.1 & 2.2[55] illustrate the synthesis and characterisation of these

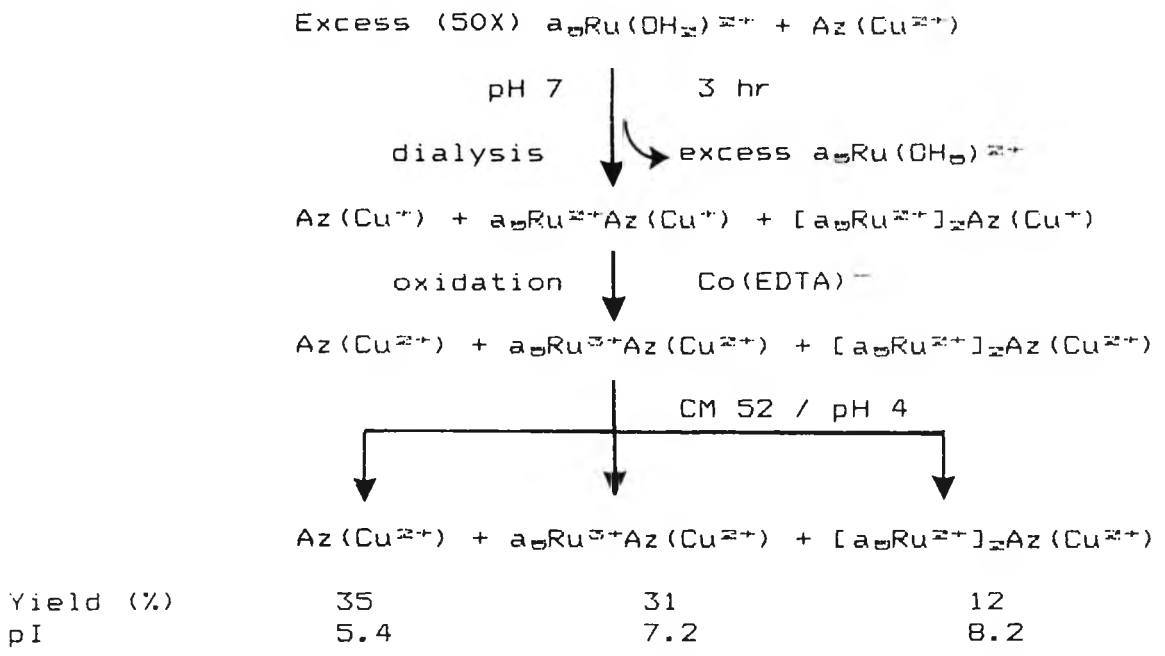

Scheme 1.1 Preparation and purification of ruthenated azurins.

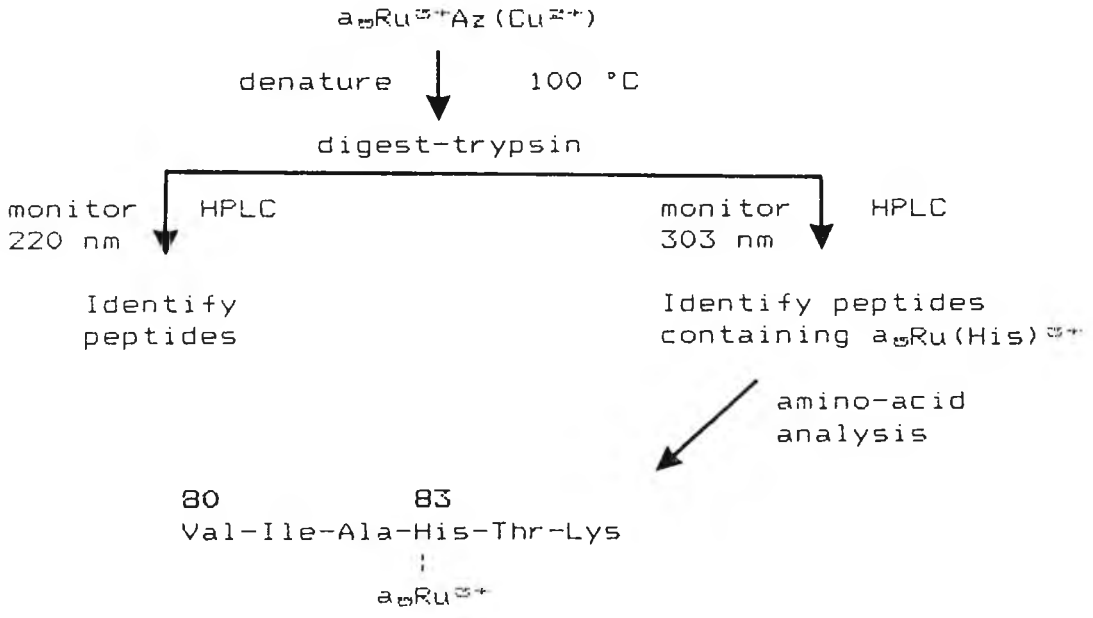

Scheme 1.2 Peptide mapping of $a_5Ru^{3+}Az(Cu^{2+})$.

species; Table 1.5 offers a comparison of the results of long-range E.T. in ruthenated derivatives of azurin, horse heart cyt c, and sperm whale Mb.

Table 1.5 Long range E.T. data for ruthenated proteins at room temperature

Protein	d /Å	E° /V	k(Ru^{2+} --→ Fe^{3+} or Cu^{2+}) /s^{-1}
a_5Ru(His-33)$^{2+}$cyt c(Fe^{3+})	11.8	0.18	30
a_5Ru(His-83)$^{2+}$Az(Cu^{2+})	11.8	0.24	2
a_5Ru(His-48)$^{2+}$Mb(Fe^{3+})	13.3	-0.02	0.02

Temperature independence of the long range E.T. in ruthenated azurin is taken to indicate a low reorganisational enthalpy at copper, supported by comparison with the results for myoglobin. The origin for the apparent enhancement in donor-acceptor coupling in the low-spin heme c(Fe^{3+}) system is not explained.

Figure 1.8 Relative geometry of the electron transfer units in ruthenium modified azurin.

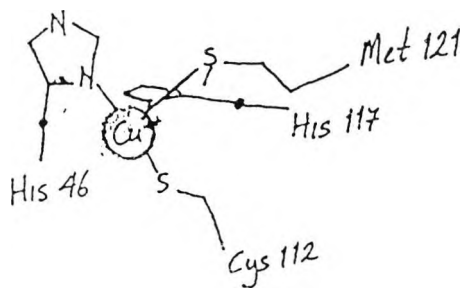

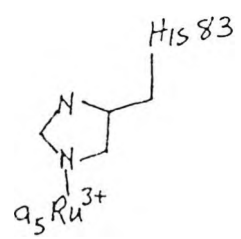

The convenient method of studying protein long range E.T. by photogeneration of powerful oxidants or reductants is not new. Excited zinc porphyrins for example, have been used as reductants both in fixed distance experiments[63,64] and in studies of long-range E.T. in protein-protein complexes[65-67]. Gray *et al.* [65] repeated experiments of this sort on blue copper proteins using excited $Ru(bipy)_3^{2+}$ [$Ru(bipy)_3^{2+*}/Ru(bipy)_3^{+}$= 0.84V SHE] and $Cr(phen)_3^{3+}$ [$Cr(phen)_3^{3+*}/Cr(phen)_3^{2+}$= 1.42V SHE] as oxidants. The kinetics of these reactions exhibit saturation, suggesting that at high protein concentrations, the excited reagent is bound to the reduced protein in an E.T. precursor complex. Analysis of their results for a mechanistic scheme incorporating this feature gave the results for the intracomplex (remote or long range) electron transfer rate constants of plastocyanin(Cu^+), azurin(Cu^+) and stellacyanin(Cu^+) indicated in Table 1.6. NMR studies revealed the binding site in plastocyanin and computer modelling gave an edge to edge distance for the long-range E.T. as 10.3 Å.

Table 1.6 Reactions of $Cr(phen)_3^{3+*}$ and $Ru(bipy)_3^{2+*}$ with reduced blue copper proteins at 22 °C.

Protein	M^{n+*}	$-\Delta G°$/V	$k_{et}/10^6 s^{-1}$
Pl(Cu^+)	Cr^{3+*}	1.06	2.5
Pl(Cu^+)	Ru^{2+*}	0.48	3.0
Az(Cu^+)	Cr^{3+*}	1.11	1.2
Az(Cu^+)	Ru^{2+*}	0.53	1.2
St(Cu^+)	Cr^{3+*}	1.23	0.20
St(Cu^+)	Ru^{2+*}	0.65	0.20

Following this lead by Gray, the semisynthetic system $p_2Ru(fp)Mb$ (p = 1,10-phenanthroline, fp = functionalised p) was prepared. By exploiting parameters of the $Ru(phen)_3^{2+}$ moiety, a superior model for the dependence of the kinetics on donor-to-acceptor distance, the inner-sphere reorganisation, the thermodynamic driving force, the nature of the intervening medium and donor-acceptor orientation is sought.

REFERENCES

1. Schopf, J.W. Evolution, W.H. Freeman, 1978.
2. Yearwood, G. M.Phil Transfer Report, City Univ., 1987.
3. Huber, R. Angew. Chem. Int. Ed. Engl., 28, 848, 1989.
4. Deisenhofer, J.; Epp, O.; Miki, K.; Huber, R.; Michel, H. J. Mol. Biol., 180, 385, 1984.
5. Ke, B.; Shuvalov, V.A. The light reactions, 8, Ed. Barber, J., 31, Elsevier, 1987.
6. Evans, M.C.W. Nature, 327, 284, 1987.
7. Haarer, D. Angew. Chem. Int. Ed. Engl. Adv. Mater., 28, 1544, 1989.
8. Creed, D.; Caldwell, R.A. Photochem. Photobiol., 180, 715, 1985.
9. Antennas and Reaction Centers of Photosynthetic Bacteria, Ed., Michel-Beyerle, M.E., Springer-Verlag, Berlin, 1985.
10. Wasielewski, M.R.; Neimczyk, M.P.; Svec, W.A.; Pewitt, E.B. J. Am. Chem. Soc., 107, 5562, 1985.
11. Wasielewski, M.R.; Neimczyk, M.P.; Svec, W.A.; Pewitt, E.B. J. Am. Chem. Soc., 107, 1080, 1985.
12. Wasielewski, M.R.; Neimczyk, M.P. J. Am. Chem. Soc., 106, 5043, 1984.
13. Pasman, P.; Mes, G.F.; Koper, N.W.; Verhoeven, J.W. J. Am. Chem. Soc., 107, 5839, 1985.
14. Penfield, K.W.; Miller, J.R.; Paddon-Row, M.N.; Cotsaris, E.; Oliver, A.M.; Hush, N.S. J. Am. Chem. Soc., 109, 5061, 1987.

15. Closs, G.L.; Calcaterra, L.T.; Green, N.J.; Penfield, K.W.; Miller, J.R. J. Phys. Chem., 90, 3673, 1986.

16. Miller, J.R.; Calcaterra, L.T.; Closs, G.L. J. Am. Chem. Soc., 106, 3047, 1984.

17. Calcaterra, L.T.; Closs, G.L.; Miller, J.R. J. Am. Chem. Soc., 105, 670, 1983.

18. Bolton, J.R.; Ho, T.-F.; Liauw, S.; Siemiarczuk, A.; Wan, C.S.K.; Weedon, A.C. J. C. S. Chem. Commun., 559, 1985.

19. Schmidt, J.A.; Siemiarczuk, A.; Weedon, A.C.; Bolton, J.R. J. Am. Chem. Soc., 107, 6112, 1985.

20. Siemiarczuk, A.; McIntosh, A.R.; Ho, T.-F.; Stillman, M.P.; Roach, K.J.; Weedon, A.C.; Bolton, J.R.; Connolly, J.C. J. Am. Chem. Soc., 105, 7224, 1983.

21. McIntosh, A.R.; Siemiarczuk, A.; Bolton, J.R.; Stillman, M.P.; Ho, T.-F.; Weedon, A.C. J. Am. Chem. Soc., 105, 7215, 1983.

22. Heitele, H.; Michel-Beyerle, M.E. J. Am. Chem. Soc., 107, 8286, 1985.

23. Oevering, H.; Paddon-Row, M.N.; Heppener, M.; Oliver, A.M.; Cotsaris, E.; Verhoeven, J.W.; Hush, N.S. J. Am. Chem. Soc., 109, 3258, 1987.

24. Verhoeven, J.W.; Paddon-Row, M.N.; Hush, N.S.; Oevering, H.; Heppener, M. Pure Appl. Chem., 58, 1285, 1986.

25. Joran, A.D.; Leland, B.A.; Felker, P.M.; Zewail, A.H.; Hopfield, J.J.; Dervan, P.B. Nature, 327, 508, 1987.

26. Joran, A.D.; Leland, B.A.; Getter,G.G.; Hopfield, J.J.;

Dervan, P.B. J. Am. Chem. Soc., 107, 1080, 1985.

27. Leland, B.A.; Joran, A.D.; Felker, P.M.; Hopfield, J.J.; Zewail, A.H.; Dervan, P.B. J. Phys. Chem., 89, 5571, 1985.

28. Moore, T.A.; Gust, D.; Mathis, P.; Mailocq, J.-C.; Chachaty, C.; Bensasson, R.V.; Land, E.J.; Doizi, D.; Liddell, P.H.; Lehman, W.R.; Nemeth, G.A.; Moore, A.L. Nature, 307, 630, 1984.

29. Isied, S.S.; Vassilian, A.; Magnuson, R.H.; Sewartz, H.A. J. Am. Chem. Soc., 107, 7432, 1985.

30. Paul, P.K.C.; Sukumar, M.; Bardi, R.; Piazzesi, A.M.; Valle, G.; Toniolo, C; Balaram, P. J. Am. Chem. Soc., 108, 6363, 1986.

31. Marcus, R.A. J. Chem. Phys., 24, 966, 1956.

32. Sykes, A.G. Chem. Soc. Rev., 14, 283, 1985.

33. De Vault, D. Quantum Mechanical Tunnelling in Biological System, 2nd ed., Cambridge Univ., Cambridge, 1984.

34. Habefi, Y. Annu. Rev. Biochem., 54, 1015, 1985.

35. Gray, H.B. Chem. Soc. Rev., 15, 17, 1986.

36. Brunschwig, B.S.; De Laive, P.J.; English, A.M.; Goldberg, M.; Gray, H.B.; Mayo, S.L.; Sutin, N. Inorg. Chem., 24, 3743, 1985.

37. Mayo, S.L.; Ellis, W.R., Jr.; Crutchley, R.J.; Gray, H.B. Science, 233, 948, 1986.

38. Winkler, J.R.; Nocera, D.G., Yocom, K.M.; Bordignon, E.; Gray, H.B. J. Am. Chem. Soc., 104, 5789, 1982.

39. Isied, S.S.; Worosila, G.; Atherton, S.J. J. Am. Chem. Soc., 104, 7659, 1982.

40. Yocom, K.M.; Shelton, J.B.; Shelton, J.R.; Schroeder, W.A.; Worosila, G.; Isied, S.S.; Bordignon, E.; Gray, H.B. Proc. Natl. Acad. Sci. U.S.A., 79, 7052, 1982.

41. Nocera, D.G.; Winkler, J.R.; Yocom, K.M.; Bordignon, E.; Gray, H.B. J. Am. Chem. Soc., 106, 5145, 1984.

42. Isied, S.S.; Kuehn, C.; Worosila, G. J. Am. Chem. Soc., 106, 1722, 1984

43. Bechtold, R.; Gardineer, M.B.; Kazmi, A.; van Hemelryck, B.; Isied, S.S. J. Phys. Chem., 90, 3800, 1986.

44. Kostic, N.M.; Margalit, R.; Che, C.-M.; Gray, H.B. J. Am. Chem. Soc., 105, 7765, 1983.

45. Timkovich, R. The Porphyrins, 7, Ed. Dolphin, D., 241, Acacademic Press, New York, 1979.

46. As ref. 40.

47. Schomacker, K.T.; Bangcharoenpaurpong, O.; Champion, P.M. J. Phys. Chem., 88, 4701, 1984.

48. Churg, A.K.; Weiss, R.M.; Warshel, A.; Takano, T. J. Phys. Chem., 87, 1683, 1983.

49. Mauk, A.G.; Gray, H.B. Biochem. Biophys. Res. Comm., 86, 206, 1979.

50. Crutchley, R.J.; Ellis, W.R. Jr.; Gray, H.B. J. Am. Chem. Soc., 107, 5002, 1985.

51. Axup, A.W.; Albin, M.; Mayo, S.L.; Crutchley, R.J.; Gray, H.B. J. Am. Chem. Soc., 110, 435, 1988.

52. Margulit, R.; Kostic, N.M.; Che, C.-M.; Blair, D.F.; Chaing, H.-J.; Pecht, I.; Shelton, J.B.; Shelton, J.R.; Schroeder, W.A.; Gray, H.B. Proc. Natl. Acad. Sci.

U.S.A., 81, 6554, 1984.

53. McGourty, J.L.; Blough, N.V.; Hoffman, B.M. J. Am. Chem. Soc., 105, 4470, 1983

54. Peterson-Kennedy, S.E.; McGourty, J.L.; Hoffman, B.M. J. Am. Chem. Soc., 107, 1070, 1985.

55. McLendon, G.L.; Winkler, J.R.; Nocera, D.G.; Mauk, M.R.; Mauk, A.G.; Gray, H.B. J. Am. Chem. Soc., 107, 739, 1985

56. Simolo, K.P.; McLendon, G.L.; Mauk, M.R.; Mauk, A.G. J. Am. Chem. Soc., 106, 5012, 1984.

57. Ho, P.S.; Sutoris, C.; Laing, N.; Margoliash, E.; Hoffman, B.M.; J. Am. Chem. Soc., 107, 1070, 1985.

58. As for Ref. 36.

59. Marcus, R.A.; Sutin, N. Biochem. Biophys. Acta, 811, 265, 1985.

60. Hopfield, J.J. Proc. Natl. Acad. Sci. U.S.A., 71, 3640, 1974.

61. Hush, N.S. Coord. Chem. Rev., 64, 135, 1985.

62. Larsson, S.J. J. Chem. Soc. Faraday Trans., 79, 1375, 1983.

63. Scott, R.A.; Mauk, A.G.; Gray, H.B. J. Chem. Ed., 62, 932, 1985.

64. Kimura, K.; Nakahara, Y.; Yagi, T.; Inokuchi, H. J. Phys. Chem., 70, 3317, 1979.

65. Pierot, M.; Haser, R.; Frey, M.; Payan, F.; Astier, J.P. J. Biol. Chem., 257, 14341, 1982.

66. Higuchi, Y.; Kusunoki, M.; Matsuura, Y.; Yasuoka, N.; Kakudo, M. J. Mol. Biol., 172, 109, 1984.

2.0 THEORY SECTION

2.1 Photochemistry

2.1.1 *Elementary Considerations.*

Most of the currently available energy resources of the world can be ascribed to the sun's radiant energy which has been captured and accumulated by photochemical reactions. These reactions range from the heating of the atmosphere during daytime by absorption in the ultraviolet region of the spectrum through processes of the kind summarized below[1];

Thermosphere:~ $O + h\nu \rightarrow O^+ + e^-$

$N_2 + h\nu \rightarrow 2N$

Mesosphere:~ $O_2 + h\nu \rightarrow O_2^+ + e^-$

$N_2 + h\nu \rightarrow N_2^+ + e^-$

Stratosphere:~ $O_3 + h\nu \rightarrow O_2 + O$

to the absorption of red and blue light by chlorophyll, and the subsequent deployment of the energy to bring about the synthesis of carbohydrates (the radiation incident upon the earth's surface spans a wavelength range of ~350 nm to 1800 nm, the maximal intensity range being from ~400 nm to 1400 nm). Thus, photochemistry is the study of chemical reactions initiated by light (Figure 2.1). To understand the interaction of light with matter we must consider two events:

1. The initial act of light absorption resulting in excitation. The *Grotthuss-Draper Law* , which states that *only the radiation actually absorbed by the reacting system can initiate reaction* . The emphasis here is on the word

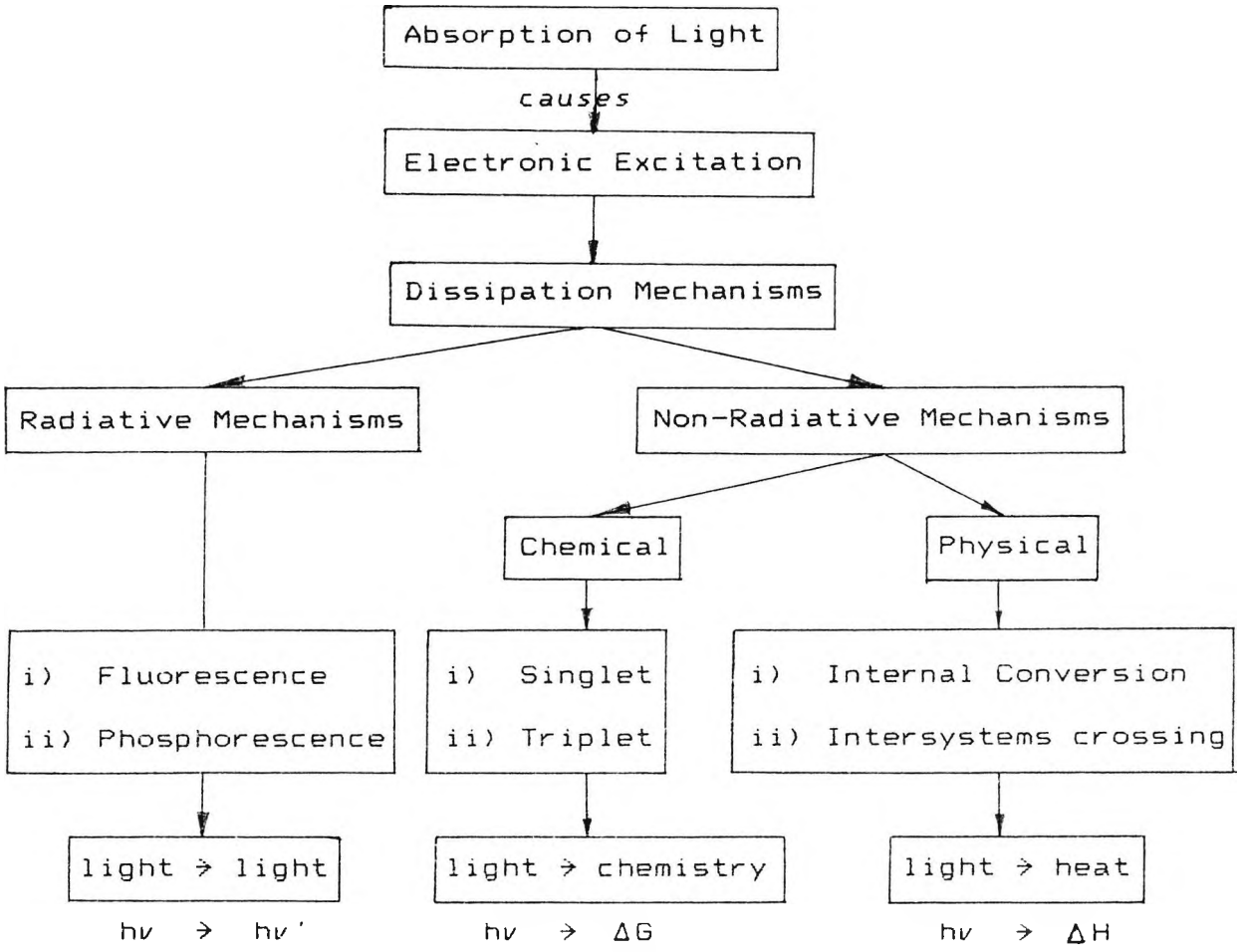

e.g. Fluorescent lights Interest! e.g. Green House Design

Figure 2.1 An overview of molecular photochemistry.

absorbed: light simply passing through does not initiate reaction. This leads naturally to the *Einstein-Stark Law* , which asserts that *one quantum is absorbed by the molecule responsible for the primary photochemical process* .

Thus we can write:-

Molecule in ground state (G.S) + $h\nu$ →

Molecule in excited state (E.S)

2. The subsequent fate of the excited molecule.

Classical physics dealt with waves and with particles and the distinction was clear. Quantum mechanics introduced the view that matter and radiation have a dual character and that either aspect of behaviour may be exhibited by the same entity. The mutual exclusiveness of these two properties (their complementarity) means that it is impossible to demonstrate simultaneously the wave and corpuscular attributes of a "particle" (see ref. 3 for an illuminating discussion). The *de Broglie* relation describes this character [eqn.1].

$$\lambda = h / p \qquad (1)$$

The wave properties of light are related by the equation (2):-

$$\nu \lambda = c \qquad (2)$$

One of the basic laws of physics relates the energy available from electromagnetic radiation of energy frequency:-

$$E = h\nu \quad \text{or} \quad E = c\, h / \lambda \qquad (3)$$

Thus, light of frequency ν , can impart energy in discrete amounts (quanta) of magnitude $h\nu$. A light beam of frequency

ν therefore, can possess an energy that is an integral multiple of $h\nu$, and could be regarded as containing an integral number of light corpuscles. These quanta of excitation, or hypothetical corpuscles, are *photons* . Each photon of wavelength $\lambda = c/\nu$ carries an energy $h\nu$ and, according to the de Broglie relation, a linear momentum of $h\nu /c$.

2.1.2 *Quantum Efficiency.*

The Einstein-Stark Law does not necessarily imply that only one product molecule is produced when one photon is absorbed: if the subsequent process is a chain reaction, the absorption of one photon might lead to several product molecules. The ratio of molecules reacting to the number of photons absorbed is called the *quantum efficiency* of the reaction and is denoted Φ (capital phi):

$$\Phi = \frac{\text{number of molecules that react}}{\text{number of photons absorbed}} \qquad (4)$$

The main mechanism by which light emission arises is by radiative dissipation of energy from an E.S.. The quantum efficiency of photoluminescence never exceeds unity.

2.1.3 *Excitation.*

A molecule can only absorb light if the *Bohr frequency condition* [eqn.5] is satisfied:

$$h\nu = E_{\blacksquare} - E_{\circ}$$

where $E_{\blacksquare}$ is the energy of the E.S.,

and $E_{\circ}$ is the energy of the G.S.

Planck's constant itself has dimensions of action (J s) and so may be regarded as the fundamental *quantum of action* . Absorption by a molecule of light in the ultra-violet region results in E.S. so high in energy that the energy absorbed is comparable with the bond dissociation energies associated with organic molecules. Thus;

Energy of excitation for one molecule = ch / λ

Energy of excitation for one mole = Lch / λ

$$= \frac{1.20 \times 10^{5}}{\lambda / (nm)} \text{ kJ mol}^{-1}$$

and for absorption at 250 nm, E=480 kJ mol^{-1}; that is greater than the bond dissociation energy of a carbon-carbon bond (D ~ 350 kJ mol^{-1})! This example serves to illustrate the great potential of applied photochemistry, that is, the ability to focus high energies regiospecifically within a molecule.

2.1.4 *Electronic Excitation.*

Absorption of radiation in the range covered by the ultra-violet (UV) to the end of the visible spectrum results in electronic excitation, that is promotion of an electron from one molecular orbital (M.O.) to another of higher energy. For organic compounds, e.g. dyes, transition metal complexes, etc., these transitions occur between orbitals which have discrete energies. From the diagram below (Fig. 2.2)[2] it is possible to see that only $\pi - \pi^*$ and $n - \pi^*$ transitions can be brought about by radiation in the accessible region of the UV - visible spectrum, and it is

these which are responsible for the majority of organic photochemical reactions.

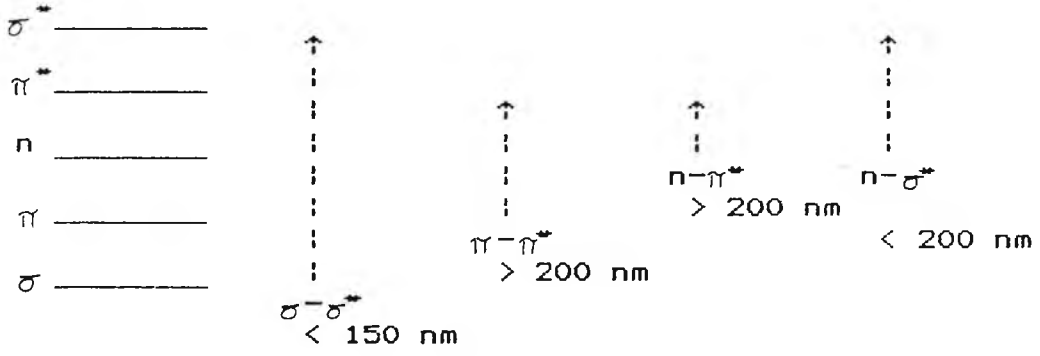

Figure 2.2 Electronic excitation processes for organic molecules.
NB. The energy of the n–π transition can be greater than that of the n–σ* transition.*

2.1.5 *Multiplicity Considerations.*

At risk of inciting shouts of "Sloppy usage!" from the ranks of our inorganic-chemistry brethren, we shall define multiplicity thus;

$$\text{multiplicity} = 2S + 1$$

where S is the overall spin quantum number. By considering the π–π* excitation process for ethene (Fig. 2.3), it is possible to understand the nomenclature for ground and excited states. Thus, the difference between an excited singlet and triplet state lies in spin pairing.

2.1.6 *Fate of Electronically Excited States.*

A common fate for the excitation energy is for it to be transferred into vibration, rotation, and translation of the neighbouring molecules. This *thermal degradation* of the energy transforms it into thermal energy of the environment.

Much more interesting is the possibility that the excited molecule may be able to take part in a chemical reaction. However, we shall be concerned mainly with *radiative decay*, which is the ability of a molecule to discard its excitation energy by emitting a photon.

The potential energy surface and simplified Jablonski diagrams (Figs. 2.4 and 2.5) illustrate the absorption of a photon, the changes to a molecule's electronic energy levels, and to their associated vibrational levels. Absorption of a photon causes the direct population of the S_1 state, a vibrationally excited singlet state (Illustrated in Figure 2.4 as S_1's vibrational level 5). This state will, if surrounded by other molecules, give energy to these neighbouring molecules as it relaxes to the lowest attainable vibrational level of the S_1 state.

Two mechanisms for the radiative deactivation have been identified, *fluorescence* and *phosphorescence*. In fluorescence, the radiation emission ceases immediately the exciting source is removed, whereas in phosphorescence it may persist for long periods (up to hours, but characteristically seconds or even fractions of a second). This difference of behaviour suggests that the former process is an immediate conversion of absorbed light into re-emitted energy, whilst in the latter, energy is stored in some kind of reservoir, from which it slowly leaks.

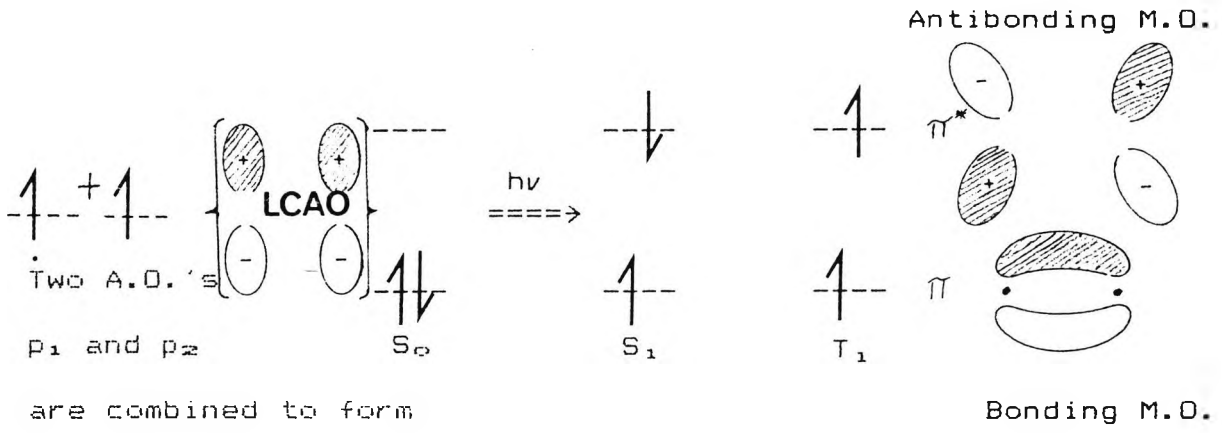

Figure 2.3 The π – π excitation process for ethene.*

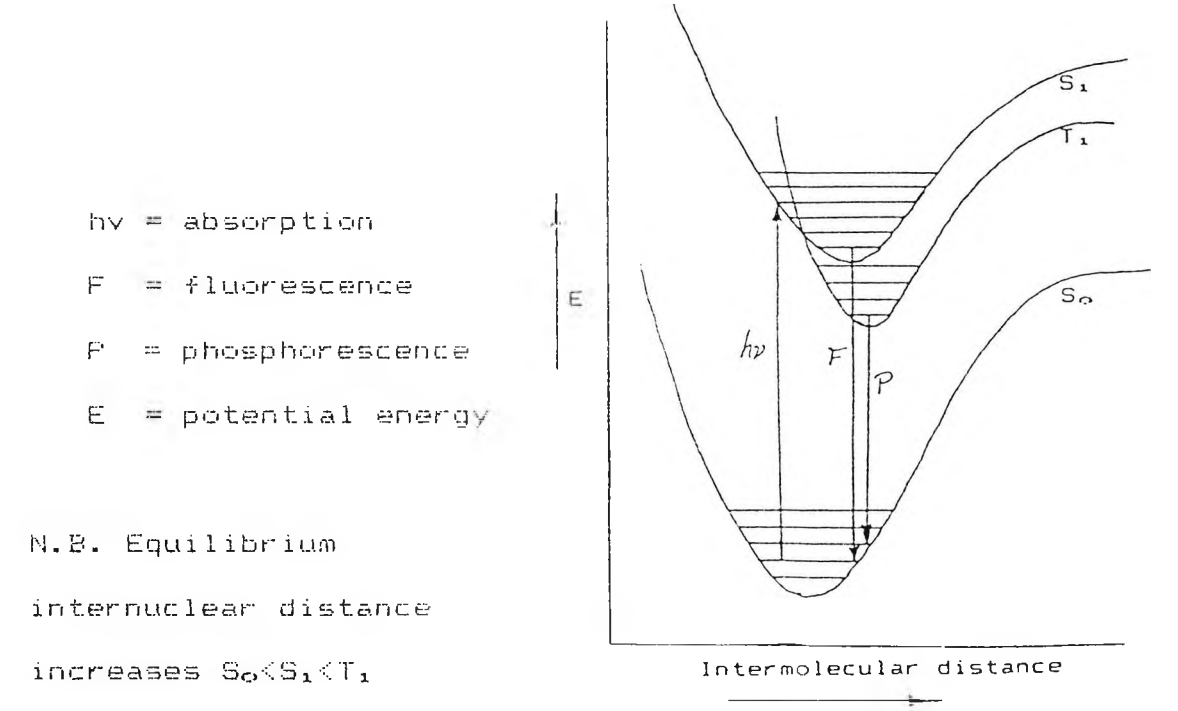

Figure 2.4 Potential energy surface diagram for a diatomic molecule.

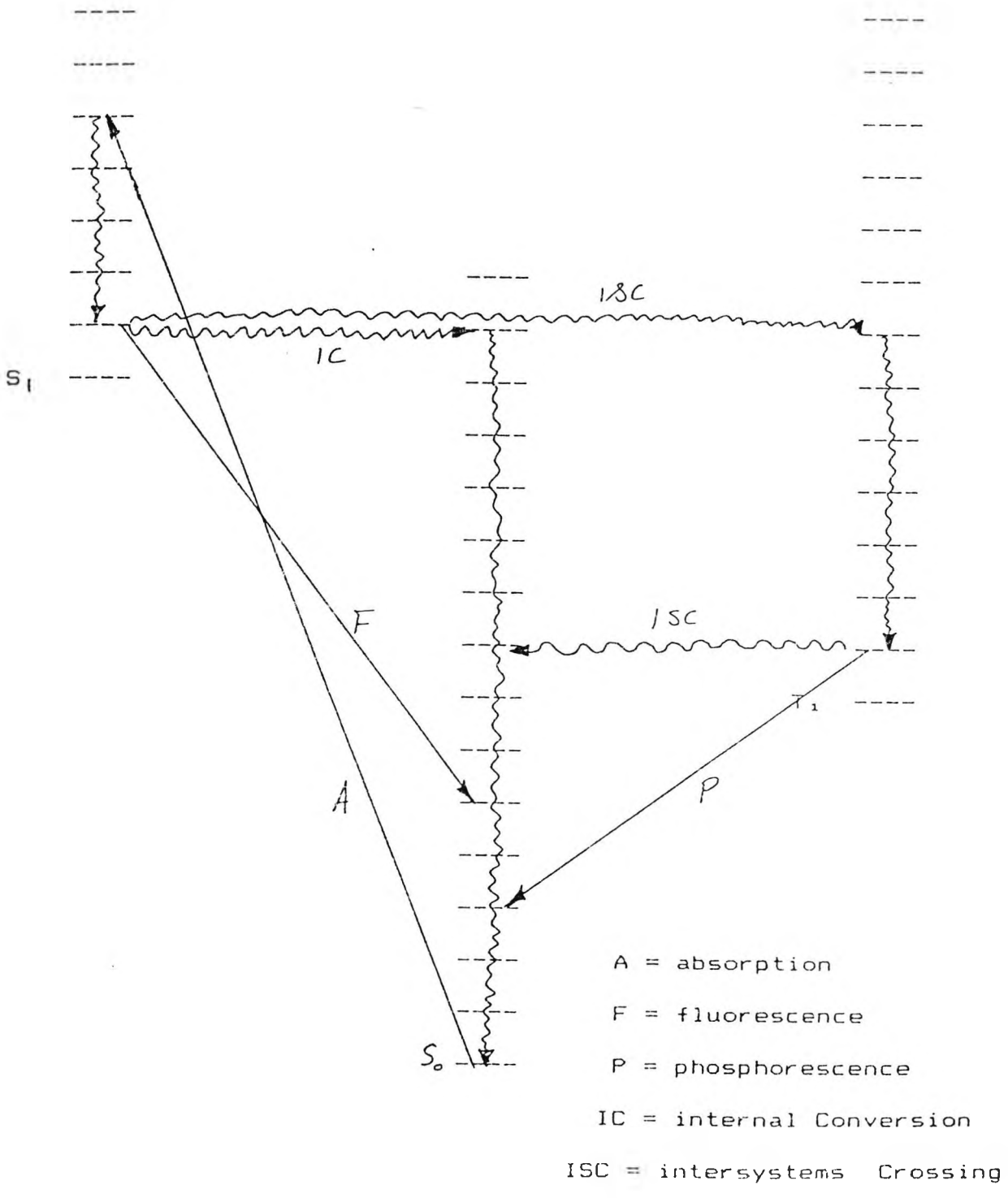

Figure 2.5 Simplified Jablonski diagram.

2.1.7 *Franck-Condon Principle.*

The Franck-Condon principle governs the intensity of spectral transitions between the vibrational levels of different states of molecules. By recognising that the absorption of light is a fast process (e.g. $\sim 10^{-15}$ s for an electronic S_0-S_1 transition, c.f. $\sim 10^{-13}$ s for one molecular vibration); it states that *electronic absorptions occur so rapidly that during it the nuclei are static* .

2.1.8 *Fluorescence and Phosphorescence.*

Above it was discussed how collisions succeeded in lowering the excited molecule down its ladder of vibrational levels, however, they may be unable to withdraw (i.e. quench) the larger electronic energy difference. The molecule might therefore live long enough to undergo a spontaneous emission, and to emit excess energy as radiation as it drops to the lower electronic state.

The downward step occurs vertically in accordance with the Franck-Condon principle, and a series of lines appear as the *flourescence spectrum* . The vibrational structure of this spectrum is characteristic of the lower electronic state (in contrast to the structure of the absorption spectrum).

The mechanism also suggests that the intensity of fluorescence should depend on the ability of the solvent to quench the excited state. Indeed fluorescence can be eliminated by selecting a different solvent. For example, a solvent with widely spaced vibrational energy levels (such as water) may be able to accept the large quantum, but one with

more closely spaced levels (such as $SeOCl_2$) might not[1].

A singlet state is transformed into a triplet state by the non radiative mechanism of *intersystems crossing* . This vibrationally excited state undergoes further energy dissipation within the triplet manifold as relaxation from v_7 to v_0 occurs. The efficency of intersystems crossing, will of course determine the extent to which the triplet state is populated. In the ground vibrational state of the excited triplet, the energy is now trapped. The solvent cannot extract the final, large quantum of electronic excitation energy, nor can the molecule radiate its energy because a return to the G.S. involves a forbidden singlet-triplet transition. The radiative transition is not completely forbidden because spin-orbit coupling is present and breaks the selection rule. The molecules are therefore able to emit slowly, and the emission may last long after the original excited state is formed.

The mechanism suggests that the phosphorescence should be most intense from solid samples. This is because the environment then collides less effectively with the molecule, and the intersystems crossing step has time to occur as the singlet excited state slowly loses vibrational energy and falls past the intersection point. It also predicts that on account of the presence of the unpaired electron spins, the excited reservoir state should be magnetic (that is paramagnetic).

It is worth introducing pause for thought at this stage,

in that an electronically E.S. may be highly polarisible, due to the presence of a half filled HOMO (electrophlic) and a half filled LUMO (nucleophilic).

2.1.9 *Luminescence: A Quantitative Approach.*

In the general terms of the preceding discussion we have allowed ourselves to distinguish quite clearly between the decay mechanisms of the E.S. However, at this stage it is necessary to introduce a new term to our vocabulary to go some way to reducing ambiguity in assignment of photophysical processes. Thus a molecule able to discard its excitation energy by emitting a photon shall be refered to as *luminescent.*

An important principle in photochemistry is the Beer-Lambert Law (eqn.6), which describes the effectiveness of a compound in absorbing radiation.

$$\lg(I_o/I) = \xi c l = \text{Optical density} \qquad (6)$$

The relationship between the quantum yield for luminescent emission and extinction coefficient is obtained in a simple form, for weakly absorbing solutions for which the optical density is small (<0.01), in terms of the rate of luminescence, Q (eqn.7).

$$Q = I_o(2.3\xi c l)\phi \qquad (7)$$

The way in which the intensity of luminescence changes with variation in the wavelength of the exciting light can be deduced from equation 7. For a solution of a single solute at a constant concentration, the luminescence intensity is

proportional to $\xi I_o \Phi_{em}$. Thus if the intensity of exciting light is kept constant as the wavelegth is varied, the luminescence intensity will be proportional to $\xi \Phi_{em}$. Plots of this function against wavelength are called *corrected luminescence spectra.*

The molar extinction coefficient is a measure of transition probability and life time of the E.S., that is strong absorption bands are associated with short E.S. life times. It should be noted that the absolute probabilities of electronic transitions themselves depend on the types of electronic states involved and determine the overall intensity of the corresponding absorption band, for example;

carbon-carbon double bond :

$\pi \rightarrow \pi^*$ transition, $\xi = 10^2$–10^4 $m^2\ mol^{-1}$,

high probability, symmetry allowed.

carbon-oxygen double bond :

$n \rightarrow \pi^*$ transition in carbonyl group, $\xi = 5\ m^2\ mol^{-1}$,

low probability, symmetry forbidden.

A variety of formulae have been derived to relate the radiative or intrinsic lifetime of the state , τ_o, to the molar extinction coefficient. The simplest to use is that given by Bowen and Wokes[4]. Translated into units of μm^{-1} this takes the form:

$$1/\tau_o = 2900 n^2 \nu_o^2 \int \xi \, d\nu \qquad (8)$$

where the integral part of the function is the area under the curve of molar extinction coefficient plotted against wavenumber (Fig. 2.6)[4], and ν_o is the wavenumber of the maximum of the absorption band.

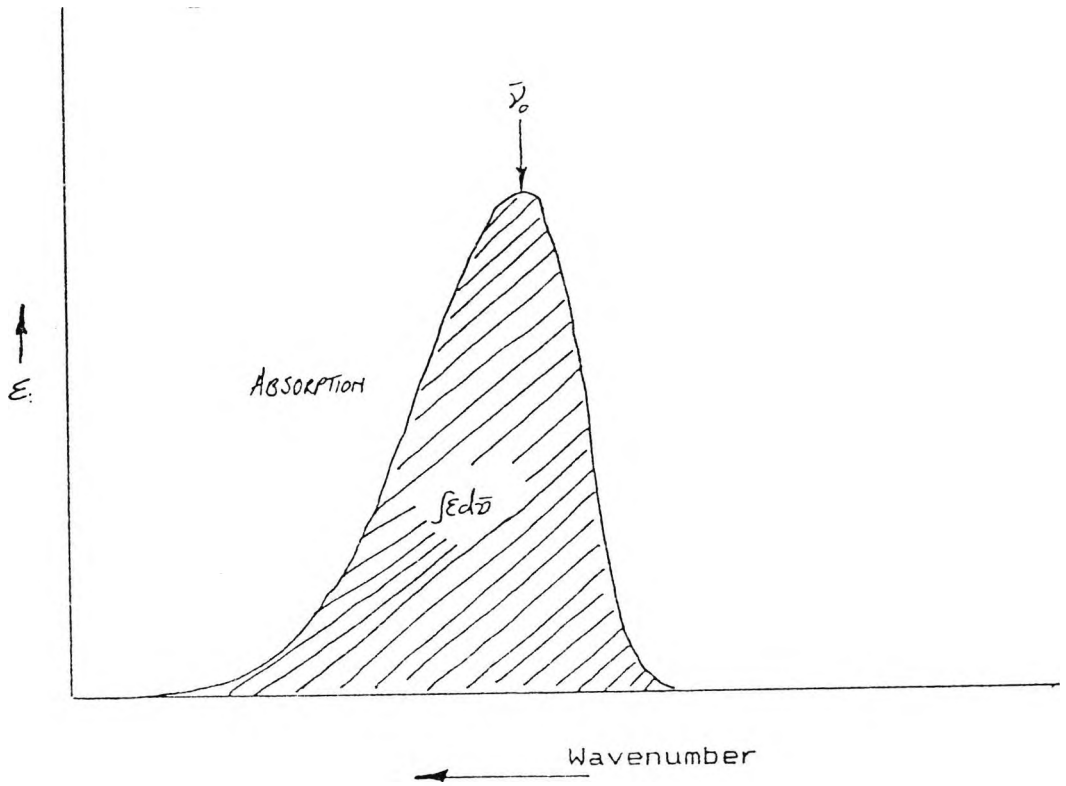

Figure 2.6 Method of calculating radiative lifetimes.

It should be noted that the intrinsic lifetime is that which would be observed in the abscence of all other processes by which the molecule can return to the G.S.

Experimental determination of the quantum yield for luminescent emission, and the intrinsic lifetime of the state can lead to an estimate of the radiative rate constant, the lifetime of the E.S., and the quenching rate constant[5]:

$$k_o = 1/\tau_o = \Phi_{em}/(\Phi_{abs})\tau \qquad (9)$$

$$k_q = 1/\tau_o \; [\; 1 - (\Phi_{em}/\Phi_{abs})\;] \qquad (10)$$

Both Φ_{em} and τ are strongly temperature dependent[6], but k_o is independent as predicted above. It has, however, been shown that the temperature dependence of the lifetime of the excited state must lie in k_q. In terms of application to luminescence from organometallic complexes assumptions in the model which best accommodates the experimental data are[7]:

(i) For D_3 complexes (Ru(II), d^6, low spin), the luminescence observed experimentally originates from three closely spaced electronic states. For C_2 complexes (e.g. *cis* - $[Ru(bipy)_2(CN)_2]$), four levels must be assumed.

(ii) Each of these states is capable of undergoing both radiative and non-radiative decay to the G.S., and these pathways are controlled by first order kinetics, with associated k_o and k_{nr} are independent of temperature.

(iii) Boltzmann equilibrium between these states is established and maintained upon time scales much shorter than the characteristic lifetimes of the states.

(iv) The manifold of these states is populated from higher excited states with unit efficiency (that is $\Phi_{isc} = 1$).

The effect of these assumptions is summarised in figure 2.7[7], where:

$$k_1 = (k_0)_1 + (k_{nr})_1$$

$$k_2 = (k_0)_2 + (k_{nr})_2$$

$$k_3 = (k_0)_3 + (k_{nr})_3$$

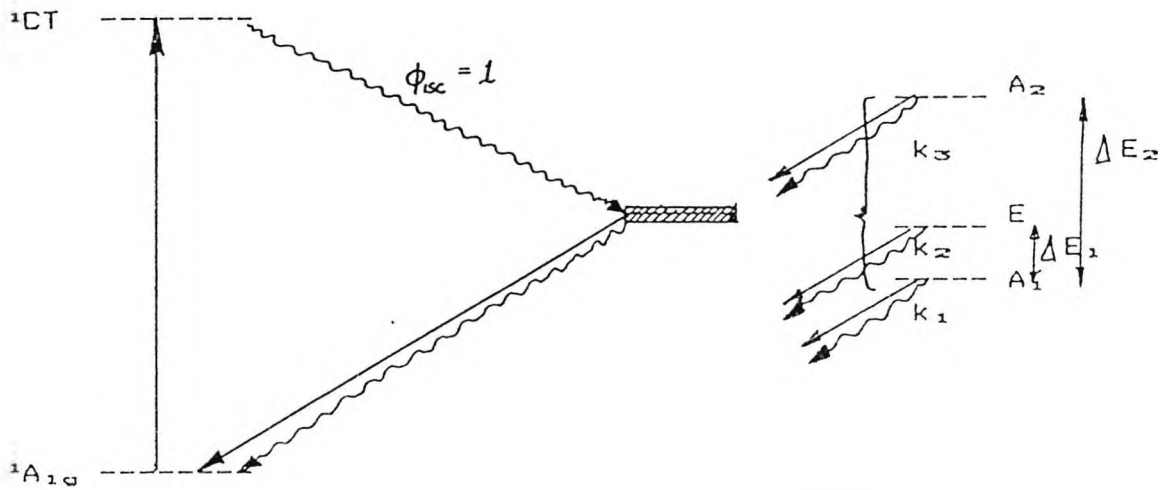

Figure 2.7 Schematic model for emission from the excited manifold of $a_2(\pi^*)$ origin for $[Ru(L-L)_3]^{2+}$.

2.1.10 *Summarizing for Tris(1,10-Phenanthroline)Ruthenium(II) Complexes and Related Species.*

In 1959, Paris and Brandt[8] reported the first observation of luminescence from $[Ru(bipy)_3]^{2+}$. They intuitively assigned this to the decay of an E.S. of the molecule created by an MLCT absorption, $(t_{2g})^6 \rightarrow \pi^*$. Although this assignment was controversial for many years, it now appears to be substantially correct. We have shown that the

intially formed E.S. undergoes non-radiative decay to an emissive E.S. manifold. At low temperature, there is insufficient thermal energy to populate A_2, and so luminescence approaches phosphorescence, emission originating from the E and A_1 states. At higher temperature, A_2 becomes populated and luminescence from that state starts to predominate; this luminescence is of a formally fluorescent nature.

Much of the above discussion has been derived from studies upon $[Ru(bipy)_3]^{2+}$. What we find when we apply the same to complexes of phenanthroline derivatives is that, in general, they are less susceptible to quenching than their bipyridine analogues - probably due to their enhanced rigidity. Moreover, the parameters of the complexes of the phenathroline derivatives are very sensitive to the substitution in the 4,7-positions, but not so markedly in the 5,6-positions[9], whereas those of the complexes of bipyridine derivatives show little change with 4,4-substitution[10]. The total splitting of the emission manifold, ΔE_2, is a measure of the "isolation" of the electron of the excited electron from the ruthenium ion. Thus, a large value of ΔE_2 represents strong coupling, and a small value weak coupling. On this naïve basis, the values in Table 2.1[10-12] suggest that ($[Ru(4,7\text{-}Ph_2phen)_3]^{2+}$) should be the most powerful reducing agent of those complexes examined, but this is not borne out by experiment (c.f. Table 2.2)[13-14].

Table 2.1 Some excited state parameters for $[Ru(L-L)_3]^{2+*}$.

Complex	Solvent	E_1/cm^{-1}	E_2/cm^{-1}
$[Zn(Ru)(bipy)_3][SO_4].7H_2O$	solid	10	80
$[Ru(bipy)_3]^{2+}$	pmma	10.1	61.2
$[Ru(4,4'-Me_2bipy)_3]^{2+}$	pmma	9.2	64.2
$[Ru(4,4'-Ph_2bipy)_3]^{2+}$	pmma	9.5	60.1
$[Ru(phen)_3]^{2+}$	pmma	8.9	52.7
$[Ru(5,6-Me_2phen)_3]^{2+}$	pmma	8.5	53.1
$[Ru(4,7-Me_2phen)_3]^{2+}$	pmma	8.5	30.4
$[Ru(4,7-Ph_2phen)_3]^{2+}$	pmma	8.5	30.1

Table 2.2 Some excited state redox potentials (*vs* SHE).

Complex	E(3+/2+*)/V	E(2+*/1+)/V
$[Ru(bipy)_3]^{2+}$	-0.84	+0.84
$[Ru(phen)_3]^{2+}$	-0.87	+0.79
$[Ru(4,7-Me_2phen)_3]^{2+}$	-1.01	+0.67
$[Ru(5,6-Me_2phen)_3]^{2+}$	-0.93	
$[Ru(5-Clphen)_3]^{2+}$	-0.77	+1.00
$[Ru(5-Brphen)_3]^{2+}$	-0.76	
$[Ru(3,4,6,8-Me_4phen)_3]^{2+}$	-1.11	
$[Ru(3,5,6,8-Me_4phen)_3]^{2+}$	-1.04	
$[Ru(4,7-Ph_2phen)_3]^{2+}$	-0.90	
$[Ru(5-Mephen)_3]^{2+}$	-0.90	
$[Ru(5-Phphen)_3]^{2+}$	-0.87	
$[Ru(5-NO_2phen)_3]^{2+}$	-0.67	

2.2 Electronic Structure

2.2.1 *Electronic Absorption Spectra.*

$[Ru(bipy)_3]^{2+}$ and $[Os(phen)_3]^{2+}$ share with complexes like $[Mo(bipy)CO_4]$, $[Re(phen)(CO)_3Cl]$, and $[Ir(bipy)_2Cl_2]^+$ the G.S. electronic configuration $(t_{2g})^6$ (in octahedral coordination) and vacant, low lying π^* orbitals on the polypyridyl ligands of appropriate symmetry to mix with the d orbitals. For the low oxidation state complexes of Mo(0) and Re(I) the carbonyl groups are necessary to mix with and stabilise the d levels thus decreasing sensitivity towards oxidation and bringing the d $-\pi^*$ energy gap into the visible region of the spectrum. In the higher oxidation state complex of Ir(III) the d levels are so stabilised by the higher effective charge at the metal that the MLCT transitions occur at high energies and can overlap with $\pi \rightarrow \pi^*$ based transitions localised on the polypyridyl ligands.

Considering the nature of possible electronic transitions in $[Ru(bipy)_3]^{2+}$, assuming it has D_3 symmetry, the d-manifold will be split according to Figure 2.8.

In the literature the π and π^* orbitals of 2,2'-bipyridine are classified according to the convention established by Orgel. Thus, rotation about the C_2 axis under the D_3 symmetry of the complex (Fig. 2.9)[7] allows classification of the π and π^* molecular orbitals (M.O.) according to whether they are symmetrical (χ) or antisymmetrical (ψ) with respect to it.

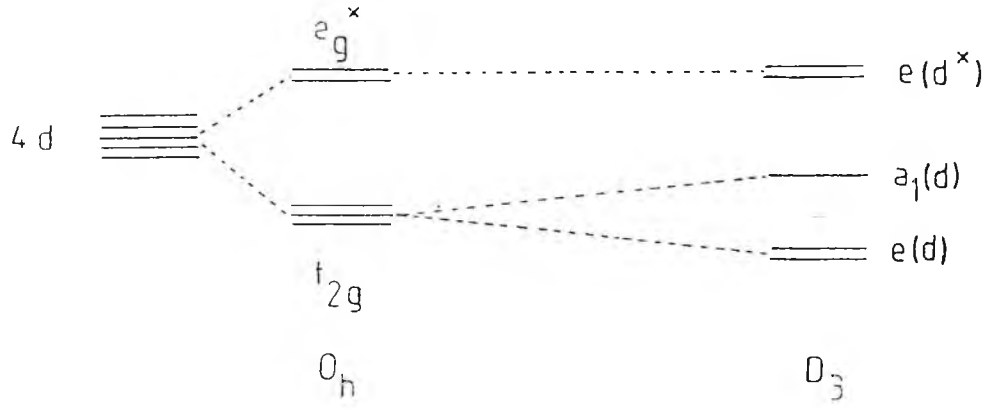

Figure 2.8 Splitting of the 4d manifold under D_3 symmetry, assuming that the bond angles do not deviate significantly from those of an octahedron.

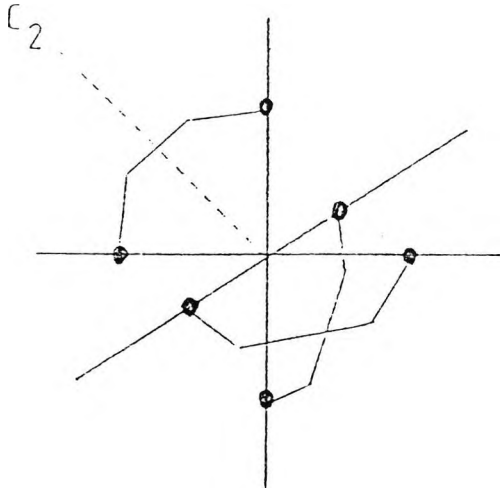

Figure 2.9 Diagram showing the C_2 axis retained by one of the bipy ligands of $[Ru(bipy)_3]^{2+}$.

Thus, upon the M.O. scheme for $[Ru(bipy)_3]^{2+}$ shown in Figure 2.10[17] (which incorporates the results of the Daul model for weak interligand coupling)[16] the highest filled molecular orbitals are $a_1(d)$ and $e(d)$ which are predominantly localised on the metal; the lowest empty M.O.s are $a_2^*(\psi)$ and $e^*(\psi)$, which are predominantly localised on the ligands. On the basis of the completely filled HOMO d set, the ground state of the complex can be ascribed as a singlet. The following electronic transitions are possible:

ligand $\pi \rightarrow \pi^*$	$\pi \rightarrow \pi^*(\psi^*)$
	$\pi \rightarrow \pi^*(\chi^*)$
metal d → d*	$e(d) \rightarrow e(d^*)$
	$a_1(d) \rightarrow e(d^*)$
MLCT (metal oxidation)	$e(d) \rightarrow \pi^*(\psi^*)$
	$a_1(d) \rightarrow \pi^*(\psi^*)$
	$e(d) \rightarrow \pi^*(\chi^*)$
	$a_1(d) \rightarrow \pi^*(\chi^*)$
LMCT (metal reduction)	$\pi \rightarrow e(d^*)$

Thus, in general[17]:

1) The visible spectrum is usually dominated by transitions to <u>MLCT excited states</u> which are largely singlet in character $^1[(t_{2g})^6(\pi^*)^1]$ and emission occurs from MLCT states[18] which are largely triplet in character, $^3[(t_{2g})^6(\pi^*)^1]$. The energies of the MLCT states vary systematically as the ligands are varied, a direct consequence of the considerable difference in electronic configuration at the metal between the E.S., and the $(d)^6$ G.S. For example, good back bonding

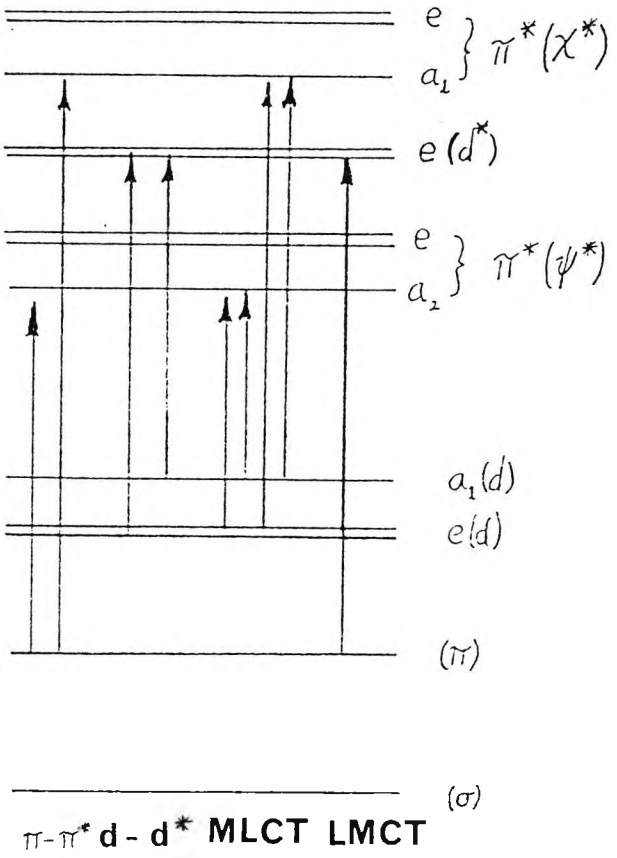

Figure 2.10 Possible types of electronic transitions within $[Ru(bipy)_3]^{2+}$ *based upon a simplified m.o. diagram incorporating the results of the Daul model for weak interligand coupling.*

ligands stabilise $(d_{2g})^6$-Ru(II) but not $(d_{2g})^5$-Ru(III) to any appreciable degree (that is good backbonding ligands lead to an increased energy gap between the E.S. and G.S.). Also, because excitation involves promotion of a non-bonding electron to an empty anti-bonding orbital, only relatively

small molecular distortions are expected to exist.

The maximum of the ^{1}MLCT at ~450nm is slightly sensitive to solvent, suggesting an instantaneous sensing of the dipolar excited state $[Ru^{3+}(bipy)_2(bipy^-)]^{2+}$.[17]

2) In the dd excited states $(t_{2g})^5(\pi^*)^1$, there is a significant increase in electronic repulsion along the ligand sigma bonding axes because of the promotion of a non-bonding electron to a sigma anti-bonding orbital. Because of their LaPorte forbiddenness, absorption bands arising from d → d transitions are weak and generally not observed for $(d\pi)^6$ polypyridyl complexes. If accessible they can play a significant role in the photochemical and photophysical properties of a complex since they are relatively short lived in solution and are often the source of photochemical instability (See Figure 2.11b)[20], arising in ligand loss.

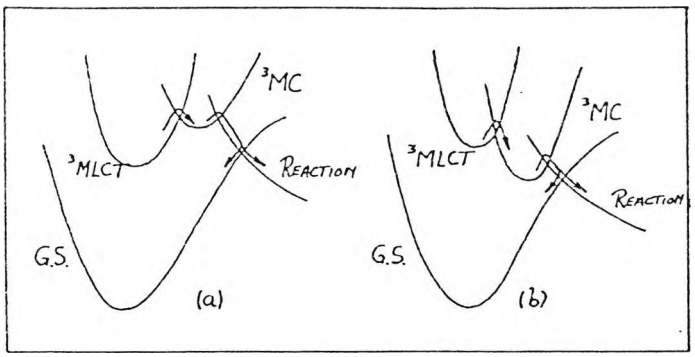

Figure 2.11 Diagramatic representation of the limiting cases for the ^{3}MC and ^{3}MLCT excited states.

It should be remembered that the dd E.S. energies above the G.S. in analogous complexes inreases ~30% in passing from

the first transition series to the second and ~30% again from the second to the third. Figure 2.11a[20] gives pictorial representation of how, thermally activated radiationless deactivation via upper lying MC E.S.can occur.

3) $\pi-\pi^*$ States-absorption bands arising from polypyridine localised $\pi \rightarrow \pi^*$ transitions appear to vary in energy with the metal and its oxidation state but generally appear at ~300 nm [$\pi \rightarrow \pi^*(\psi^1)$] and ~185 nm [$\pi \rightarrow \pi^*(\chi^1)$]. Because of the lack of dipole character, the E.S. so produced is relatively insensitive to solvent variations.

2.2.2 *Changes After Optical Excitation.*

For $[Ru(bipy)_3]^{2+}$, optical excitation throughout the $t_{2g} \rightarrow \pi^*$ spectral region results in the rapid appearance of an emitting ^{3}MLCT manifold.

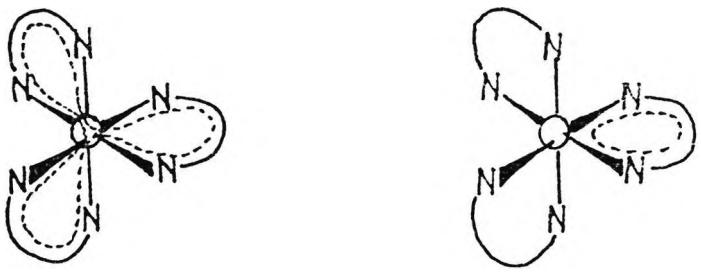

Figure 2.12 Interligand interaction upon electron promotion to MLCT ; a) delocalised molecular orbitals over the whole molecule, and b) localised ligand state - weak interligand interaction.

An interesting question exists for multiple chelates. Is the electron localised on a single ligand as in $[(bipy)_2Ru^{III}(bipy^{\cdot-})]^{2+*}$, possibly with rapid exchange occurring between ligands, or does the excited electron occupy a molecular orbital which is delocalised over all three ligands (Figure 2.12) ?

Experimental evidence[21] is available showing that in fluid solution the electron is initially localised during the

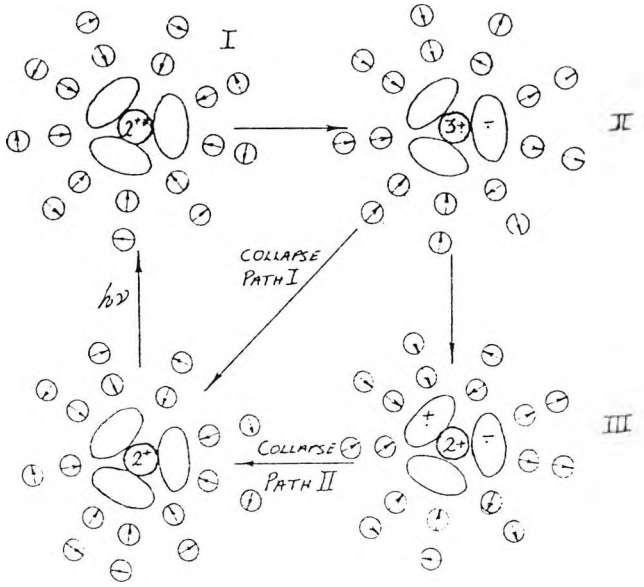

Figure 2.13 Changes wrought after optical excitation in $Ru(phen)_3^{2+}$; changes in the atomic and orientation polarisation of the solvent molecules are indicated by the small spherical shapes. The collapse of the thermally populated interligand C.T. state (structure III) would not be expected to involve the same electron transfer processes followed by the localised MLCT state II. It is also fair to say that the rate constant for collapse path II may reflect a different reorganisation process with respect to path I.

electronic transition. The G.S. of $[Ru(bipy)_3]^{2+}$ has D_3 symmetry, and no permanent dipole moment. If optical excitation produced a delocalised E.S. then this condition will be preserved and MLCT absorption band energies should be independent of the solvent. The converse is found by experiment, consistent with dipole induction as a result of electron localisation on a single ligand[7] (Illustrated in Figure 2.13). Further convincing evidence for localised ligand states has been obtained from low temperature cyclic voltametry[22,23], electron spin resonance[24,25], electronic absorption spectra[26-28], NMR[29], and resonance Raman spectra[30].

2.3 Photoinduced Electron Transfer

2.3.1 *Quenching Reactions.*

The excited state of $[Ru(phen)_3]^{2+}$, usually reacts *via* outer sphere electron transfer or energy transfer. These reactions are in direct competition with luminescent decay to its G.S.:

$$[Ru(phen)_3]^{2+*} \rightarrow [Ru(phen)_3]^{2+} + h\nu$$

Quenching by electron transfer occurs by a one electron reaction in which an electron jumps from an occupied orbital of one reactant to an unoccupied orbital on the other. During oxidative quenching, $[Ru(phen)_3]^{2+*}$ acts as a reducing agent similar to, but not as powerful as, $[Ru(phen)_3]^{+}$; during reductive quenching, $[Ru(phen)_3]^{2+*}$ acts as an oxidising agent similar to, but not as powerful as, $[Ru(phen)_3]^{3+}$. In either case, quenching by E.T. is manifest by a charge

separation with repect to starting materials[31,32].

Quenching by energy transfer can take place through two mechanisms. In the electron exchange mechanism, two single E.T. events occur, one in each direction, resulting in the sensitiser's G.S. and the quenchers E.S. Energy transfer by the dipole-dipole mechanism operates by Coulombic resonance interactions, in which the oscillating electrons of an E.S. sensitiser are coupled with those of the quencher by an induced dipole interaction[33,34].

2.3.2 *Quenching by Electron Transfer in Linked Systems.*

Photoinduced E.T. has been demonstrated in many molecules where the donor and acceptor are linked together intramolecularly. Not surprisingly, the efficiency of E.T. in such systems is strongly dependent upon the separation distance and the structure of the molecular link.

Possible behaviour is summarised in Figure 2.14[32]. For flexible connecting links, the possibility exists for formation of encounter complexes and exiplexes, giving rise to E.T. being influenced by chain length, it's steric nature and the solvents viscosity. In rigid systems, the situation is less complex, leading to the separation distance, and the donor-acceptor orientation being the primary factors for consideration.

For E.T. between widely separated molecules, a mechanism considering through-space interaction is clearly inappropriate. What is found is that E.T. *via* through-bond coupling of the donor-acceptor orbitals with the σ-orbitals

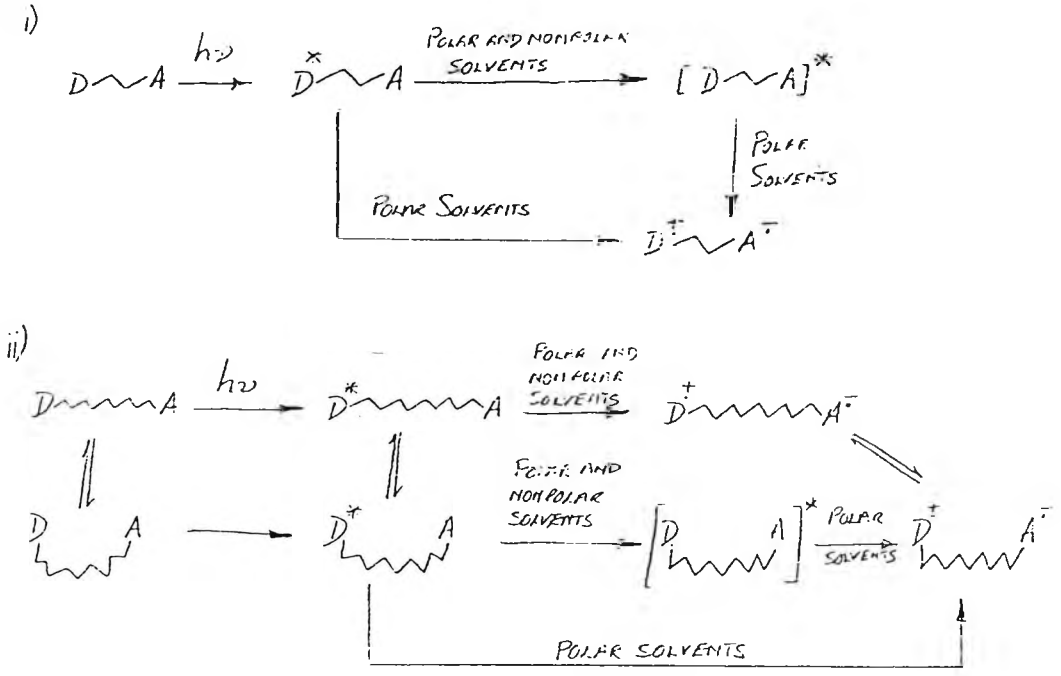

Figure 2.14 Electron transfer in systems linked, i) by short chains; ii) by long chains.

of the intervening spacer serving as a "conduit" for the passage of the electron occurs as a possible pathway[55]. This mode has been deduced for coupling between donor and acceptors separated by as many as twelve bonds[56] by the appearance of intramolecular charge-transfer absorption and emission.

This mechanism falls into the classification "inner-sphere" E.T., as the bridging ligand is covalently linked to the metal centres. The strong coupling induced by the spacer can enhance the rate of electron transfer, as has been recorded in the case of proteins, membranes, and other biological structures.

An interesting point to note is the similarity of structure (II)[37], (Figure 2.13) to that of a diagramatic representation of a twisted intramolecular charge transfer (TICT) state[38-40].

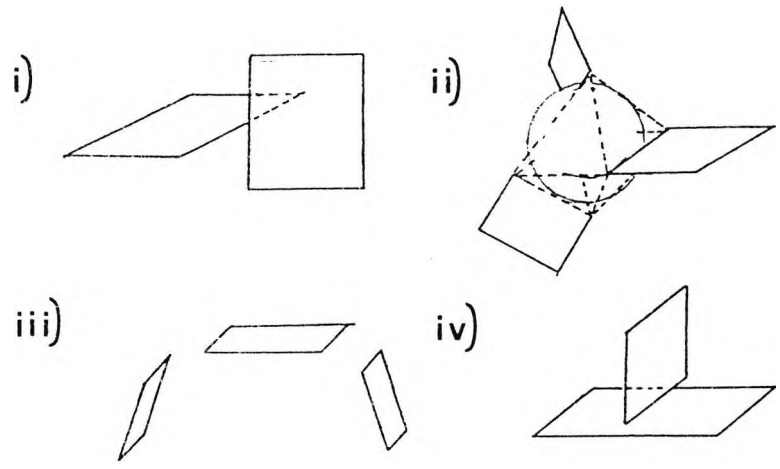

Figure 2.15 Small-overlap arrangements in various multichromophoric π - systems:

i) π - orthogonality by twisting;

ii) octahedral arrangement in Ru(phen)$_3^{2+}$;

iii) juxtaposition of chromophores in the photosynthetic reaction centre and σ - coupled model DIAS's;

iv) T- (or Y -) shaped conformations, e.g. the triptycene molecules.

A generalisation of TICT states are biradicaloidal charge transfer states[41-43] which encompass both TICT compounds with twisted, essential single bonds; alkenes with twisted, essential double bonds, and a large variety of compounds on the borderline (triphenylmethane and cyanine dyes, substituted stilbenes) as well as larger

supramolecular systems like the reaction centre in photosynthesis[49] and through bond-coupled space separated chromophores[35,46] and transition metal complexes with relatively small $\pi - \pi$ overlap. Figure 2.15[37] summarises several possibilities for small overlap arrangements of chromophores.

2.3.3 *Energetics.*

The feasibility of E.T. between an excited-state sensitizer and quencher is dictated by the overall change in free energy, ΔG, which accompanies the reaction.

For a bimolecular E.T. between two G.S. species, the standard free energy change is given by;

$$\Delta G = IP_D - EA_A \qquad (11)$$

When one of the reactants is an excited-state molecule, the role of free energy in E.T. can be examined in terms of the simplified M.O. diagrams in Figure 2.14[35,36] . If the donor is excited, then eqn. (11) takes the form;[49]

$$\Delta G = IP_D - EA_A - E^{0-0} \qquad (12)$$

To treat the case of reactants in solution, we must consider the Coulombic interactions and solvent stabilising effects of E.T. Recognising, also, that the ionisation potential and electron affinity in solution are related to the redox potentials of the donor and acceptor, it is then possible to derive the Weller equation[49,52]. It follows that since excited state has a higher energy content, it will be both a stronger reductant and a stronger oxidant than the corresponding ground state. To a first approximation, the redox potentials

for the E.S. couples may be calculated from the potentials of the G.S. couples and the zero-zero excitation energy $E^{\circ-\circ}$ (Scheme 2.1)[35]:

$$E(D^{+}/D^{*}) = E(D^{+}/D) - E^{\circ-\circ}$$

$$E(D^{*}/D^{-}) = E(D/D^{-}) - E^{\circ-\circ}$$

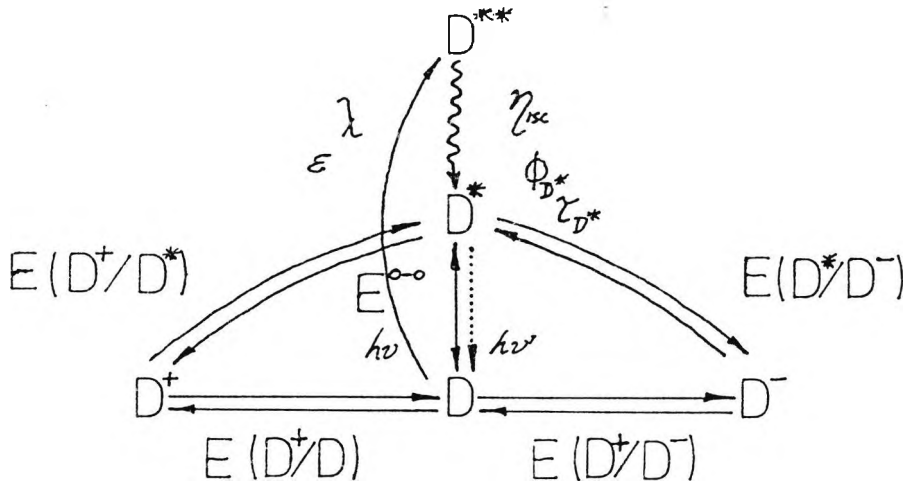

Scheme 2.1 Diagram showing molecular quantaties that characterise an excited state from the point of view of an electron transfer process.

For the system where the ion pair is separated by a distance exceeding ~ 7 Å in a solvent of high dielectric constant, equation (13) simplifies to[36]:

$$\Delta G = (\text{kcal mol}^{-1}) = 23.06[E(D^{+}/D) - E(A/A^{+})] - E^{\circ-\circ} \quad (13)$$

However, in the derivation of the Weller equation it is assumed that the geometry of the E.S. does not differ from

[36] footnote(13) is a simplified form of that derived by Mayer[48], however due to ambiguity on a previous line, he has quoted ΔG as $(-\Delta G)$.

the G.S. and that entropy changes accompanying the radical ion pair formation from the reactants are negligible.

The process of electron transfer from an E.S. to a G.S. molecule and the subsequent reactions are described by Scheme 2.2[47].

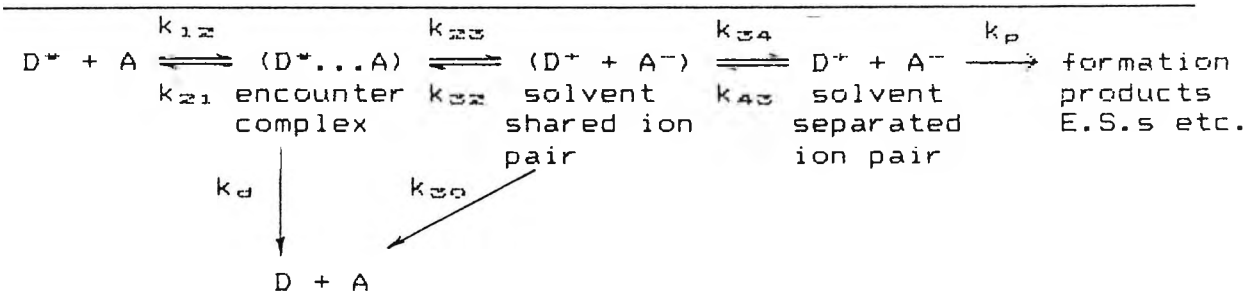

Scheme 2.2. Detailed mechanism for an electron transfer event, where:

k_d = rate constant for unimolecular decay of E.S. (1/)
k_{12}, k_{21} = diffusion controlled rate constants
k_{23}, k_{32} = bimolecular "activation energy controlled" rate constant
k_{30} = rate constant for reversible E.T. to G.S. reactants
k_{34}, k_{43} = rate of radical ion dissociation/association
k_p = rate constant for trapping reactions in the presence of scavengers

Application of a steady state treatment to the various intermediates of this scheme leads to relationship for the observed quenching rate constant k_q:

$$k_q = \frac{k_{12}}{1 + (k_{21}/k_{23}) + (k_{21}k_{32}/k_{30}k_{23})} \qquad (14)$$

Equation(14) can be simplified if it is assumed[15] that E.T. is exothermic*. Given this assumption, $k_{32} << k_{23}$ and equation(14) becomes:-

* This generalisation has been applied to show that E.T. from excited singlet and triplet aromatic to methyl viologen is exothermic except when the aromatic hydrocarbons contain

strongly electron withdrawing substituents such as cyano and nitro[51].

$$k_q = \frac{k_{23}k_{12}}{k_{23} + k_{21}} \qquad (15)$$

Introducing a further assumption that $k_{12} = k_{21}$ leads to the following relationship:

$$\frac{1}{k_q} = \frac{1}{k_{23}} + \frac{1}{k_{12}} \qquad (16)$$

However, if we now consider a system where D and A are held apart by a rigid spacer group, we lose the term in k_{12} to leave us with $k_{23} \sim k_q$, that is, the measured rate is related to the barrier for electron transfer.

Utilising the following relationships[50];

$$k_{23} = Ak_{et} \qquad (17)$$

where

$$k_{et} = Z\exp(-\Delta G^{\ddagger}_{23}/RT) \qquad (18)$$

where A is the frequency of interaction within the DIAS, Z is a constant which reflects the electronic barrier of the reaction, and $\Delta G^{\ddagger}$ is the free energy of activation representing contributions from nuclear barriers. Either electronic barriers primarily influence the rate ($Z<<1$ and $\Delta G^{\ddagger}_{23} = 0$), or nuclear barriers are rate determining ($Z \sim 1$ and $\Delta G^{\ddagger}_{23} > 0$).

On the basis of many experimental results, Rehm and Weller derived an empirical relationship (19). ΔG_{23} is given by eqn(13).

$$\Delta G^{\ddagger}_{ij} = \Delta G_{ij}/2 + ([\Delta G_{ij}/2]^2 + [\Delta G^{\ddagger}_{ij}(0)]^2)^{1/2} \qquad (19)$$

$G^{\ddagger}(0)$ is the activation free energy for a reaction in which

there is no free energy change and corresponds to the intrinsic barrier to electron transfer. According to Scandola and Balzani[52] this equation predicts, that for a value of $\Delta G^{\ddagger}(0)$ = 2 kcalmol^{-1}, $\Delta G^{\ddagger}$ should vary as a function of G as shown by the Rehm-Weller (R-W) line in Figure 2.17.

An alternative relationship (20), based on absolute reaction-rate theory, has been derived by Marcus[53-55] and Hush[56-57].

$$\Delta G^{\ddagger}_{ij} = \Delta G^{\ddagger}_{ij}(0)[1 + (\Delta G_{ij})/4\Delta G^{\ddagger}_{ij}(0)]^2 \qquad (20)$$

Not satisfied that this theoretical derivation accounted for all experimental observations (paricularly in exoergonic reactions), Scandola and Balzani developed a further relationship based on a "thermodynamic-like treatment of concerted reaction kinetics", equation (21). This equation predicts $\Delta G^{\ddagger}$ to vary with $\Delta G^{\ddagger}_{ij}$;

$$\Delta G^{\ddagger}_{ij} = \Delta G_{ij} + (\Delta G^{\ddagger}_{ij}(0)/\ln 2)\ln\{1+\exp[-\Delta G_{ij}\ln 2/\Delta G_{ij}(0)]\} \qquad (21)$$

(as shown in Fig. 2.17) in a similar way to the R-W empirical relationship.

Utilising (21), Balzani *et al.* [60] computed plots of log k_q versus redox potentials (Fig. 2.18) and showed how the $\Delta G^{\ddagger}(0)$ term ~~is~~ affects the shape. The term $\Delta G^{\ddagger}(0)$ is affected by two main reorganisational processes shown in eqn. (22):

$$\Delta G^{\ddagger}(0) = \Delta G^{\ddagger}_{i} + \Delta G^{\ddagger}_{o} \qquad (22)$$

(i) changes in internal nuclear coordinates of the molecule ("inner sphere" reorganisational energy, $\Delta G^{\ddagger}_{i}$) and (ii) from changes in the solvent arrangement around the molecule ("outer sphere" reorganisational energy, $\Delta G^{\ddagger}_{o}$). It was

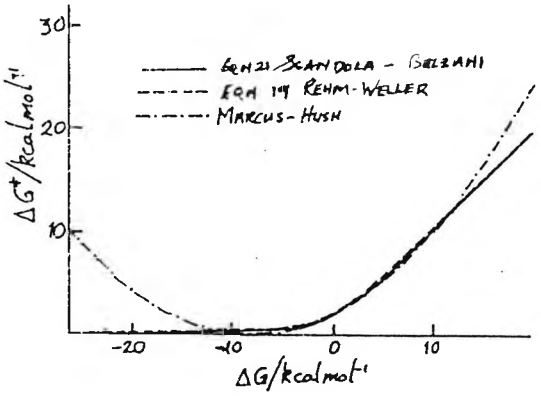

Figure 2.17 Graphical representation of the free energy relationship for electron transfer processes (calculation performed with $\Delta G^{*}_{(o)} = 2$ *kcal* mol^{-1} *).*

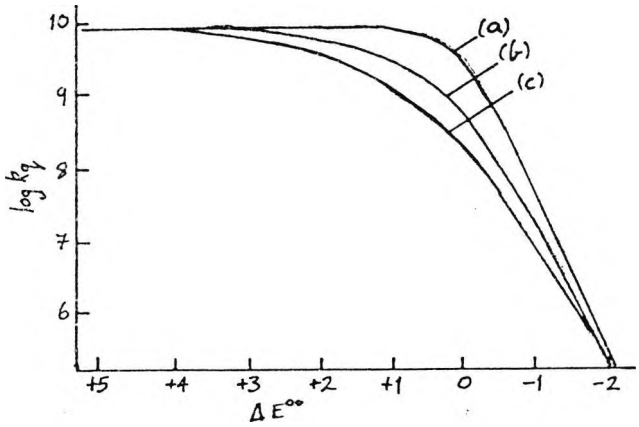

Figure 2.18 Influence of the intrinsic reorganisational energy on the shape of the plot of log k_q *versus redox potential from equation (14); (a)* $\Delta G^{*}_{(o)} = 250cm^{-1}$; *(b)* $=1000cm^{-1}$; *(c)* $=1250cm^{-1}$.

pointed out that ΔG^{*}_{σ} may well be negligible for E.T. reactions from a delocalised (eg. π) orbital, but significant when a localised (eg. π^{*}) orbital is involved.

As far as practising chemists are concerned, the difficulty of using eqn. (20) is that one has to employ curve fitting to obtain the relevant parameters. Thus the temptation to apply the simple relationships (23) and (19) empirically derived by R-W is very great.

$$k_q/\mathrm{lmol^{-1}s^{-1}} = 2.0*10^{10}/[1+0.25\exp(\Delta G^{*}/RT) + \exp(\Delta G/RT)] \quad (23)$$

Bock *et al.* [61] have shown in a most convincing way that the degree of reorganisation ("inner" and "outer sphere") plays an important part in determining the energetics of E.T. reactions and hence plots of log k_q against the energy of the appropriate redox couple.

The treatment of Balzani *et al.* [60] in eqn. (21) places a different emphasis upon the reorganisational processes compared with that by the Marcus and Hush approach and point out that any attempt to predict k_q must take account of the relative importance of $k_{\sigma\sigma}$ and $k_{\sigma\sigma}$. It is unfortunate that steady state kinetics do not directly give these values and one is forced to time-resolved experiments which have the problem that multi-exponential decays have to be analysed.

REFERENCES

1. Atkins, P.W. Physical Chemistry, 2nd ed., Oxford University Press, 1982.
2. Yearwood, G. M.Phil Transfer Report, City Univ., 1987.
3. Bohm, D. Quantum Theory, Prentice-Hall, New Jersey, 1951.
4. Parker, C.A. Photoluminescence of Solutions, Elsevier, London, 1968.
5. Demas, J.N.; Crosby, G.A. J. Am. Chem. Soc., 93, 2841, 1971.
6. Lytle, F.E.; Hercules, D.M. J. Am. Chem. Soc., 91, 253, 1969.
7. Harrigan, R.A.; Hager, G.D.; Crosby, G.A. Chem. Phys. Lett., 21, 487, 1973.
8. Paris, J.P.; Brandt, W.W. J. Am. Chem. Soc., 81, 5009, 1959.
9. Seddon, S.A.; Seddon, K.R. The Chemistry of Ruthenium, Elsevier-Oxford, 1984.
10. Hager, G.D.; Crosby, G.A. J. Am. Chem. Soc., 97, 7037, 1975.
11. Hager, G.D.; Watts, R.J.; Crosby, G.A. J. Am. Chem. Soc., 97, 7031, 1975.
12. Harrigan, R.W.; Crosby, G.A. J. Phys. Chem., 59, 3468, 1973.
13. Lin, C.-T.; Bottcher, W.; Chou, M.; Creutz, C.; Sutin, N. J. Am. Chem. Soc., 98, 6536, 1976.
14. Creutz, C.; Sutin, N. Inorg. Chem., 15, 496, 1976.

15. Orgel, L.E. J. Chem. Soc., 3683, 1961.

16. Belser, P.; Daul, C.; von Zelewsky, A. Chem. Phys. Lett., 79, 596, 1981.

17. Meyer, T.J. Pure Appl. Chem., 58, 1193, 1986.

18. Kober, E.M.; Meyer, T.J. Inorg. Chem., 21, 3697, 1982.

19. Kober, E.M.; Sullivan, B.P.; Meyer, T.J. Inorg. Chem., 23, 2098, 1984.

20. Cannon, R.D. Electron Transfer Reactions, Butterworths, London, 1980.

21. Kober, E.M.; Sullivan, B.P.; Meyer, T.J. Inorg. Chem., 23, 2098, 1984.

22. Ohsawa, Y.; De Armond, M.K.; Hanck, K.W.; Morris, D.E.; Whitten, D.G.; Neveux, P.E.Jr. J. Am. Chem. Soc., 105, 6522, 1983.

23. Ohsawa, Y.; Whanglo, M.-H.; Hanck, K.W.; De Armond, M.K. Inorg. Chem., 23, 3462, 1984.

24. Molten, A.G.; Hanck, K.W.; De Armond, M.K. Chem. Phys. Lett., 79, 541, 1981.

25. Morris, D.; Hanck, K.W.; De Armond, M.K. J. Am. Chem. Soc., 105, 3032, 1983.

26. Elliot, C.M. J. Chem. Soc. Chem. Commun., 261, 1980.

27. Heath, G.A.; Yellowlees, L.J.; Braterman, P.S. J. Chem. Soc. Chem. Commun., 287, 1981.

28. Heath, G.A.; Yellowlees, L.J.; Braterman, P.S. Chem. Phys. Lett., 92, 646, 1982.

29. Ohsawa, Y.; De Armond, M.K.; Hanck, K.W.; Moreland, C.G. J. Am. Chem. Soc., 107, 5383, 1985.

30. Angel, S.M.; De Armond, M.K.; Donshoe, R.J.; Hanck, K.W. Wertz, D.H. J. Am. Chem. Soc., 106, 3688, 1984.

31. Jaris, A.; Balzani, V.; Barigelletti, F.; Campagna, S.; Belser, P.; von Zelewsky, A. Coord. Chem. Rev., 84, 85, 1988.

32. Kavarnos, G.J.; Turro, N.J. Chem. Rev., 86, 401, 1986.

33. Forster, T. Disc. Faraday Soc., 27, 7, 1959.

34. Turro, N.J. Modern Molecular Photochemistry, Benjamin/Cummings, Menlo Park, 1978.

35. Beratan, D.N. J. Am. Chem. Soc., 108, 4321, 1986.

36. Verhoeven, J.W.; Paddon-Row, M.N.; Hush, N.S.; Oevering, H.; Heppener, M. Pure Appl. Chem., 58, 1285, 1986.

37. Rettig, W. Supramolecular Photochemistry, Ed. Balzani, V., NATO ASI Series C, 214, 329, 1987.

38. Bischof, H.; Baumann, W.; Detzer, N.; Rotkiewicz, K. Chem. Phys. Lett., 116, 180, 1985.

39. Rettig, W.; Gleiter, R. J. Phys. Chem., 89, 4676, 1985.

40. Rettig, W. Angew. Chem. Int. Ed. Engl., 25, 971, 1986.

41. Bonacic-Koutecky, V.; Michl, J. J. Am. Chem. Soc., 107, 1765, 1983.

42. Bonacic-Koutecky, V.; Koutecky, J.; Michl, J. Angew. Chem. Int. Ed. Engl., 26, 170, 1987.

43. Bonacic-Koutecky, V.; Kohler, J.; Michl, J. Chem. Phys. Lett., 104, 440, 1984.

44. Warman, J.M.; de Haas, M.P.; Oevering, H.; Verhoeven, J.W.; Paddon-Row, M.N.; Oliver, A.M.; Hush, N.S. Chem. Phys. Lett., 128, 95, 1986.

45. Heitele, H.; Michel-Beyerle, M.E.; Finckh, P. Chem. Phys. Lett., **134**, 273, 1987.

46. Joran, A.D.; Leland, B.A.; Geller, G.G.; Hopfield, J.J.; Dervan, P.B. J. Am. Chem. Soc., **106**, 6090, 1984.

47. Gust, D.; Moore, T.A. J. Photochem., **29**, 173, 1985.

48. Meyer, T.J. Progr. Inorg. Chem., **30**, 389, 1983.

49. Davidson, R.S. Adv. Phys. Org. Chem., **19**, 1, 1983.

50. Sutin, N. Acc. Chem. Res., **15**, 275, 1982.

51. Davidson, R.S.; Bonneau, R.; Fournier De Violet, P. Chem. Phys. Lett., **78**, 471, 1981.

52. Scandola, F.; Balzani, V. J. Am. Chem. Soc., **101**, 6140, 1979.

53. Marcus, R.A. J. Chem. Phys., **24**, 966, 1956.

54. Marcus, R.A. Disc. Faraday Soc., **29**, 21, 1960.

55. Marcus, R.A. Ann. Rev. Phys. Chem., **15**, 155, 1964.

56. Hush, N.S. Trans. Faraday Soc., **57**, 557, 1961.

57. Hush, N.S. Progr. Inorg. Chem., **8**, 391, 1967.

58. Hush, N.S. Electrochem. Acta., **13**, 1005, 1968.

59. Hush, N.S. Chem. Phys., **10**, 361, 1975.

60. Belzani, V.; Bolletta, F.; Scandola, F. J. Am. Chem. Soc., **102**, 2152, 1980.

61. Bock, C.R.; Connor, J.A.; Gutierrez, A.R.; Meyer, T.J.; Whitten, D.G.; Sullivian, B.P.; Nagle, J.K. J. Am. Chem. Soc., **101**, 4815, 1979.

3.0 SYNTHESIS OF RUTHENIUM(II) COMPLEXES OF MODIFIED 1,10-PHENANTHROLINES

3.1 Introduction

3.1.1 *Strategy.*

In the analysis of the photoinduced electron transfer event illustrated by:

$$D^* + A \rightarrow D^+ + A^- \qquad (1)$$

there were three fundamental questions the project was to address:

1) Over what distance can the electron be transferred?

2) To what extent are solvent molecules involved?

3) Can a protein act as a solvent or as a conduit for an electron?

Our approach to the elucidation of pertinent parameters governing event (1) was the synthesis of molecular rectifier components of the form donor-insulator-acceptor system (DIAS). Ergodynamics of a photoexcited DIAS would follow the form:

a) Local electronic excitation as a result of absorption of a photon h_A by the donor chromophore.

b) Reaction of this local excited state (LES) resulting either in deactivation of the ground state by photon emission h_D or electron transfer through the insulating medium to the acceptor, resulting in complete charge separation.

c) Charge recombination of the dipole state (DS) by reverse electron tunnelling (possibly with the emission of a photon h_{CR}).

The energy difference between the LES and the DS, is known as the driving force for charge separation. The excess energy trapped in the DS is called the redox power.

It can be seen that DIAS's have a huge potential as catalysts. Thus, maximum redox power from such systems is obtained by optimising the charge separation in competition with deactivation by reducing the driving force.

The important kinetic parameters of a DIAS are the natural lifetime of the excited donor towards deactivation, τ_D; the forward electron transfer time, τ_{ET}; and the charge recombination time, τ_{CR}. Thus, if $\tau_{ET} \ll \tau_D$, then the charge separated state can be populated with greater efficiency, and if τ_{CR} is long compared with the timescale for activity on the reaction co-ordinate, then the DIAS will interact with the environment.

3.1.2 *Systems.*

Bridging groups between the donor and acceptor can be divided into four sub-groups: each poses interesting barriers to donor-acceptor coupling.

I) *RIGID BRIDGES*

i) Classical electron transfer bridges

These are inner-sphere moieties allowing coupling of remote centres by virtue of conjugated double bonds, for example:

Resulting delocalisation within these systems means complete charge transfer cannot occur.

ii) Quantum-mechanical charge-transfer bridges

Weak interaction between donor-acceptor sites can be achieved by employing rigid paraffinic bridge systems such as bicyclo [2.2.2] octane polymers.

or, by derivatisation of a steroid molecule.

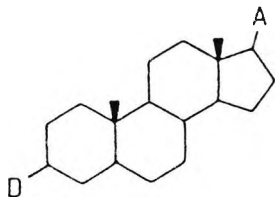

Electron-transfer in such a system would be dependent on the symmetry of the donor and acceptor orbitals relative to the linker orbitals.

II) *FLEXIBLE CHAINS*

Flexible spacer molecules may permit the formation of encounter complexes. Under these circumstances, the fate of charge separated intermediates formed by electron-transfer will reflect the structure and dynamic conformations of the molecular link. Also included under this heading are polyamide bridges of the form:

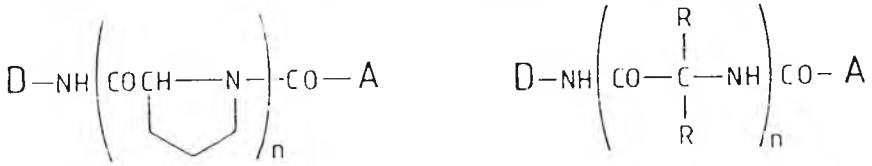

III) *PENDANT CHAINS*

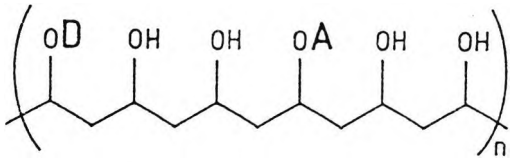

Such systems represent an extension of the flexible concept and add further complication as to the elucidation of the coupling processes between the donor and acceptor species. In such cases the nature of the donor and acceptor may be difficult to fathom.

IV) *MODIFICATION OF PROTEIN STRUCTURES*

Protein structures can be viewed as "cooled dimethyl formamide solutions". As such, modified derivatives can be studied for the effect of "through-space" coupling enhancement, for the propagation of electron-transfer. The model proposed is the surface modification of metalloproteins with suitable donor moieties. This should yield information on electron-transfer processes through proteins using the metal centre as an acceptor (e.g. Fe^{III}-heme).

3.1.3 *Suitable Donor-Acceptors.*

As indicated in 3.1.1, a major design requirement of the donor, is luminescence. Whilst luminescence is not necessarily a pre-requisite for photo-redox behaviour, it's presence is a desired property as a convenient probe of the excited state and it's redox potentials (the term luminescence is used to avoid any confusion in formal excited state labelling).

Other requirements imposed by our approach to molecular engineering are as follows:

i) The system should exhibit room temperature luminescence.

ii) The system should exhibit chemical stability of both excited and ground state, in a range of solvent systems.

iii) The system should allow ready chemical functionalisation through synthetic manipulation.

iv) The system should allow tunability of excited state.

v) The systems redox potentials should be compatible with electron transfer.

Compiled below are the excited-state energies; redox potentials; lifetime data; and intersystems crossing efficiencies for organic sensitisers (Table 3.1) and metal complex sensitisers (Table 3.2). Redox potentials of typical quenchers are listed in Tables 3.3 and 3.4.

For the organic sensitisers, it should be noted that: (i) although the singlet-states may be more effective in electron transfer quenching than the respective triplet-states, singlet-singlet energy transfer may populate lower lying singlet states of the quencher; and (ii) where the singlet lifetime is short and the intersystems crossing efficiency is high, the singlet-states of such species are usually ineffective as singlet electron transfer sensitisers. However, their triplet-states may be capable of functioning in redox reactions.

Table 3.1 ORGANIC SENSITISERS - Photophysical and Electrochemical Data. [1,2]

Sensitiser	$\lambda_{(S_0-S_1)}$ /nm	$E(D^+/D)$ /V	$E(A/A^-)$ /V	E_{S_1} /eV	Φ_f	τ_{S_1} /ns	Φ_{ST}	E_T /eV	τ_T /μs
Acetophenone	363		-1.85	3.41	0.00		1.00	3.20	0.41
Anthracene	375	1.16	-1.93	3.31	0.27	5.3	0.72	1.85	500
Benzophenone	384		-1.68	3.23			1.00	3.00	12
Chrysene	360	1.40		3.43	0.12	43.0	0.82	2.43	
CN	320		-1.98	3.88		8.92		2.49	
DCA	433		-0.89	2.86		19.6			
TCA	440		-0.45	2.82		15.2			
DCB	290		-1.60	4.27		9.7			
DCN	359		-1.28	3.45		10.1		2.41	
Fluorene	301	1.55		4.12	0.68	10.0	0.32	2.94	
MON	318	1.42		3.90	0.42	15.0		2.60	
Naphthalene	311	1.60	-2.29	3.99	0.21	150	0.80	2.64	74
Perylene	435	0.85		2.85	0.87	6.0	$9E^{-3}$	1.52	
Phenanthrene	345	1.58	-2.20	3.59	0.13	61.0	0.85	2.69	
Pyrene	372	1.20		3.34	0.53	475	0.38	2.09	
PCA	391		-1.67	3.17		12.5			
t -stilbene	304		-2.26	3.53		$7E^{-3}$		2.12	
Triphenylene	342	1.64	-2.22	3.62	0.07	37.0	0.89	2.88	
NTMB	345	0.32		3.60	0.30	10.0	0.63		

Abbreviations:-

CN= 1-cyanonaphthalene DCA= 9,10-dicyanoanthracene
TCA= 2,6,9,10-tetracyanoanthracene DCB= *p* -dicyanobenzene
DCN= 1,4-dicyanonaphthalene MON= 2-methoxynaphthalene
PCA= pyrene-3-carboxylic acid
NTBM= N,N,N',N'-tetramethylbenzidene

Table 3.2 LUMINESCENT METALLO-COMPLEXES - Photophysical and Electrochemical Data.

Complex	λ_{max} /nm	$E(D^+/D)$ /V	$E(A/A^-)$ /V	E^* /eV	Φ_{em}	τ /μs	ref.
$Cr(bipy)_3^{3+}$	455	>1.6	-0.26	1.71		77.0	(3)
$Cu(dpp)_2^{+}$	439	0.39		1.80	$4E^{-4}$	0.31	(4)
$Pt_2(P_2O_5)_4H_8^{4-}$	452	<1.0	-1.4	2.50	0.52	9.8	(5)
$Re_2Cl_8^{2-}$		>1.25	-0.85	1.75		0.14	(6)
$Rh_2(dicp)_4^{2+}$	553	0.89	-1.4	1.69		8.5	(7)
$Ru(bipy)_3^{2+}$	452	1.29	-1.35	2.12	0.042	0.62	(1&8)
UO_2^{2+}	420		0.06	2.54	~1	6.6	(9)
ZnTMPyP^{4+}		0.94		1.57	0.90	6.55	(10)
ZnTPP	560	0.71	-1.35	1.59	0.88	1200	(10&11

Table 3.3 ORGANIC QUENCHERS - Photophysical and Electrochemical Data.[1]

Quencher	$E(D^{+}/D)$ /V	$E(A/A^{-})$ /V	E_s /eV	E_T /eV
Methoxy compounds:				
o -dimethoxybenzene	1.45			
2-methoxynaphthalene	1.42		3.70	1.65
1,3,5-trimethoxybenzene	1.49			
Nitro compounds:				
p -dinitrobenzene		-0.69		
nitrobenzene		-1.15	>4.25	2.65
Cyano compounds:				
1,4-dicyanonaphthalene		-1.28	4.27	3.06
tetracyanoethylene		0.24		
Viologens:				
1,4-methyl viologen		-0.45		3.10
Quinones:				
p -benzoquinone		-0.51		2.30
chloroanil		0.02		2.70
Miscellaneous:				
oxygen		-0.78	0.98	

Table 3.4 METAL ION QUENCHERS - Photochemical and Electrochemical Data.[1]

Quencher	$E(D^+/D)$ /V	$E(A/A^-)$ /V	E^* /eV
$Ce(aq)^{3+}$	1.20		3.55
$Eu(aq)^{3+}$		-0.64	2.17
$Eu(aq)^{2+}$	0.67		3.88
$Fe(aq)^{3+}$		-0.53	1.60
$Fe(aq)^{2+}$	0.50		1.30
$Mn(aq)^{2+}$	1.27		
$Ti(aq)^{3+}$		-0.60	1.90
$Tl(aq)^{3+}$		-0.59	>4.50
UO_2^{2+}		0.06	2.54

It is largely as a consequence of the complicated nature of the excited-state reactivity of organic molecules (i.e. which state is involved) that our attention was drawn to metallo complexes. What is more these often show absorption in the visible spectrum, and exctation here results in low energy, long lived, and in many cases emitting excited states (Table 3.2). These excited states, by virtue of their low oxidation and high reduction potentials, enable them to react to both as electron donors and acceptors. It should be noted that electron transfer is not always the exclusive quenching pathway; energy transfer has also been documented.

As has been indicated, the photoinduced redox properties of $Ru(bipy)_3^{2+}$ has spurred numerous studies of this complex and it's related derivatives, leading to a detailed

understanding of this chemistry[12]. The initial motive for intense research was that of sensitised water splitting by sunlight[13]. However, in recent years the photophysical characteristics of these complexes, and the elucidation of photochemical transformations involving their excited states have been the topics of greatest interest[14].

It is not surprising to see why this complex has attracted so much attention. Its excited state is produced efficiently after excitation ($\Phi_{ISC} \sim 1$) has a lifetime of $\sim 0.6\mu s$; it emits strongly, allowing conveniently for study by Stern-Volmer techniques; and, most significantly, $Ru(bipy)_3^{2+}$ has a low oxidation and high reduction potential.

Both electron and energy transfer have been confirmed for this sensitiser. Both are normally rapid, being influenced by the solvent shell reorganisation (outer-sphere mechanism), since bond length changes during electron transfer are negligible. Slow reactions can sometimes be traced to bond reorganisational changes in the quencher molecules or non-adiabatic effects due of poor orbital overlap.

Such is the wealth of information about this molecule that we felt it's selection as a donor moiety gave a firm foundation on which to build.

To maintain a link with electron transfer in natural systems, our acceptor molecule was to have been derived from the quinone family (Table 3.3). As demonstrated by the work of Alvin Joral *et al* [15], synthetic manipulation of the

benzoquinone skeleton with electron withdrawing or donating groups can dramatically alter it's half-wave reduction potential. Thus, synthesis of DIAS's with the same donating function and with different substituted benzoquinones as acceptors gives rise to a series of molecules in which the exothermicity varies. This would then allow analysis of electron transfer as a function of ΔG without major perturbation to overall electron structure in a series of DIAS's.

Metal ions can also be used as acceptor species. This can be accomplished by linking cavelands to the insulator bridge, illustrated for chromium below:

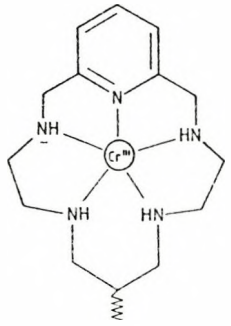

Our goal in the semi-synthetic protein DIAS's was envisaged as proceeding via utilisation of the Fe^{3+} heme in structurally characterised metalloproteins. In this spirit our first choice for derivatisation was myoglobin (see Section 1.0). The methodology would then be applied to investigation of the proteins horseradish peroxidase and microperoxidase. By attaching (labelling) a ruthenium complex to the protein, electron transfer between the metal sites could be studied.

Many proteins are not involved in natural electron

transfer cascades. Their incorporation into semi-synthetic DIAS's as the insulator moiety provides a powerful method of assessing favourable selections and compositions of amino-acids for electron mediation. Thus, by comparison with heme proteins in DIAS's of a similar donor-acceptor separation, it may be possible to reveal the extent of interaction of intervening functionalities. An importaant question we wished to pose is why, in natural electron transfer systems, -helical conformations are selected for protein rigidity and why sulphur (except where it is used in a co-ordinating capacity) is excluded.

An ideal opportunity to study these often taken for granted features, is presented by -chymotrypsin. A detailed knowledge of the catalytic mechanism and structure of this protein has led to the design of non-reversible inhibitor molecules. Since these species form covalent bonds only at the reaction centre, it is possible to specifically mono-functionalise this protein. Hence, affinity labelling chymotrypsin with a suitable derivatised ruthenium complex results in a new metalloprotein.

3.2 Ligand Synthesis

3.2.1 *Introduction.*

From the outset, it was recognised that the rigid, conjugated system in 1,10-phenanthroline would be advantageous in fulfilling one of our first aims, namely, a relatively long lived excited state of the ruthenium complex.

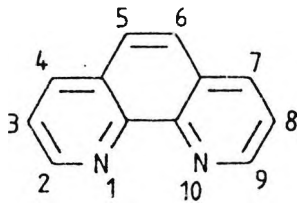

To employ Ru(II) complexes as donors in DIAS design, requires that the phenanthroline skeleton be functionalised with reactive groups. Described is the synthesis of some ligands formally derived from phenanthroline[16,17].

In the octahedral coordination sphere of ruthenium(II), three phenanthrolines are accommodated. Our strategy was to substitute the complex at only one of these.

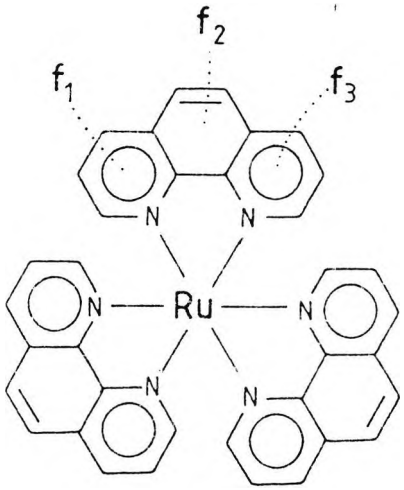

Competitive arguments between charge localisation and delocalisation of the promoted electron in the excited state have been summarised (see Section 2.2.2). Meyer *et al* [18] have suggested that by altering the electron accepting properties of one of the ligands, one might be able to manifest one of these conditions preferentially. Thus, a series of ligands are synthesised in which the phenanthroline electronic system has been modified. By this method, it was

hoped to be able to tune the excited state of the complex, e.g. by lowering the energy of the MLCT.

Another line of interest centred upon minimising the reverse reaction that follows the photo-induced electron transfer, and converting the one-photon, one-electron redox steps into more useful multi-electron transfer reactions. Although a number of dimeric Ru(II) systems have previously been prepared (mostly for the purpose of studying the intervalence charge transfer transitions in mixed valence systems[19]), none satisfy the criteria of field strength and/or coordination about each Ru^{2+} necessary for luminescence. Consequently, preparation of luminescent bimetallic ruthenium(II) complexes demands a bridging ligand that resembles, as closely as possible, 2,2-bipyridine. Examples of this type are presented.

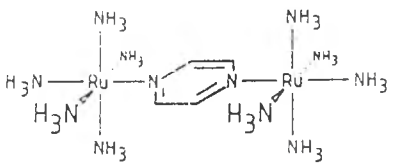

Creutz-Taube ion: a pyrazine bridged, mixed valence dimer.

Intramolecular electron transfer induced photo-fragmatisation as a route to free radicals has important implications in imaging technology[20]. Given "the groups" of interest in such areas, and the possible use of such substrates as sensitive monitors for long range electron transfer led to the synthesis of an aromatic disilane derivative for investigation.

3.2.2 *Synthesis.*

The carbonyl group, by way of being susceptible to nucleophilic attack, makes it a desirable functionality. Introduction of this moiety into the phenanthroline system was achieved by particularly efficient route (Scheme 3.1.1).

Scheme 3.1.1

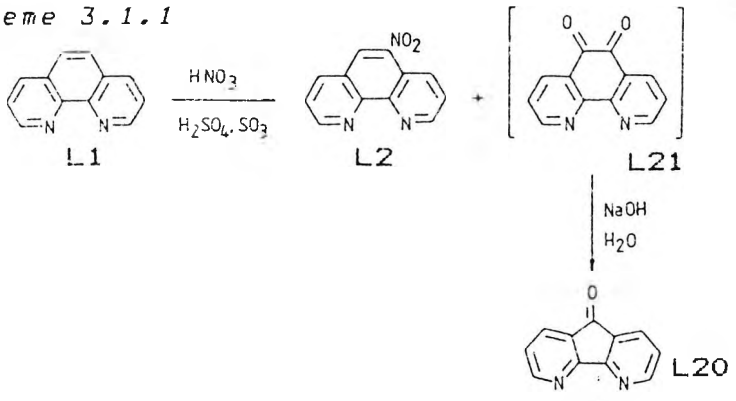

Hence under the conditions required for nitration of the heterocycle[221], oxidation also occurs, generating 1,10-phenanthroline-5,6-quinone (L21). Yield of this valuable by-product was maximised by using both fuming nitric and sulphuric acids. L21 can be isolated directly by work up, after Dickinson and Summers[222] (who generated L21 by oxidation of 5-amino-1,10-phenanthroline [L3]) or treated *in situ* with base to yield 4,5-diazofluoren-9-one[223] (L20). The comments of Smith and Inglet[223] about this reaction are ambiguous; while they imply loss of a carbon monoxide unit as a gaseous molecule, there is no reference in the paper to it's direction, nor have we observed such an event. It may be that their description ("decarbonmonoxidation") implies no more than the stoichiometric loss of a CO unit.

Reduction of 5-nitro-1,10-phenanthroline (L2) was found to be very reagent sensitive. Catalytic hydrogenation with

10% Pd(C) proceeded in only 40% yield.

Scheme 3.1.2

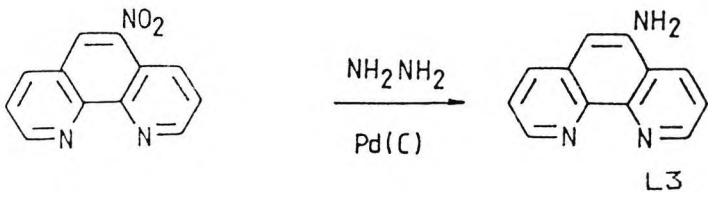

L3

Even then, the product was contaminated with a difficult-to-remove component [4.2(m) and 2.9(m)] presumably:-

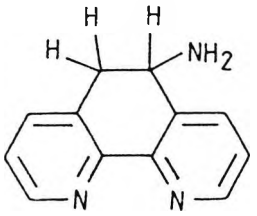

Reduction by either zinc or tin in either hydrochloric acid or acetic acid again gave poor yields (<30%). Amongst the other side reactions (reduction of the phenanthroline ring) yields were found to have been reduced by complexation of the ligand.

The highest yields of L3 (80% after recrystallisation) were achieved by reduction of the nitro group using hydrazine/palladium on charcoal reagent . Unfortunately, the best reagent combination requires that the palladium/charcoal catalyst be added to the refluxing mixture. This potentially hazardous procedure is rewarded by an efficient and clean reaction.

Thus, in a short space of time we had introduced nucleophilicity and electrophilic behaviour into the

phenanthroline nucleus, as well as generating an alternative diaza cavity (L20) has been ~~to~~ shown not to ligate the ferrous ion)[25].

Synthesis of 4,7-dichloro-1,10-phenanthroline (L5) by the method of Snyder and Freider[24] (Scheme 3.2) was eventually achieved, but not without minor modification to the reaction conditions.

Scheme 3.2 I

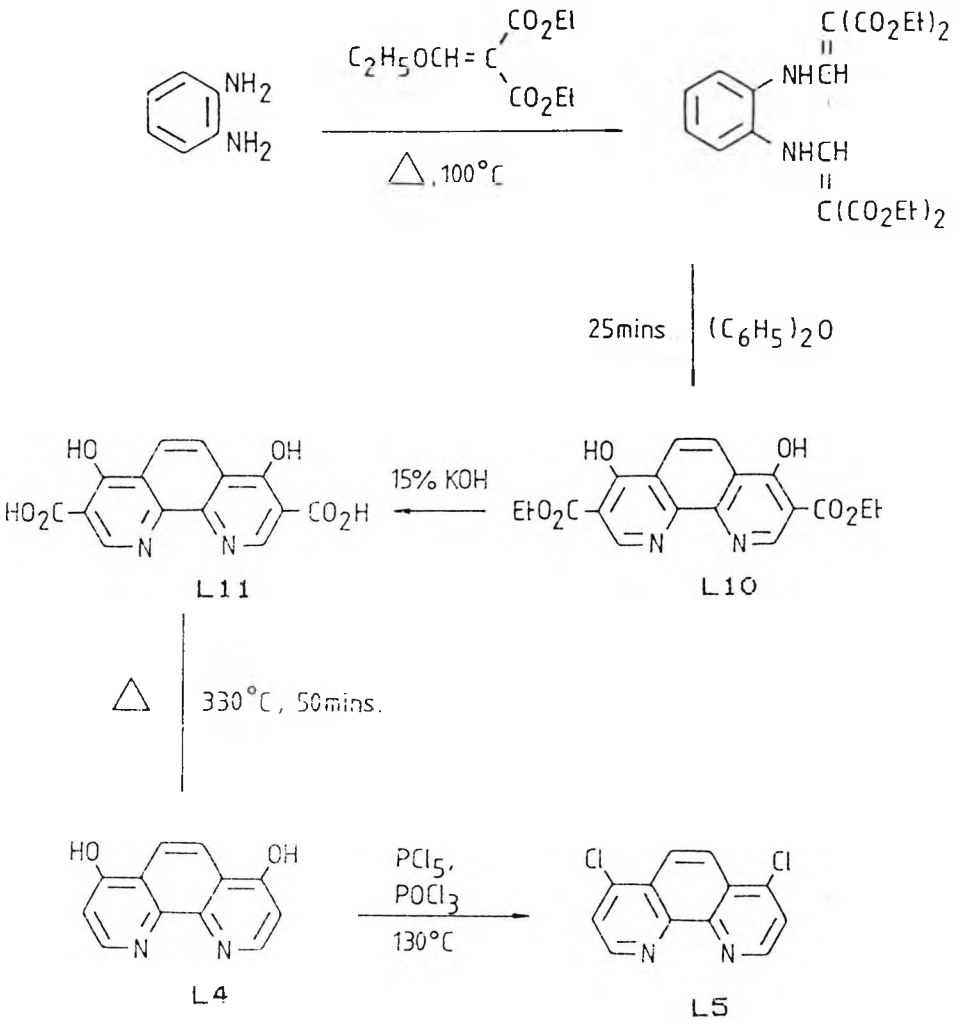

Of the reaction sequences denoted, two of the steps proved to be particularly difficult to reproduce;

i) Thermal cyclisation: The published method utilised diphenyl ether as the high temperature solvent. It was found that this procedure resulted only in a 60% yield (c.f. 93% quoted) at best, and was difficult to achieve consistently. By employing diphenyl and using a bunsen burner as the heat source, yields in excess of 90% were attained. Diphenyl was removed from the product far more efficiently than diphenyl ether, especially when triturated in hot toluene.

ii) Hydrolysis: This proceeds in near quantitative yield (c.f. 83%) if the 3,8-dicarbethoxy-4,7-dihydroxy-1,10-phenanthroline (**L11**) is first refluxed in methanol and a 5% potassium hydroxide solution is added dropwise over a period of time (typically 30 minutes). The hydrolysis solution is reported to attain a red colouration. This not observed.

It was deemed interesting to evaluate the effect of heavy atom substitution to the luminescence properties of the ruthenium complexes. Hence, **L4** was smoothly converted to the bis bromo derivative, **L6** using phosphorous oxybromide. Despite the high purity claimed for the latter by the manufacturer, distillation to yield the crystal clear reagent (60%) was necessary in order to achieve high yields.

Upon achieving synthesis of 4,7-dichloro-1,10-phenanthroline attempts were made to displace the halogens with a variety of aliphatic and aromatic amines. Despite the rigorous exclusion of both moisture and oxygen, mild

conditions resulted in the the recovery of starting material and severe conditions caused extensive decomposition.

Scheme 3.2 II

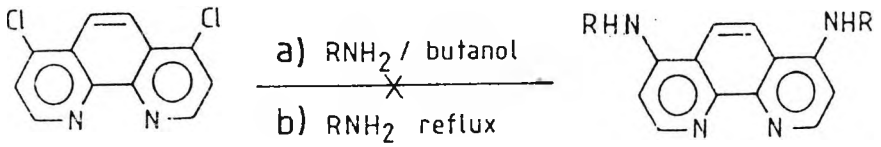

The complicated and inseparable mixtures so obtained were seen as testament to the reactivity of the 5,6-(carbon-carbon) "double bond". As expected, no Grignard reagent could be formed (lack of reactivity, plus complex formation).

An alternative route to extending functionalisation at the 4,7- positions was, therefore sought.

Scheme 3.2 III

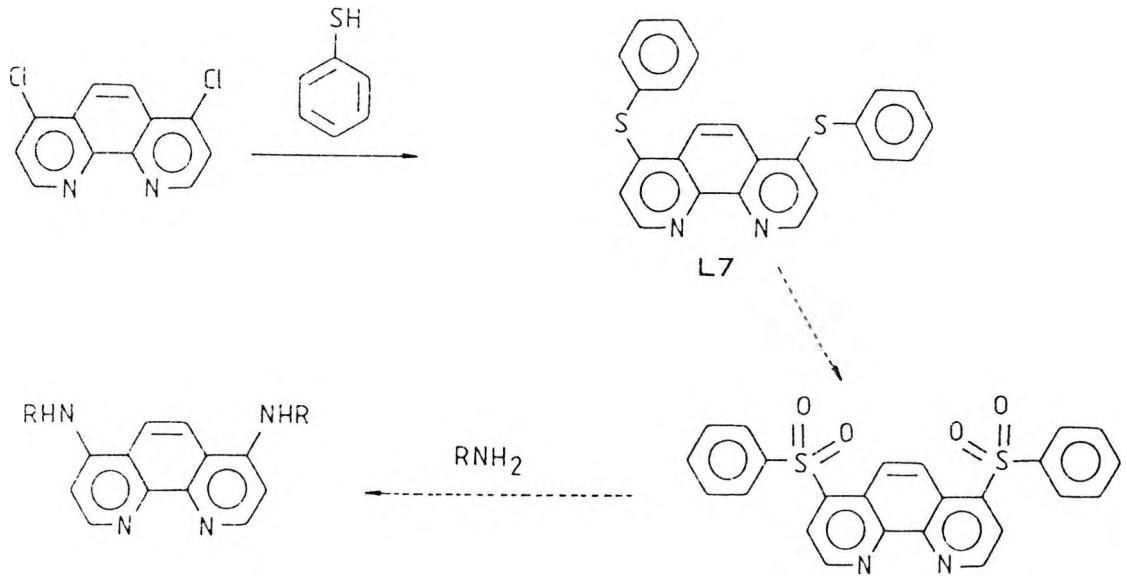

Cook *et al* [39] chose a route in the synthesis of analogues of 4-amino-1,10-phenanthroline (L7) employing

thiophenol (Scheme 3.2.III illustrates this approach in our system). Attempts to oxidise selectively to the sulphone failed. Whilst it's presence (the sulphone) could be inferred from ^{1}H NMR of the reaction mixture (appearance of a doublet at ~ 9 δ) yield was poor and purification was but a dream!

With these results, derivatisation in this series was thus planned to progress through 3,8-decarboxy-4,7-dihydroxy-1,10-phenanthroline (**L11**). However, as a result of solubility problems, and the known quenching properties of the 4,7-*bis* hydroxy function, it was necessary to functionalise this ligand further. Scheme 3.3 shows how the 3,8-dicarbethoxy derivative **L10** was converted to the functionalised 4,7-dichloro species **L12** and O-alkylated to give **L13**.

Scheme 3.3

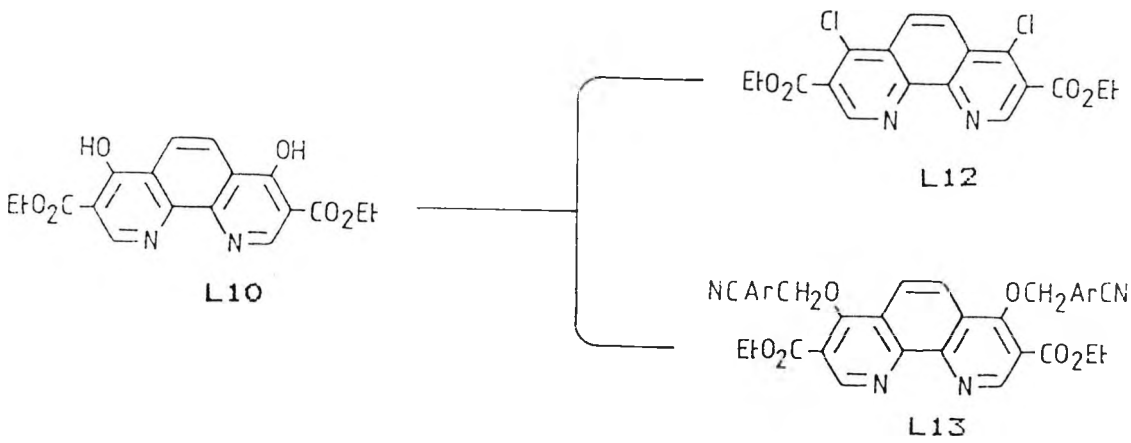

Proton NMR work on 5,6- substituted phenanthrolines[26], and our own NMR work on complexes containing **L2** and **L3** indicated some excitng perturbations to the ring electronic system. Conventional wisdom has it that only substitution at

the 4,7- postions in phenanthroline dramatically alters the properties of ruthenium complexes[1,2] of these ligands.

In order to further study the effects of substitution at these positions (5,6-) in ruthenium complexes, it was decided to place aza substituents here. First by placing an aza bridge in the phenanthroline skeleton **L14**, having 5,6-substituents (**L30** and **L31**) and generating the triazaphenanthroline **L28**.

Hence, 2-chloro-3-nitropyridine was coupled by Ullmann "condensation" (Scheme 3.4)[27], giving 3,3-dinitro-2,2-bipyridyl (**L15**). Mild reduction of this compound with aqueous sodium sulphide resulted in the desired 4,5,9,10-tetra-azaphenanthroline (**L14**).

Scheme 3.4

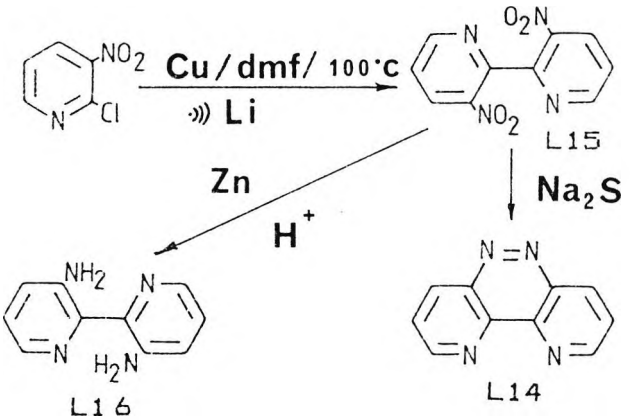

In our hands, Ullmann coupling to **L15** proceeded very poorly (average yield 12%; c.f. a reported 77%). Given the interest in sonochemistry of the group, this reaction was repeated using this technique. Having located a suitable energy maximum within the sono-bath (perforation of aluminium

foil), powdered lithium in dry dioxan (stored over sodium wire) was sonicated for six hours in a thin-bottomed conical flask with an equimolar amount of the 2-chloro-3-nitropyridine. With the reaction proceeding under a nitrogen atmosphere, a 46% yield of **L15** was isolated. The major side-product of this reaction appeared to be 3-nitropyridine (as monitored on the NMR coordinate). Work up was found to be uncomplicated.

Condensation of suitable *o*- phenylenediamine derivatives with **L21** (Scheme 3.5.1) lead to derivatives of the dipyrido [3, 2-a : 2',3'-c] phenazine system **L30** and **L31**.

Scheme 3.5.1

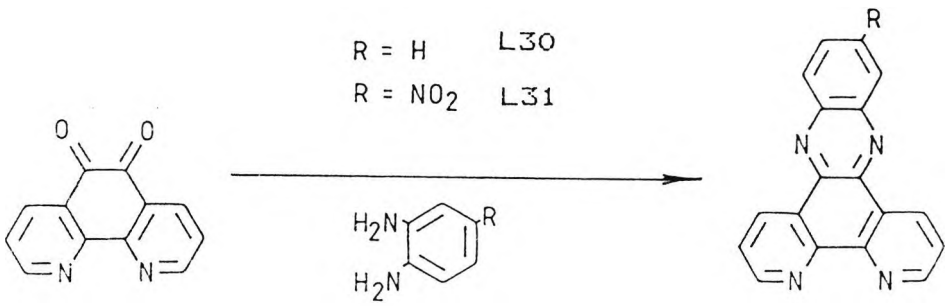

The intermediate system between these two skeleton types was achieved by converting **L20** to it's oxime, and then subjecting this to a Beckmann rearrangement (Scheme 3.5.2).

Scheme 3.5.2

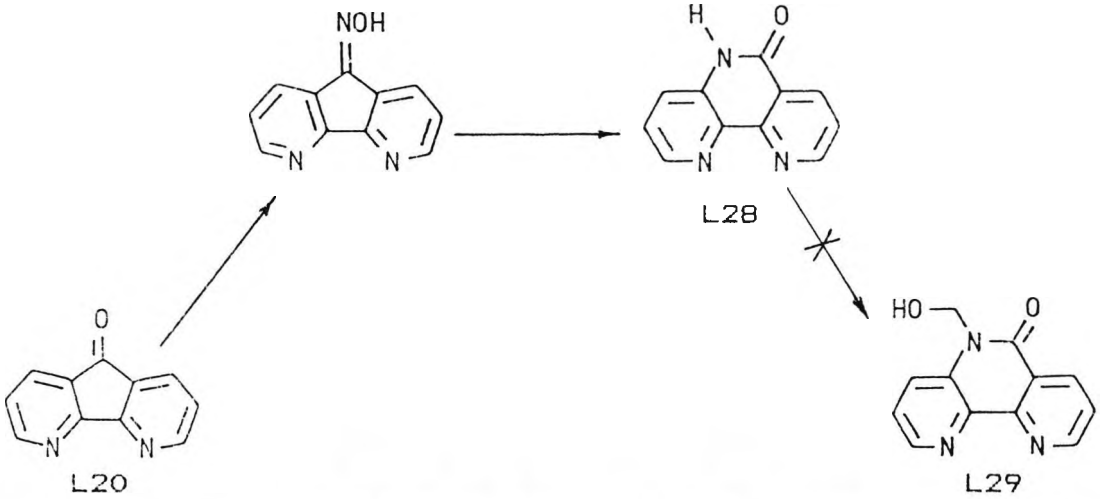

An attempt was made to trap the lactam tautomer of 4,5,9-triaza-10-hydroxyphenanthroline **L28**, however, infra-red data on **L28** did not lend much credence to such a move (i.e. band at 1725 cm^{-1} weak). Despite subjecting **L28** to a number of forcing conditions, **L29** could not be isolated.

Functionalisation through the 2- position of phenanthroline opened further pathways to a series of reactive probes. However, substituents at this position impose a certain steric constraint upon coordination to the octahedral ruthenium ion, which we felt should modulate the excited state properties of the complex.

Following Chandler *et al* [39], 2,9-dimethyl-1,10-phenanthroline (Scheme 3.6.1) was oxidised by treament with selenium dioxide to the 2,9-dicarboxaldehyde **L22**. The procedure documented results in the product still being contaminated with selenium dioxide. Repeated recrystallisation of the product with THF was necesary to achieve a pure product.

Scheme 3.6.1

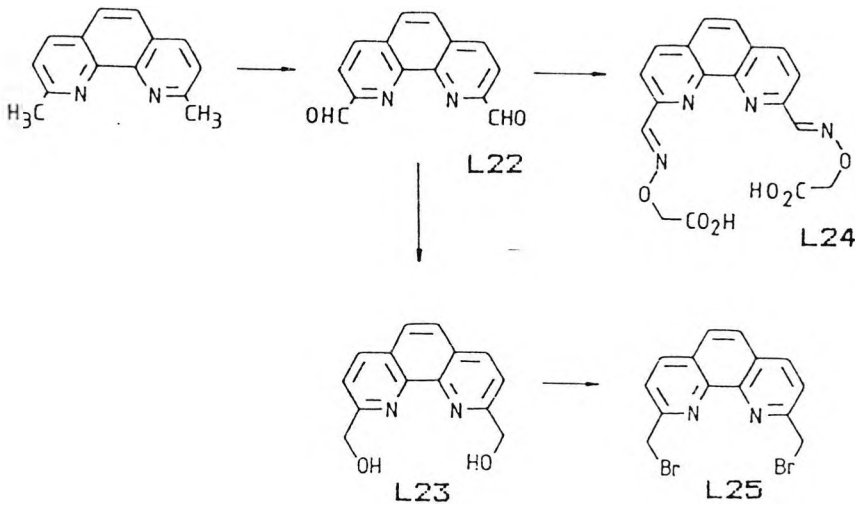

Derivatisation of **L22** was by condensation with carboxymethonylamine[27] to give the Schiff base 1,10-phenanthroline-2,9-dicarboxaldehyde *bis* (O-carboxymethyl) oxime, **L24.** Attempts to reduce this material to the *bis* (N-aryl-O-alkylcarboxy hydroxylamine) did not appear to work. This reaction used the borane/THF reducing system, and, whilst complete characterisation of the product was <u>not</u> achieved, reaction appeared to proceed to yield the corresponding phenanthroline diamine.

Further functionality was added by reducing **L22** to the *bis* (hydroxymethyl) compound, **L23**, which was brominated giving 2,9-*bis* (bromomethyl)-1,10-phenanthroline, **L25.** Direct bromination of 2,9-dimethyl-1,10-phenanthroline, under a variety of free radical conditions, with N-bromosuccinimide proved unsuccessful. Evidence for the formation of a bromo-derivative was provided by use of ^{1}H NMR to monitor progress along the reaction coordinate. By this method, it was clearly evident that the required product was a minor component

(~2%).

Scheme 3.6.2

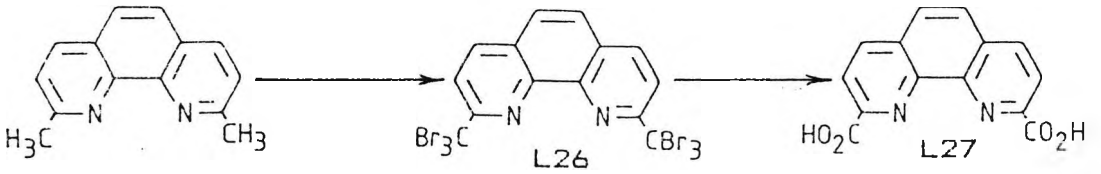

Treatment of 2,9-dimethyl-1,10-phenanthroline with bromine in acetic acid gave the *bis* (tribromo⟷methyl) **L26** product in 78% yield (Scheme 3.6.2). Following hydrolysis with 10% sulphuric acid **L27** was obtained in an overall 40% yield. As direct oxidation of the dimethyl starting material had provided some difficulty for other members of the group, it was hoped that this would provide a valuable alternative route.

Complexes derived from commercially available bathophenanthroline upon conjugation to proteins were giving rise to non-self consistent side reactions. These dark process-side reactions (Section 6) were attributed to over functionalisation of the probe molecule (**C8**). This hypothesis was tested by synthesis of active substituents in the 4-position on the phenanthroline ring (Scheme 3.7).

Scheme 3.7

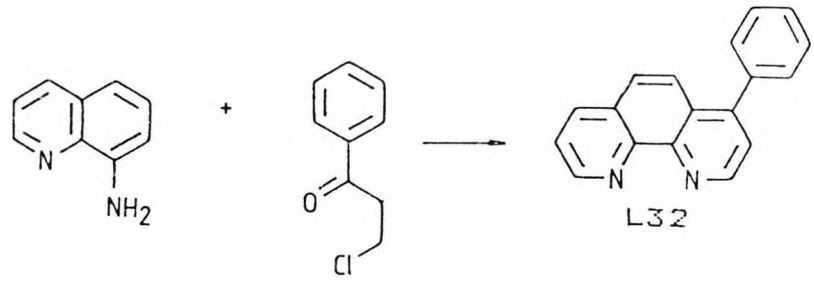

Thus, the readily functionalised phenyl substituent was introduced by means of Skraup's reaction from 8-aminoquinoline and 3-chloropropiophenone[30,31]. The product (**L32**), was only once isolated as a solid, despite repeated purification by column chromotography. We are grateful to Mr. P. Crick for an analytical sample. In improving the synthesis, he has achieved a melting point 11°C higher than the literature. Complexation of our crude material proceeded smoothly to give a pure ruthenium complex, and it was in this form that functionality was introduced (see Section 3.4).

Scheme 3.8

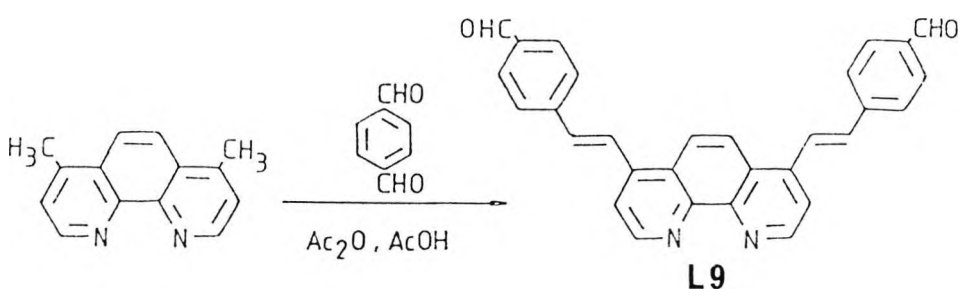

It was also found that simple condensation at the methyl substituents in 4,7-dimethyl-1,10-phenanthroline (Scheme 3.8) could be achieved. Using an acetic acid/acetic anhydride couple as a dehydrating agent[xx], terephthaldehyde in 1.6 fold excess reacted to yield 4,7-*bis* [2-(4-formylphenyl)ethenyl]-1,10-phenanthroline (**L9**).

Molecules required to give the ligand field for luminescent binuclear complexes are described in Scheme 3.9. The action of hydrazine on 2-cyanopyridine[xx] yields the interesting dihydro derivative **L18**. Oxidizing this with

Scheme 3.9

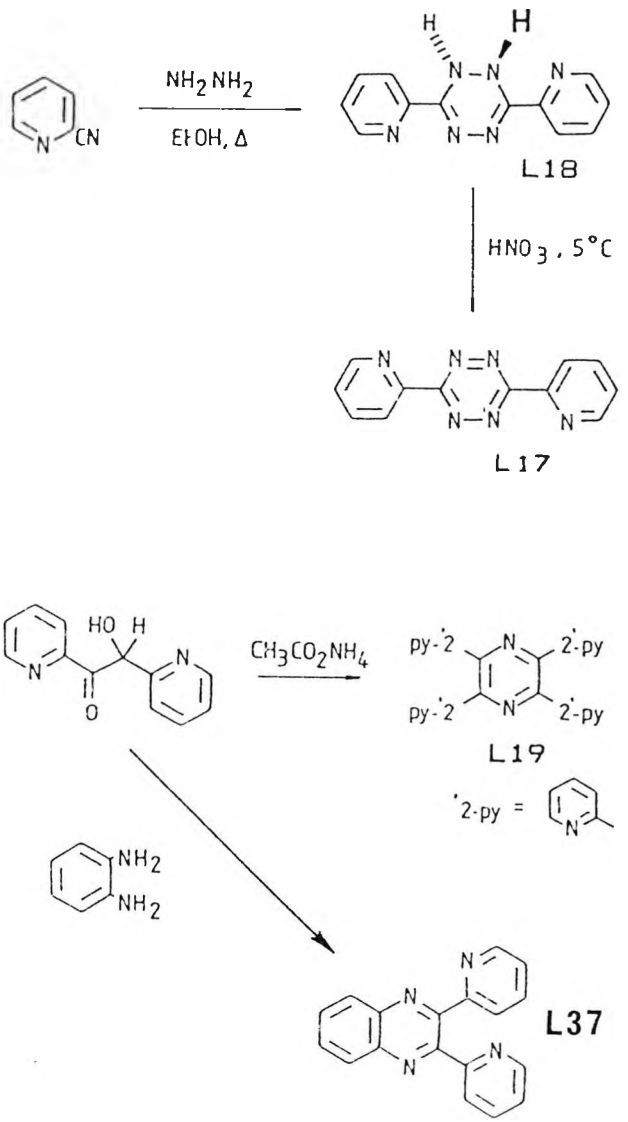

nitric acid affords 2,6-bis (2'-pyridyl)-1,2,4,5-tetrazine (L17). It is worth noting that this compound exhibits an intense pink colour in the solid state. Condensation of phenylenediamine and -pyridoin yielded 2,3-dipyridylquinoxaline. Included here is the synthesis of 2,3,5,6-tetrakis(2'-pyridyl)-pyrazine[34](L19). We required this ligand to further expand our knowledge of the luminescence requirements of polyazacavity complexes ruthenium(II).

Scheme 3.10

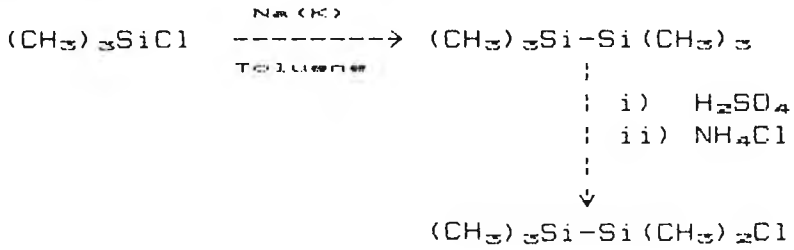

Synthesis of the proposed radical generating substituent is shown in Scheme 3.10. That coupling trimethylchlorosilane by the method of Wilson and Smith[35] (seemingly the preferred route by workers in the field) proceeded in relatively low (half the anticipated) yield was probably a reflection on over cautious handling of the reagents. Conversion to the activated pentamethylchlorodisilane[36] appeared to proceed in quantitative yield as monitored by NMR). However, isolation by the published method was not possible due to extensive decomposition. Simply subjecting the reaction mixture to vacuum distillation yielded a crude product free of concentrated sulphuric acid, which was further purified by fractionation.

3.3 Complex Formation

The most common route to $Ru(bipy)_2Cl_2$ described in the literature is a direct reaction of $RuCl_3.x\ H_2O$ and 2,2'-bipyridine in dimethylformamide. In the method of Whitten and co-workers[37], the mixture is concentrated after three hours, treated with acetone, the residue is then suspended in aqueous ethanol and heated with an excess of lithium chloride. The ethanol is then removed and the residue recrystallised from water.

In the synthesis of $Ru(phen)_2Cl_2$, we adapted the procedure of Meyer and co-workers[38]. Here, the lithium chloride is added with the other reagents to the DMF: yield of the desired intermediate was always greater than 60%. It should be noted that this compound should be stored with some care as degradation appears to occur with repeated exposure to air and fluorescent strip lights.

The complexes $[Ru(phen)_2L]^{2+}$ and $[(phen)_2RuLRu(phen)_2]^{4+}$ can be prepared by direct reaction of the free ligand, L, with *cis*- $Ru(phen)_2Cl_2$. The conditions previously employed by "this group" to effect substitution at the metal employed refluxing ethanol, DMF or water as the reaction medium. This method can give good yields (in our hands never better than 60%, and frequently closer to 25%), but is wasteful of ligand and at times prone to fail altogether! The lengthy synthetic procedures for the preparation of substituted derivatives of phenanthroline argue against this as a good synthetic route.

An alternative route involving an intermediate diacetone

complex (produced when the co-ordinated chlorine is precipitated as silver chloride) has been explored[39] by the route shown in Scheme 3.11.

Scheme 3.11

i) *cis*- $Ru(phen)_2Cl_2 + 2\ AgO_3SCF_3 \xrightarrow{Acetone}$

$$cis\text{-}\ Ru(phen)_2(CH_3COCH_3)_2^{2+} + AgCl_{(s)} + 2CF_3SO_3^-$$

ii) *cis*- $Ru(phen)_2(CH_3COCH_3)_2^{2+} + L \longrightarrow$

$$[Ru(phen)_2L]^{2+} + 2CH_3COCH_3$$

This route, while appearing more efficient, introduces it's own problems.

Sargeson *et al* [40], succeeded in synthesising cobalt(II) amine complexes of the labile unidentate trifluoromethane sulphonate anion ($CF_3SO_3^-$). Their work was repeated by us, but using $Ru(phen)_2Cl_2$, to yield the triflate complex quantitatively. Not only is this complex easy to handle and store, but co-ordination reactions proceed smoothly and rapidly, especially from anhydrous acetone. Typical times to co-ordination were three hours, whereas two-day refluxes were the norm for the original route. A brief survey of the literature suggests this extension to triflato ligand chemistry to be novel.

Scheme 3.12

$RuCl_3.3H_2O \xrightarrow[DMF]{Phen/LiCl} Ru(phen)_2Cl_2$ (purple)

$Ru(phen)_2Cl_2 \xrightarrow{CF_3SO_3H/\ N_2\ bubbled} Ru(phen)_2(OSO_2CF_3)_2$ (bright red) **(CTf)**

$Ru(phen)_2(OSO_2CF_3)_2 \xrightarrow{L17} [(phen)_2Ru\ L17\ Ru(phen)_2]$ (dark green) **(C28)**

The complex described in Scheme 3.12 was originally synthesised by us using the "ethanol substitution" method, and brought home the importance of being sure of the purity of products; recrystallisation alone rarely yielded pure materials. This lead to the introduction of the technique of molecular exclusion chromatography[12]. This represents a very costly procedure, and it, too is not without disadvantages. For example, Figure 3.1 displays the 360 MHz ^1H N.M.R. of **C28**; (a) prepared from the ruthenium(II)dichloride and separated on sephadex LH20 (acetonitrile eluent) in approximately 40% yield; and (b) derived from the triflate intermediate and chromatographed on alumina (MeOH : H_2O : $CHCl_3$ :: 4 : 0.5 : 6). Not only is it obvious that the latter route gives a cleaner product, the isolated yield of **C28** was 84%.

Subsequently, all co-ordination reactions were performed under these conditions. Where ligand solubility dictated, however, glycerol was used as the reaction solvent. Employing a minimum volume eases work-up, and reduces reaction time.

All complexes, with the exception of **C7**, were isolated as the hexafluorophosphate salts. This large counter anion removes the dangers associated with the use of perchlorate ion, and gives complexes with high covalent character. This then allows complex isolation and purification (as previously illustrated) by conventional organic chemistry techniques.

The complex **C7** was isolated simply by altering the dielectric constant of the medium. Thus quenching the

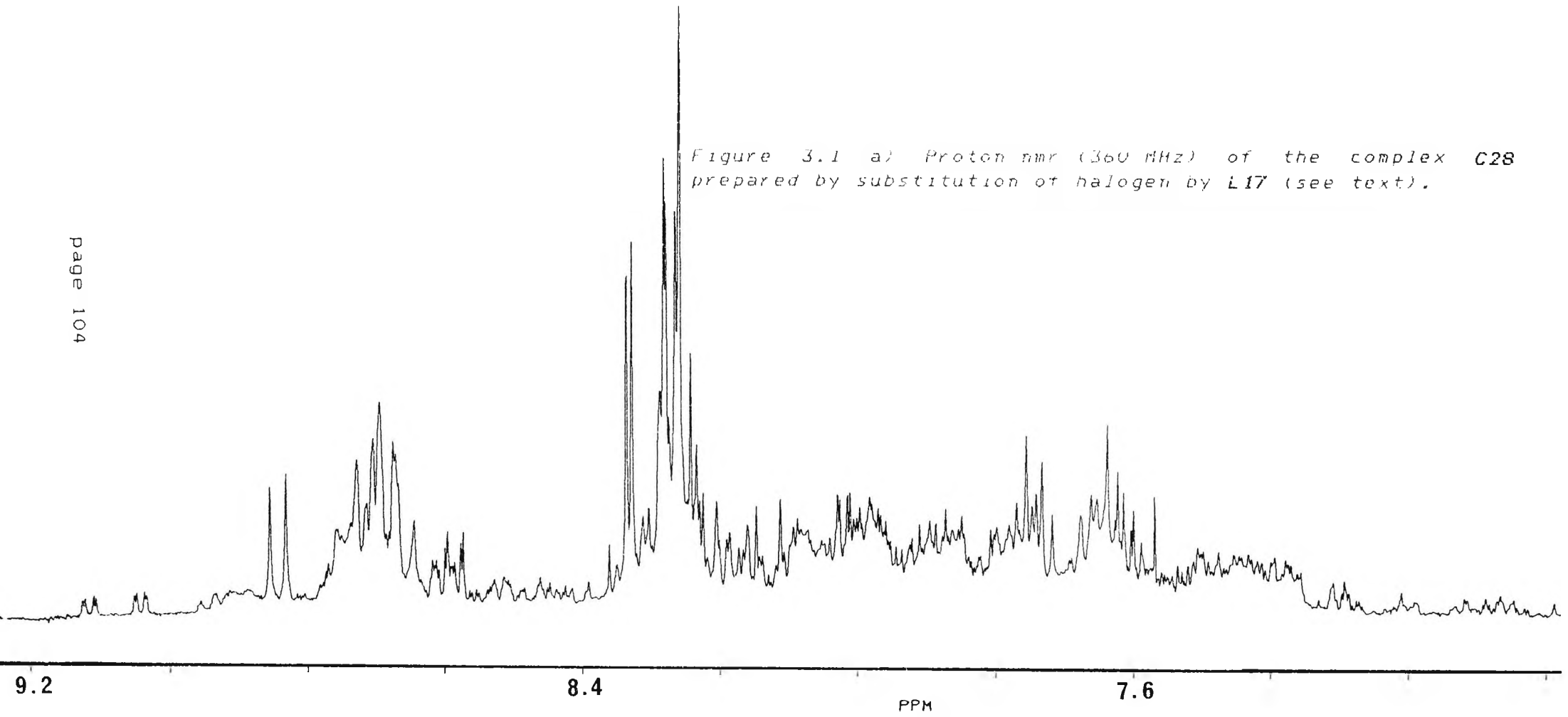

Figure 3.1 a) Proton nmr (360 MHz) of the complex ***C28*** *prepared by substitution of halogen by* ***L17*** *(see text).*

Figure 3.1 b) Proton nmr (360 MHz) of the complex ***C28*** *prepared using the triflate intermediate* ***CTf.***

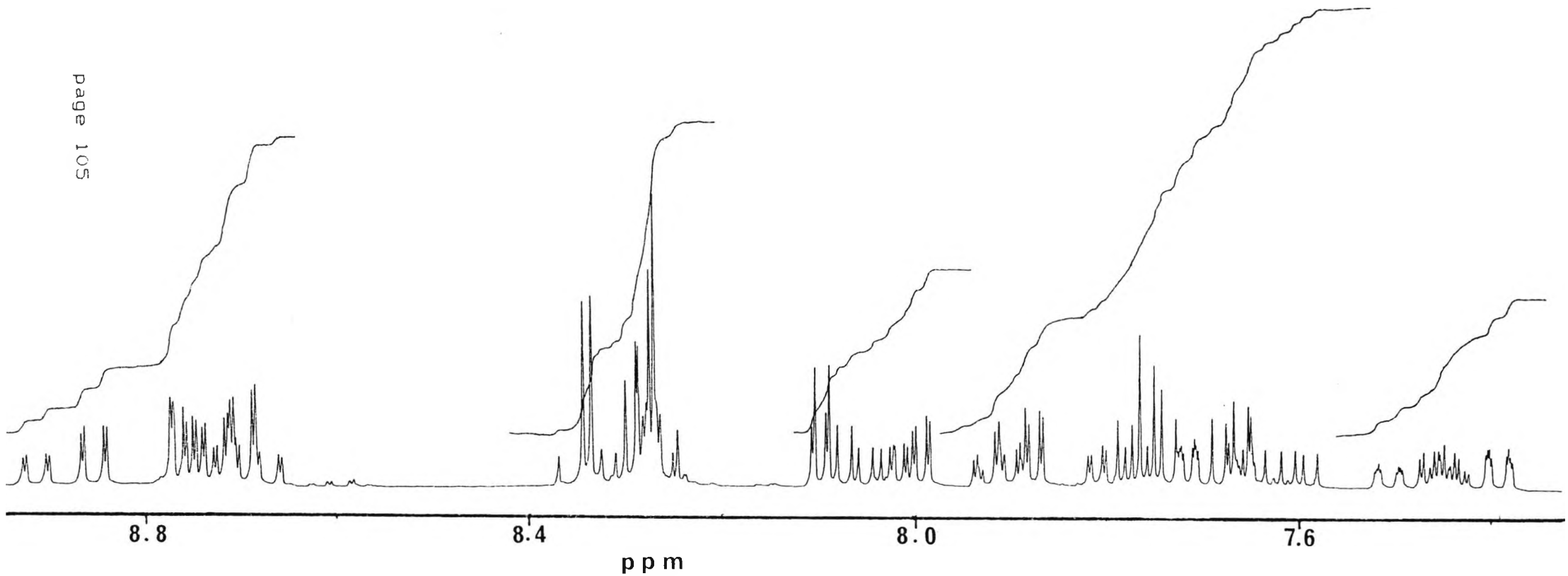

reaction mixture for theillustrated in Scheme 3.13 with a large volume of acetone, results in a crystalline deposit of C7.

Scheme 3.13

$$Ru(phen)_2(OSO_2CF_3)_2 \xrightarrow[Na_2BPDS]{glycerol} Ru(phen)_2BPDS$$
(CTf) (C7)

Na_2BPDS= bathophenanthroline disulphonic acid, disodium salt:

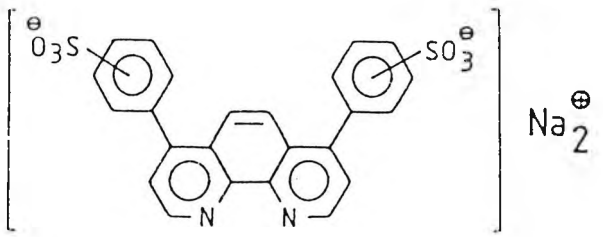

It appeared that the sulphonate group was a sufficiently strong acid to form the counter ion of the complex.

3.4 Complex Modification

The chemical "inertness" of octahedral, *tris* (aza-bidentate) ruthenium(II) complexes to ligand substitution opens another avenue to functionalised derivatives. We have keenly exploited this property, especially in situations such as:-

i) where it has been difficult to ensure ligand purity [as in the case of commercially available bathphenanthroline disulphonic acid disodium salt (Aldrich)-Na_2bpdp and our own L32.

ii) where a ligand insolubility has hampered it's reactivity e.g. L4.

iii) where electronic considerations in a ligand have made it difficult to target reactivity, e.g. L3.

In each of these cases, co-ordination of the ligand concerned to form a poly-azacavity, co-ordinately saturated ruthenium complex, lead to ready transformation to the desired products.

Thus, 5-amino-1,10-phenanthroline, L3, could not be 5-N-derivatised under a variety of conditions employing numerous reagents (Scheme 3.14). However, upon binding to ruthenium, rapid smooth conversion to the acetate was achieved. The freeing of the amine lone pair was attributed to efficient π-electron back donation from the metal.

Scheme 3.14

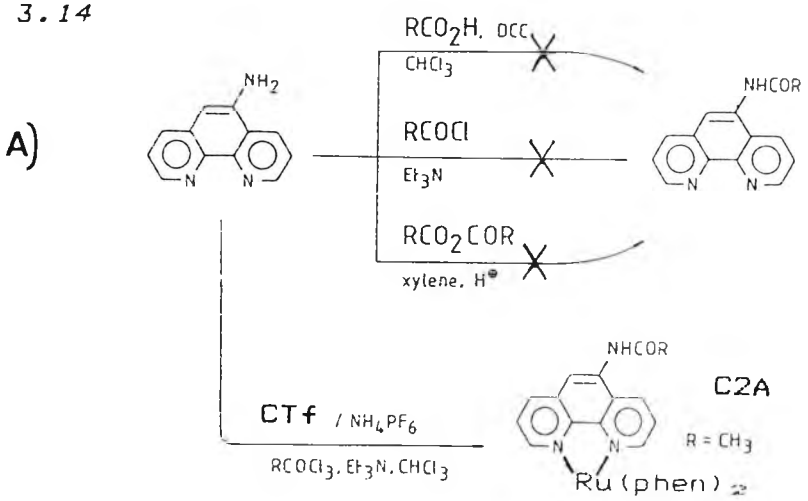

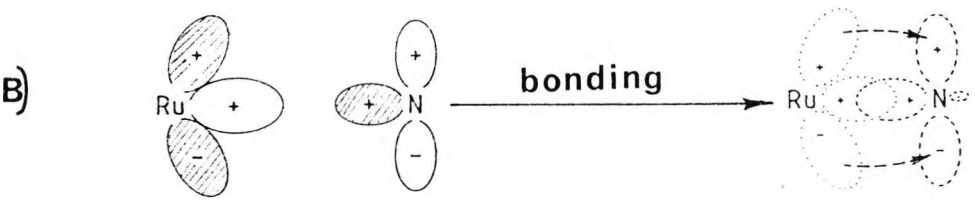

It was also found that 100% conversion to amides could

Ru ≡ [Ru(phen)$_3$]$^{2+}$ mfx,y Ru ≡ Ru functionalised at one phen in position x,y of that ring.

tfx,y Ru ≡ Ru functionalised at all three phens in positions x,y on each ring.

a)

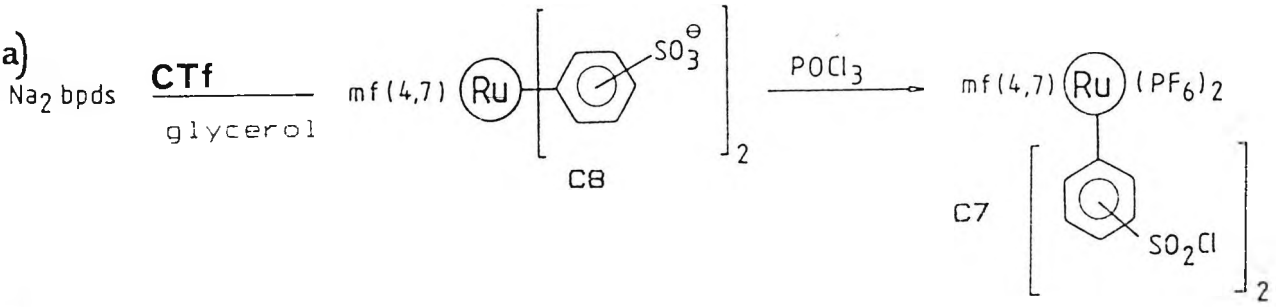

b)

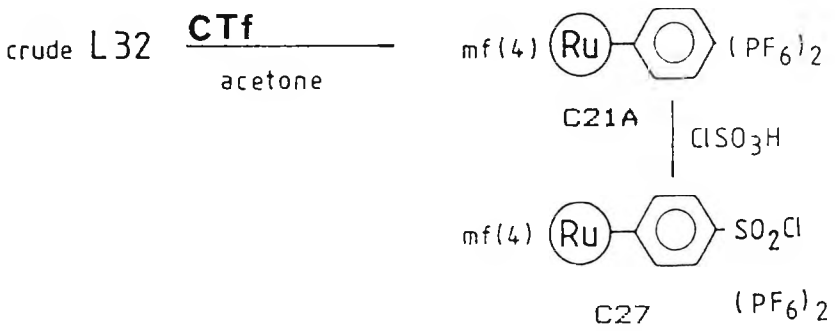

c)

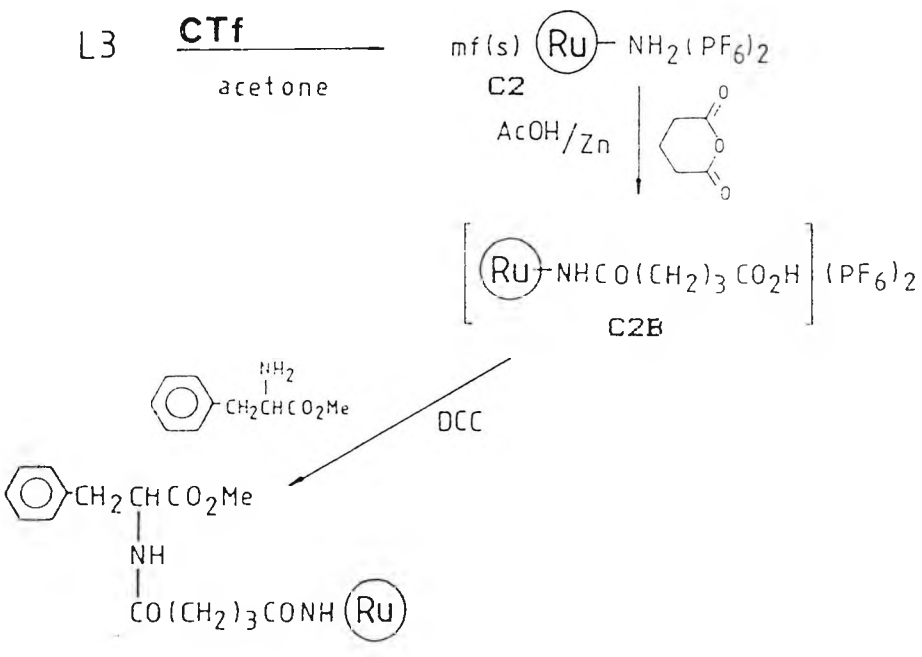

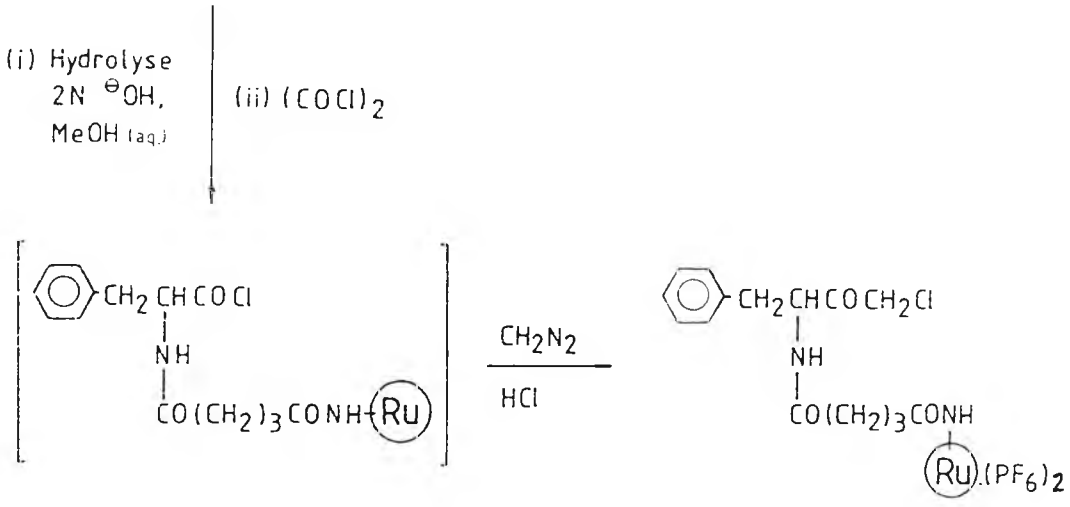
(i) Hydrolyse
2N ⊖OH,
MeOH (aq.)
(ii) (COCl)2
CH2CHCOCl
NH
CO(CH2)3CONH
Ru
CH2N2
HCl
CH2CHCOCH2Cl
(PF6)2

d)

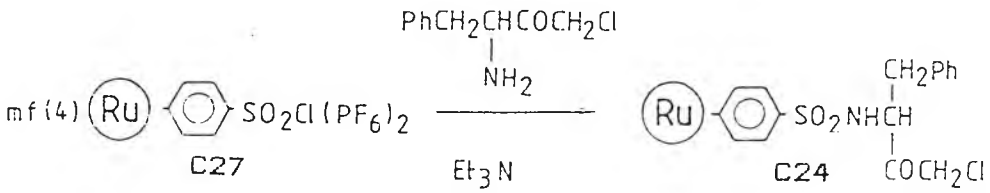
PhCH2CHCOCH2Cl
NH2
mf(4)
Ru
SO2Cl(PF6)2
C27
Et3N
SO2NHCH
CH2Ph
COCH2Cl
C24

e)

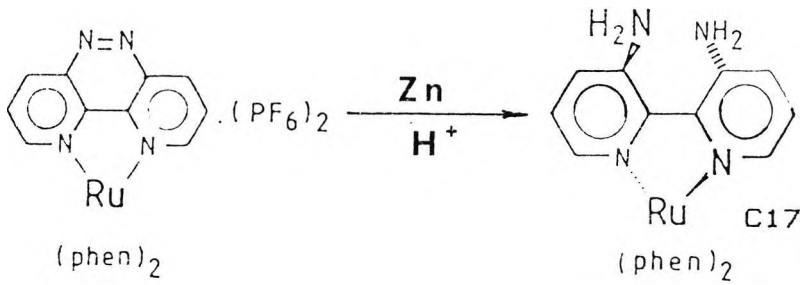
N=N
N
Ru
(phen)2
(PF6)2
Zn
H+
H2N
NH2
C17

be obtained merely by stirring the complex with the desired acid anhydride in acetic acid, in the presence of finely divided zinc. In the absence of zinc, significant quantities of starting material remained.

The 4,7-dihydroxyphenanthroline, **L4**, proved to be practically insoluble in almost every solvent. Ligation to ruthenium and isolation of the resulting complex as the hexafluorophosphate salt, allowed ready O-alkylation in acetone.

Reaction of **C3** with pentamethyldisilyl chloride gave an extremely unstable material which was not identified (non luminescent derivative decomposed rapidly to give luminescent products).

Coordination of Na$_2$bpds allowed ready conversion to the bis(sulphonyl chloride) complex **C8**, by heating **C7** in phosphorous oxychloride under reflux. Isolation of solid **C8** was achieved by precipitation from an ice cold dilute hexafluorophosphoric acid solution. The required product being easily separated from the starting material by virtue of the organic solvent soluble nature of **C8**.

Despite numerous attempts to purify the ligand 4-phenylphenanthroline, **L32**, we could not isolate the "white crystalline" material described in the literature. On obtaining good NMR and mass spectral data, we coordinated this to ruthenium. Subjecting the product of the reaction to chromatography, yielded a pure complex (**C21A**). Sulphonation of this material with chlorosulphonic acid[41] appeared to result in yield of purely the <u>para</u>-sulphonyl

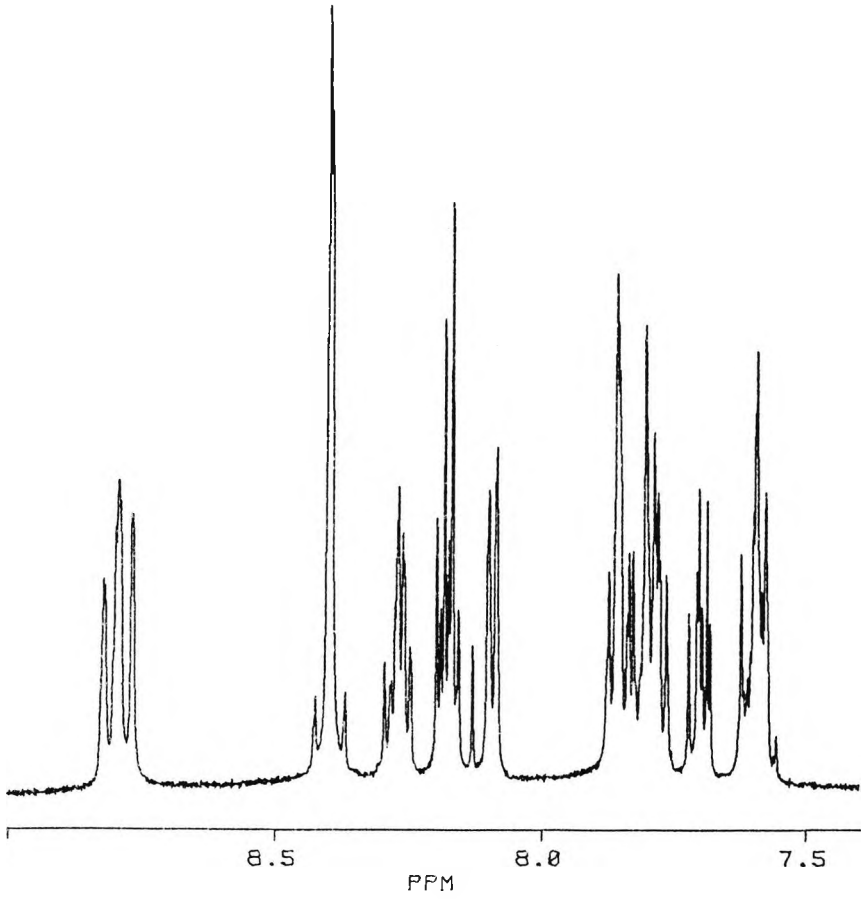

Figure 3.2 Proton nmr (360 MHz) of complex **C7** *with phase sensitive (symmetrised) cosy plot.*

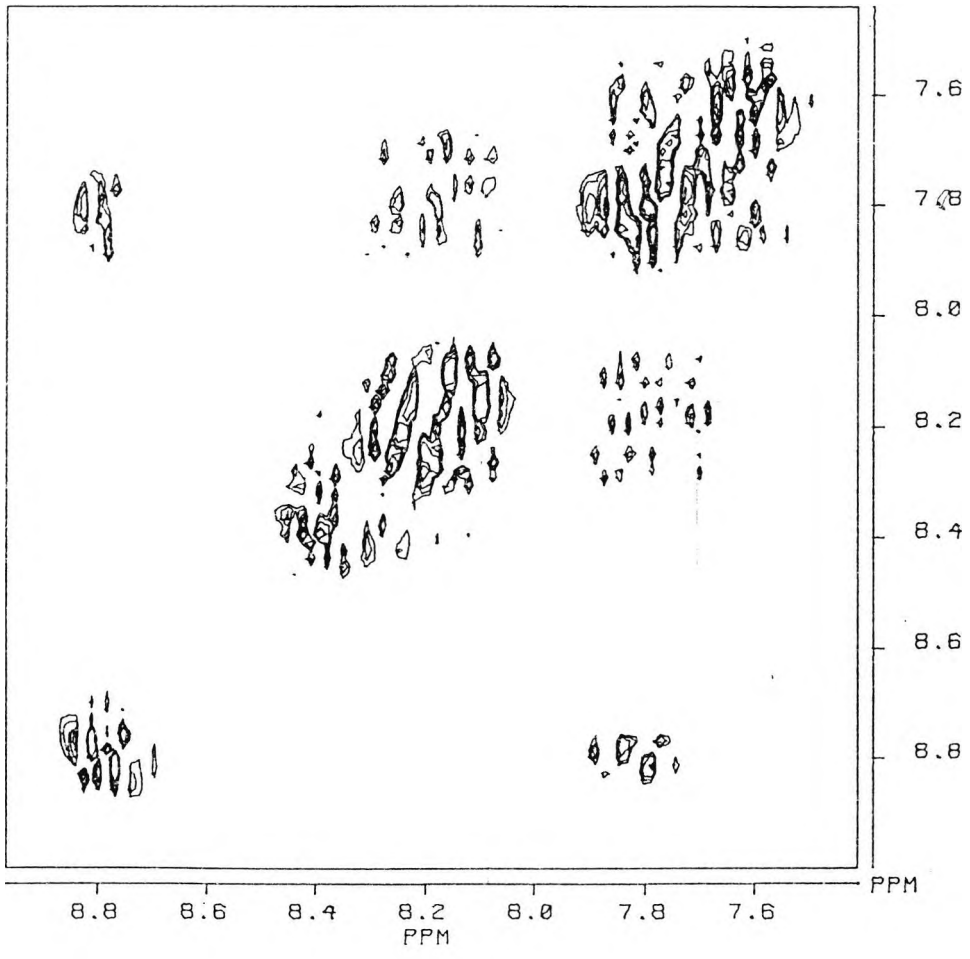

chloride isomer (NMR) (C27).

This was not the case with respect to C7. Figure 3.2 presents the 360 ^{1}H NMR of this complex. Despite repeated chromatography to separate the various substitutional isomers (and managing to obtain beautiful red-needle crystals), clearly something is amiss. Derivatives of the sulphonyl chloride C8 also could not be unambiguously identified with respect to their isomeric purity.

Synthesis of probe complexes for the affinity labelling of chymotrypsin were initially derived from C2. Thus, amide formation using glutaric anhydride followed by active ester coupling by the dicyclohexylcarbodiimide method to L-phenylalanine methyl ester gave the required framework. The chloromethyl ketone functionality was introduced by first, hydrolysis of the ester, then chlorination by reflux in oxalyl chloride and finally reaction with diazomethane in the presence of a stream of hydrogen chloride gas. The desired material was obtained with no detected racemisatation (NMR).

Subsequent discovery that L-phenylalanine chloromethyl ketone was commercially available (Sigma), lead to a sample of this being reacted with C27 to give C24. This material, having been synthesised on a larger scale, was investigated extensively in our labelling studies.

3.5 Competitive Scene and Comments

It was considered useful to develop some multi-electron transfer agents. By comparison with the μ-pyrazine mixed

valence compounds[43,44], photo-electron transfer from a 2^{+}-$2^{\pm}$ -bridged binuclear species should result in significant alteration of the systems visible absorption spectra. This could give us a probe by which further direct evidence of the nature of the photo-reactions occurring can be assigned. As work progressed, a literature survey revealed that we would not be the first to prepare a luminescent binuclear ruthenium complex.

Two earlier papers are of particular note; the first is the saturated-bridge complexes of Tinnemans *et al* [37]. A series of simple open chain ligands containing two phenanthroline moieties were described (Table 3.2), as well as *bis* (disubstituted) complexes $[(bipy)_2RuLRu(bipy_2)]^{4+}$ prepared by reaction of the free ligand, L, with <u>*cis*</u> - $(bipy)_2RuCl_2$.

Table 3.2 PREPARED STARTING MATERIALS.

phen = 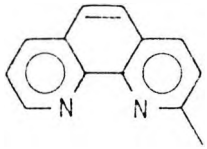

1. phen - OCH_3

phen - $(OCH_2CH_2)_nO$ - phen

2. n = 2

3. n = 3

4. n = 4

5. $(phen - OCH_2CH_2)_3N$

6. phen - CONH - nC_3H_7

phenCONHCH$_2$CH$_2$(OCH$_2$CH$_2$)$_n$NHCOphen

7. n = 1

8. n = 2

phenCONH—(CH$_2$)$_n$NHCOphen

9. n = 1

10. n = 2

These flexible link species do not appear sufficiently widely separated to prevent quenching by energy transfer. However, in the text these compounds are reported as being "highly fluorescent when irradiated in the visible", but no luminescence data ~~is~~ are given.

Closer to home was the dimeric complex synthesised by Baker *et al* [49]. In this, what appears to be the first documented luminescent bimetallic ruthenium complex, the metal centres are bridged by a polydentate unsaturated ligand (Figure 3.3). That this complex is luminescent, when the bridged dimer (bipy)$_2$Ru(2,2'-bipyrimidine)Ru(bipy)$_2^{4+}$ is not (Figure 3.4) is argued on the basis of decreased interaction between the metal ions. Thus, the minimal interaction in (bipy)$_2$Ru(bpp)Ru(bipy)$_2^{4+}$ [dpp = 2,3-*bis* (2-pyrimidyl)pyrazine], is attributed to steric coordination octahedra about each Ru(II) ion from being coplanar. This implies localisation of the excited electron in the pyridyl part of the dpp ligand. It follows that the observed luminescence is simply that from the probability proportion of this transition (and similarity with the two bipyridines

in the coordination sphere), with respect to the thermodynamically more favoured (and more efficiently deactivated) localisation onto the bridging pyrazine part.

Figure 3.3

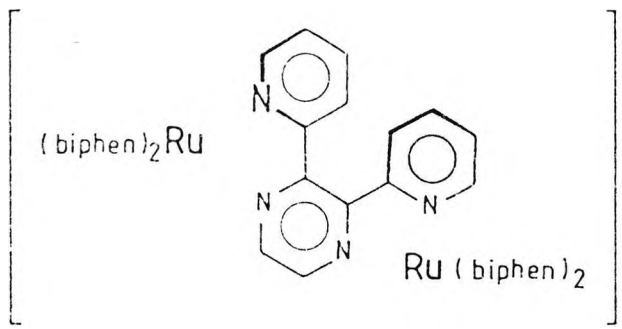

Luminescent bimetallic complex[45]

Figure 3.4

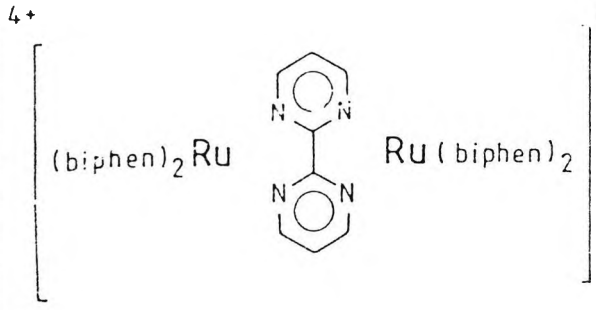

Non-luminescent bimetallic complex[46,47,48]

Baker *et al* [47] published further in late 1987 detailing the synthesis of a polydentate "planar bridging ligand" bimetallic ruthenium complex, using 4',7'-phenanthroline-5',6',5,6-pyrazine (ppz). He states that since the complex is luminescent, it "clearly establishes that steric factors involving the bridging ligand are of minor importance". We feel, from the examination of molecular models, that the ppz ligand is more rigidly puckered than dpp (Figure 3.5), and vibrational relaxation allowing orbital coupling would require substantial concerted atomic motion. This considered, we feel our previous discussion more pertinent, and the arguments in this later paper represent an over complication of the luminescence description of these species.

Figure 3.5

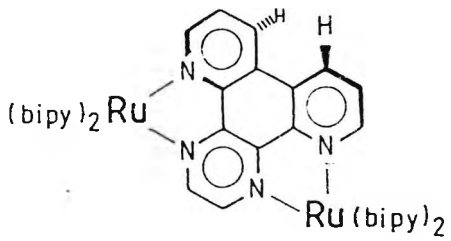

As the pure dimeric complex **C28** was being isolated in late 1987, it was discovered Kaim *et al* [50] had synthesised binuclear complexes with **L17** with low spin d^6 metal-complex fragments. These included $[Ru(bipy)_2]^{2+}$! It is interesting to note the small amount of analytical data he gives (he comments on CHN data only) on this compound. It is described as being obtained as the analytically pure <u>tetrahydrate</u> in 23% yield[50], by direct reaction of *cis* $Ru(bipy)_2Cl_2$ with **L17** (2:1), and isolation as the tetrabis(hexafluorophosphate) salt, initially with λ_{max}=688nm[50] and then with λ_{max}=755 and 390nm[51].

In light of these publications, it was felt that our contribution to this field would be reduced. However, it was hoped to coordinate indium to **L17** and see if energy transfer could be observed. This work was never undertaken as a result of delayed potassium hexachloroiridate(IV) delivery by Aldrich (six months!)

Scheme 3.18 illustrates our approach to the synthesis of a DIAS, wherein the spacer group was a conformationally restricted polyamide. The complex **C4** had only just been

synthesised when the work of Schanz and Sauer[95] was published.

Scheme 3.18

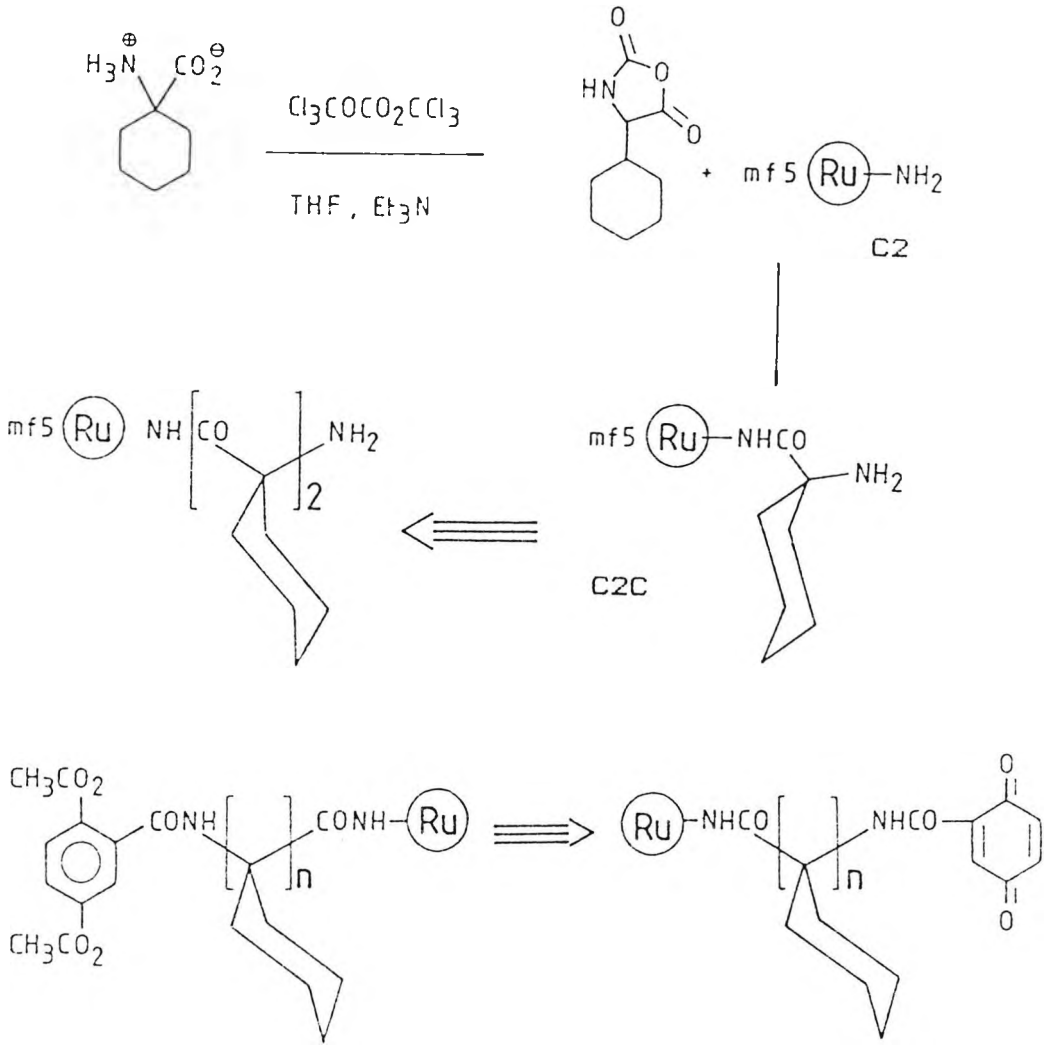

Their strategy employed L-proline oligomers as the bridging ligand between *bis* (2,2'-bipyridyl)(5-amino-1,10-phenanthroline) ruthenium(II) and benzoquinone. Whilst showing that the electron transfer rate decreased with increased with increasing chain length their decay data were complicated by the existence of multiple conformational isomers. Isied *et al* [95] showed that oligoprolines are

stabilised to single extended conformations in aqueous solution. However, when Schanze and Sauer placed their DIAS in protic solvent, they observed effects consistent with the reduction of the quinone; apparently by reaction with the solvent.

Whilst investigation of our system was tempting, we were not far enough down the track to investigate associated sidings to make this work worthwhile.

REFERENCES

1. Turro, N.J.; Kavarnos, G.J. Chem. Rev., **86**, 401, 1986.
2. Murov, S.L. Handbook of Photochemistry, Marcel Decker, New York, 1973.
3. Balzani, V.; Bolleta, F.; Gandolfi, M.T.; Maestri, M. Top. Curr. Chem., **75**, 1, 1978.
4. Dietrich-Buchecker, C.O.; Marnst, P.A.; Sauvage, J.-P.; Kirchhoff, J.R.; McMillin, D.R. J. Chem. Soc. Chem. Commun., 513, 1983.
5. Heuer, W.B.; Totten, M.D.; Rodman, G.S.; Herbert, E.J.; Tracy, H.J.; Nagle, J.K. J. Am. Chem. Soc., **106**, 1163, 1984.
6. Nocera, D.G.; Gray, H.B. J. Am. Chem. Soc., **103**, 7349, 1981.
7. Milder, S.J.; Goldbech, R.A.; Kliger, D.S.; Gray, H.B. J. Am. Chem. Soc., **102**, 6761, 1980..
8. Kalyanasundarum, K. Coord. Chem. Rev., **43**, 161, 1982.
9. Burrows, H.D.; Kemp, T.J. Chem. Soc. Rev., 3, 1974.
10. Darwent, J.R.; Douglas, P.; Harriman, A.; Porter, G.; Richoux, M.C. Coord. Chem. Rev., **44**, 83, 1982.
11. Gamache, R.E.; McMillin, D.R.; Marnst, P.A.; Sauvage, J.-P. J. Am. Chem. Soc., **107**, 1141, 1985.
12. Seddon, S.A.; Seddon, K.R. The Chemistry of Ruthenium, Elsevier-Oxford, 1984.
13.. Photochemical Conversion and Storage of Solar Energy., Ed., Connolly, J.S., Academic Press, New York, 1981.
14. Jaris, A.; Balzani, V.; Barigelletti, F.; Campagna, S.;

Belser, P.; von Zelewsky, A. Coord. Chem. Rev., 84, 85, 1988.

15. Joran, A.D.; Leland, B.A.; Felker, P.M.; Zewail, A.H.; Hopfield, J.J.; Dervan, P.B. Nature, 327, 508, 1987.

For a review of the synthesis and properties of the phenanthrolines, see 16. and 17.

16. Wanda, S. Heterocycles., 12, 1207, 1979.

17. Summers, L.A. Adv. Het. Chem., 22, 2, 1978.

18. Nagle, J.K.; Bernstein, J.S.; Young, R.C.; Meyer, T.J. Inorg. Chem., 20, 1760, 1981.

19. Creutz, C. Prog. Inorg. Chem., 30, 1, 1983.

20. Eaton, D.F. Pure Appl. Chem., 56, 1191, 1984.

21. Smith, G.F.; Cagle, F.W. J. Org. Chem., 12, 781, 1947.

22. Dickerson, J.E.; Summers, L.A. Aust. J. Chem., 23, 1023, 1970.

23. Inglett, G.E.; Smith, G.F. J. Am. Chem. Soc., 72, 842, 1950.

24. Snyder, H.R.; Freider, H.E. J. Am. Chem. Soc., 68, 1320,1976.

25. Cook, M.J.; Katritzky, A.R.; Nadji, S. J. Chem. Soc. Perkin II., 1215, 1978.

26. Carman, R.M.; Hall, J.R. Aust. J. Chem., 17, 1354, 1964.

27. Kausktanaporn, S.; MacBride, J.A.H. J. Chem. Soc. Perkin I., 1126, 1978.

28. Chandler, C.; Deady, J.; Reiss, L.W. J. Het. Chem., 18, 599, 1981.

29. Blinko, S. Internal commun., 1989

30. Case, F.H. J. Org. Chem., **16**, 1541, 1951.

31. Case, F.H.; Strohm, P.F. J. Org. Chem., **27**, 1641, 1962.

32. Cockburn, E. Internal commun., 1988.

33. Buttee, D.F.; Case, F.H. J. Org. Chem., **26**, 4691, 1961.

34. Goodwin, H.A.; Lions F. J. Am. Chem. Soc., **81**, 6415, 1959.

35. Wilson, G.R.; Smith, A.G. J. Org. Chem., **26**, 557, 1961.

36. Kumada, M.; Yamaguchi, M.; Yamamoto, Y.; Nakajima, J.; Shiina, K. J. Org. Chem., **21**, 1264, 1956.

37. Sprintschnik, G.; Sprintschnik, W.; Kirsch, P.P.; Whitten, D.G. J. Am. Chem. Soc., **99**, 4947, 1977.

38. Sullivan, B.P.; Salmon, D.J.; Meyer, T.J. Inorg. Chem., **17**, 3334, 1978.

39. Tinnemanns, A.H.A.; Timmer, K.; Reinten, M.; Kraaijkamp, J.P.; Alberts, A.H.; van der Linden, J.G.M.; Schmitz, J.E.J.; Saaman, A.A. Inorg. Chem., **20**, 3698, 1981.

40. Dixon, N.E.; Jackson, W.G.; Lancaster, M.J.; Lawrance, G.A.; Sargeson, N. Inorg. Chem., **20**, 470, 1981.

41. Blair, D.; Diehl, H. Talanta, **7**, 163, 1961

43. Ford, P.; Rudd, D.F.P.; Gaunder, R.; Taube, H. J. Am. Chem. Soc., **90**, 1187, 1968.

44. Creutz, C. Progr. Phys. Org. Chem., **30**, 1, 1983.

45. Braunstein, C.H.; Baker, A.D.; Strekas, T.C.; Gafney, H.D. Inorg. Chem., **23**, 857, 1984.

46. Rillema, D.P.; Mack, K.B. Inorg. Chem., **21**, 3849, 1982.

47. Dose. E., Wilson, L.J. Inorg. Chem., **17**, 2660, 1978.

48. Hunziger, M.; Ludi, A. J. Am. Chem. Soc., 99, 7370, 1977.

49. Fuchs, Y.; Loftens, S.; Dieter, T.; Shi, W.; Morgan, R.; Strekas, T.C.; Gafney, H.D.; Baker, A.D. J. Am. Chem. Soc., 109, 2691, 1987.

50. Kohlman, S.; Ernst, S.; Kaim, W. Angew. Chem. Int. Ed. Engl., 24, 685, 1985.

51. Ernst, S.; Kasack, V.; Kaim, W. Inorg. Chem., 27, 1146, 1988.

52. Schanze, K.S.; Sauer, K. J. Am. Chem. Soc., 110, 1181, 1988.

53. Isied, S.S.; Vassilian, A.; Magnuson, R.H.; Schwartz, H.A. J. Am. Chem. Soc., 107, 7432, 1985.

4.0 PHOTOPHYSICAL DATA

4.1 General Procedures

Acetonitrile was the solvent of choice for spectral studies. This was of HPLC grade, stored over activated 3A molecular sieve under a nitrogen atmosphere.

Fluorescence spectra for the complexes were obtained on a Perkin-Elmer MPF-4 spectrometer. Calculation of quantum yields for the complexes were made using tris(bipyridyl)-ruthenium(II) dichloride as a standard, and assuming the quantum yield for this compound at room temperature in acetonitrile to be, $\Phi = 0.06$. Degassed samples were achieved by subjecting them to three freeze-pump-thaw cycles (oil diffusion vacuum pump), purging the solutions with argon having proved unsatisfactory.

Lifetimes were measured on a Carl Zeiss fluorescence microscope (LAB 16), equipped with a 40/0.75 Neofuar objective. Sample excitation employed a helium cadmium laser: model 4240 NB (Liconix, Sunnyvale, U.S.A.), wavelength 442 nm, output power 50 mW; together with a selective mirror FT 510 and an emission long pass filter LP 520 (Carl Zeiss). Gating of the 4 m (diameter) continuous wave beam was by an acousto optical shutter [rise time 50 ns (A.A. France)] controlled by a micro-computer C64 (Commodore, Braunschweig, F.R.G.). The photomultiplier tube R446 (Hamamatsu, Japan) was powered by a regulated H-V supply (the Isotope Developments EHT unit, type 532/A). Output from the PMT following the excitation pulse was monitored on an oscilloscope-transient

waveform recorder. Digitisation of data points was by a Tektronix digitiser TD20T (Beaverton, U.S.A.). A micro-computer (Atari 1040ST) was utilised to apply curvilinear regression routines to analyse the spontaneous decay data (base line reference:- same trigger, no light) in terms of a quadratic expression over defined regions.

We acknowledge the expertise of Dr. Martin Hilchenbach and thank him for his time and help.

4.2 Treatment of Data

Using luminescent DIAS's, analysis of the time-resolved luminescence decays allows us to calculate the rate constants for electron transfer from:

$$k_{et} = 1/\tau_i - 1/\tau \qquad (24)$$

where τ is the observed luminescence lifetime of the donor-insulator couple in the absence of E.T.

In a simplified argument, for a molecule which loses its excitational energy by only a radiative mechanism and a radiationless decay process, we can write:

$$\Phi_{em} = k_r/(k_r + k_{nr}) \qquad (25)$$

giving $$k_{nr} = k_r(1/\Phi_{em} - 1) \qquad (26)$$

Substituting Equation 9 and applying our conditions for the excited state in ruthenium complexes;

$$k_{nr} = (1 - \Phi_{em})/\tau \qquad (27)$$

This equation allows us to say something about substituent effects on radiationless pathways, solvent and temperature constant.

For a more rigorous treatment[1], it is necessary to recognise the existance of temperature dependent and independent non-radiative decay paths.

$$1/\tau = k_r + k_{nr} + k_{nr}(T) \qquad (28)$$

As to the temperature dependent paths, the principal configurations that are involved are MC or LC:

$$k_{nr}(T) = k_{nr}(T)^{LC} + k_{nr}(T)^{MC} \qquad (29)$$

Substituting into eqn. 28, it becomes evident that under certain experimental conditions, it is possible to neglect some of the contributions. Limiting cases of interest are:

a) T = 77 K, deuterated solvent,

$$1/\tau^{(77\ K)}(S_D) = k_r \qquad (30)$$

b) T = 77 K, solvent,

$$1/\tau^{(77\ K)}(S) = k_r + k_{nr}(S) \qquad (31)$$

c) T = 300 K, deuterated solvent,

$$1/\tau^{(300\ K)}(S_D) = k_r + k_{nr}(T)^{MC} + k_{nr}(T)^{LC} \qquad (32)$$

This gives;

$$k_{nr}(S) = 1/\tau^{(300\ K)}(S) - 1/\tau^{(300\ K)}(S_D)$$

$$k_{nr}(T) = 1/\tau^{(300\ K)}(S_D) - 1/\tau^{(77\ K)}(S_D)$$

4.3 DISCUSSION

Tabulated are the spectroscopic and photophysical data pertaining to the mononuclear and dinuclear complexes synthesised.

4.3.1 The Excited State Energy Level.

A casual glance at energy values of the emission band for functionalised phenanthroline complexes reveals that

Table 4.1 Spectroscopic and Photophysical Data. This table lists the lowest energy absorption maximum (Ab_{max}) at room temperature, the emission maximum (Em_{max}), the emission lifetime (τ, proportions of multiples are superscripted) and the quantum yield (Φ) at R.T. in solvent S. Appended to these are the calculated values for the non-radiative decay constant. Wavelengths are in nm, lifetimes in μs and the non-radiative decay rate constant is expressed in Ms^{-1}. Emission is assumed to occur from ^{3}MLCT.

Complex	Ligand Composition		S	Ab_{max}	Em_{max}	τ	Φ	k_{nr}
C1	1 1	1	H_2O	447	603	0.92		
C1	1 1	1	ACN	477	583	0.5	0.09	1.82
C2	1 1	3	ACN	450	590	0.4	0.04	2.40
C2	1 1	3	H_2O	444	605	1.2		
C3	1 1	4	H_2O	433	630	0.8		
C3	1 1	4	ACN	429	635	0.5	0.09	1.82
C3	1 1	4	H_3O^+	429	635	1.0		
C4	1 1	5	ACN	434	620	1.6	0.11	0.56
C4	1 1	5	H_2O	434	620	1.4		
C5	1 1	6	ACN	436	610	3.3	0.10	0.27
C6	1 1	7	ACN	483	610	3.3		
C7	1 1	BPDS	PBS	460	622	3.73		
C7	1 1	BPDS	H_2O	460	622	2,80		
C7	1 1	BPDS	ACN	453	610	0.8	0.12	1.10
C8	1 1	BPDSCL	ACN	445	635	3.58	0.08	0.26
C9	1 1	10	ACN	485	655	WEAK		
C10	1 1	11	H_2O	478	643	WEAK		
C11	1 1	12	ACN	465	632	0.4		
C12	1 1	14	ACN	440	780	WEAK		
C13B	1 1	17	ACN	459	-	-		
C14	1 1	20	ACN	440	650	WEAK		
C15	1 1	21	ACN	456	658	WEAK		
C16	1 1	9A	ACN	441	612	1.70	0.07	0.55
C17	1 1	16	ACN	428	610	3.6^a:1.5^b	0.02	0.27^a:0.65^b
C18	1 1	28	ACN	430	610	~1		
C19	1 1	30	ACN	455	615	0.68		
C20	1 1	31	ACN	436	602	0.2		
C21	1 1	34	ACN	448	605	6.10		
C21	1 1	34	ACN(O_2)			0.50		
C22	1 1	35	PBS	452	605	3.70		
C22	1 1	35	PBS(O_2)			0.98		
C22	1 1	35	ACN			5.8^a:2.2^b	0.09	0.16^a:0.41^b
C23	1 1	NO_2 NO_2	ACN	423	680	0.5^1:0.15^1		
C24	1 1	36	PBS	450	600	3.7		
C24	1 1	36	PBS(O_2)			1		
C25	5 5	5	ACN	457	650	3	0.14	0.28
C26	6 6	6	ACN	452	650	3.6^a:1.8^b	0.08	0.25^a:0.51^b

Table 5.1 Spectroscopic and Photophysical Data. This table lists the lowest energy absorption maximum (Ab_{max}) at room temperature, the emission maximum (Em_{max}), the emission lifetime (τ, proportions of multiples are superscripted) and the quantum yield (Φ) at R.T. in solvent S. Appended to these are the calculated values for the non-radiative decay constant. Wavelengths are in nm, lifetimes in μs and the non-radiative decay rate constant is expressed in Ms^{-1}. Emission is assumed to occur from ^{3}MLCT.

Complex	Ligand Composition	S	Ab max	Em max	τ	Φ	knr
Polynuclear Complexes							
C28	1 1 1 1 17	ACN	700	890	WEAK		
C29	1 1 1 1 33	ACN	602	810			

H_2O, water; ACN, Acetonitrile; PBS, Phosphate buffered saline (0.1 M, pH 7.8)

these vary little with substitution at phenanthroline. This is very surprising, as one would expect some perturbation of the excited manifold with change in electron density.

Exceptions to this trend are **C10** and **C15**, De Amond *et al* [2] have correlated a molecular orbital study of the substituent effects of di- substituted bipyridines and their redox properties. They found that MINDO studies on 5,5'-$(CO_2H)_2$bipy correlated with observed results for 5,5'-$(CO_2Et)_2$bipy to predict a lowering in energy of the low lying unoccupied π^* level with respect to bipyridine. This seems to tie in fairly well with the observation here, emission being particularly red-shifted with respect to the parent ruthenium trisphenanthroline complex.

In **C15**, ligand **L21** is particularly electron poor.

However, a potentially interesting interaction exists for the excited state. ie. partial localisation of the excited electron upon a quinone oxygen. This would be particularly susceptible to vibronic deactivation. It should be noted that this complex was the first one to bring our attention to the possible influence of 5,6-substitutions to excited state properties (see Section 5).

The other complexes which exhibit marked lowering in the excited state, whilst maintaining a similar weak field about the ruthenium are with ligands other than phenanthroline.

Thus, the complex **C14** is formed rapidly and in very high yield from $Ru(phen)_2Cl_2$! Large metal ions (d_{M-L}= 0.89Å) are known to favour the formation of five membered rings during ligation. Presumably **L20**, by virtue of the relative geometry of the pyridyl rings (with respect to phenanthroline), provides an optimal fit at ruthenium, resulting in better overlap with the e_g set (hence more efficient interaction with the t_{2g} orbitals). That luminescence from this complex was weak was possibly due to the presence of the carbonyl function (cf. **C15**).

The tetra aza ligand **L14** yields the largest red shift of the emission band. That this ligand maintains the same weak field about ruthenium (λ_{max}= 440 nm) suggests that it is not an effect conferred by energy levels within this ligand. It is proposed that diazo bridge acts as a probase[1,2,3], resulting in partial localisation upon this π-electron deficient functionality. This in turn suggests that the

excited state of **C13** should be environment sensitive.

The complex **C23** is an interesting material. Nitrite anion was coordinated ostensibly as it preserved the same weak field about the ruthenium and to see if the complex would still be luminescent. Reaction of the triflate intermediate with nitrite yields a bright red, luminescent solid. On boiling with water (in order to recrystallise the solid), the dried solid was no longer luminescent, and was deep red-brown in colour (When wetted, the crystals appeared bright red!). Meyer and Goodwin[5] assumed that their products were *cis-* as their starting materials were *cis-* . However, comparing their IR data with ours (Appendix II) suggests that the previously synthesised $Ru(phen)_2(NO_2)_2$ material described in the literature is in fact *trans-* , isomerisation ocurring at the relatively low temperatures (ie.>60°C). Thus, we propose that the material we synthesised is the *cis-* isomer. It is weakly luminescent at room temperature in solution, with a quantum yield sixty times less than $Ru(bipy)_3^{2+}$. The lifetime was poorly resolved at 350ns (noisy signal). The uv/visible absorption spectrum of the *trans-* isomer was determined (see Section 5.4).

4.3.2 Estimate of the Non-radiative Decay Constant.

The overall impression from the luminescence data is that, substitution at phenanthroline seems primarily to influence the non-radiative decay pathways and their efficiencies, of the complexes[4].

Given the broad nature of the absorption band, and the

negligible dependence of the emission band on substituents, it does not seem to be valuable to correlate any energy difference with functionality in the complex.

Looking instead at the calculated values of k_{nr}, we have made the following observations/comments:

i) Deactivation of **C1** is greater than $[Ru(bipy)_3]^{2+}$ (k_{nr}=0.935 Ms^{-1}), possibly indicating a greater degree of localisation of the electron in the excited state. Cook *et al* obtained a value of k_{nr}=2.18 Ms^{-1} for the chloro salt of **C1** in EtOH:MeOH (4:1).

ii) The unexpectedly high k_{nr} value recorded for **C2** may point to the formation of the type illustrated (Scheme 4.1).

Scheme 4.1

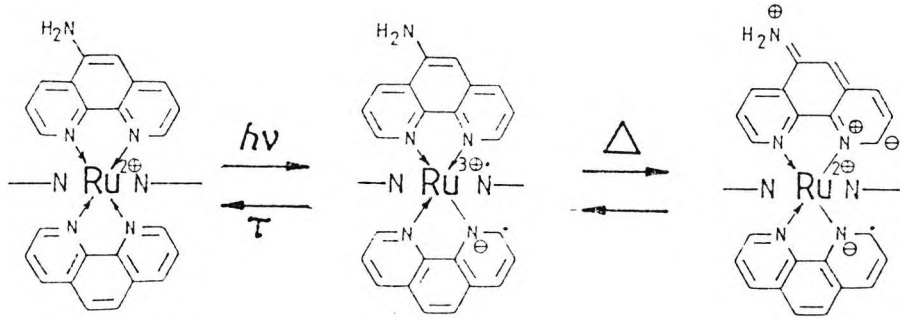

The non-radiative decay constant would be expected to hold components for deactivation at phenanthroline and others associated with deactivation at L3. If such a contribution to the excited state existed, it may explain why the presence of Zn^{0} (metallic zinc) is required to facilitate reaction at the

amino group when the reaction mixture is not protected from light.

iii) In acetonitrile, **C3** behaves rather like **C1**. However, as Wrighton *et al* [5] have demonstrated, in suitable solvents, the greater acidity of **L4** in the excited state complex dramatically influences k_{nr}.

iv) Introduction of halogen into the coordination sphere does not lead to heavy atom quenching, but rather the reverse. The magnitude of k_{nr} for **C4** is reduced dramatically with respect to **C1**; **L5** being 4,7-disubstituted with chlorine. The non-radiative decay constant falls by a factor of two (relative to **C4**) on introduction of bromine to the coordination sphere, as observed for **C5**.

Upon complete substitution in the octahedral coordination sphere by **L5**, **C25**, the value of k_{nr} was halved (cf.**C4**). Cook *et al* [4] obtained a value of k_{nr}=0.63 Ms^{-1} for *tris* (4,7-dichloro-1,10-phenanthroline) ruthenium(II) dichloride in their solvent system (EtOH:MeOH::4:1). It is noted that this is of a similar magnitude greater as their value for **C1** as the halogens salt under these conditions.

For the hexabromo substituted complex **C26**, k_{nr} is only slightly decreased (cf.**C5**), possibly indicating that delocalisation contributes little in this instance [cf. (i)].

v) Aryl substituents in the 4,7- positions seem to confer, from a simplistic view point, one of two properties, either shielding of the localised excited state on the substituted phenanthroline from solvent mediated vibronic quenching (eg.

C7) or TICT state formation through localisation on the aryl ring (eg. C8). This may go some way to accounting for the different lifetimes observed for C22.

vi) The low values of k_{nr} calculated for C17 suggest that in the excited state, by comparison with argument (ii), electron promotion is into L16. That two values are resolved for C17 may indicate that the reduction was incomplete, as illustrated in Scheme 4.2 , or behaviour described in Scheme 5.4.

Scheme 4.2

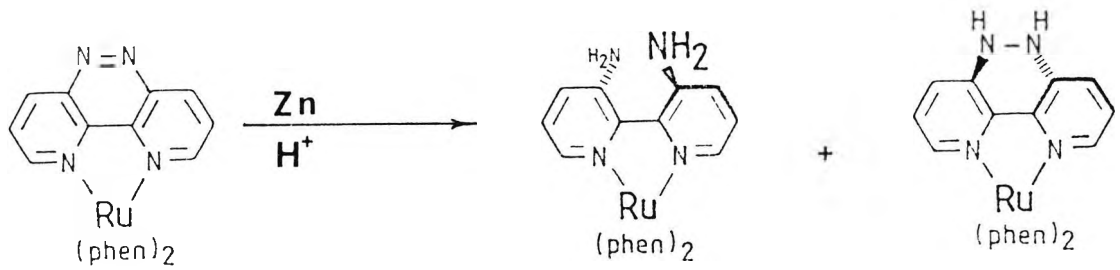

4.3.3 General Observations.

The longest lifetime observed was for the sulphonate ester complex C34. The lifetime so obtained (6.10 s) is of a magnitude observed in *tris* (4,7-diarylphenanthroline) complexes[3]. Other mono and *bis* aryl substituted complexes synthesised show longer lifetimes than those of other functionalised species, all falling in the range of 3 s. The complex C22 shows anomolous behaviour in acetonitrile, and

may indicate partial TICT formation (Section 3.4.2).

The binuclear complexes proved fascinating. Unfortunately their emission bands appear at the detection limits of our photomultipliers. As such, the apparatus was not sensitive enough to extract quantitative data. It should, be noted that weak luminescence at 610 nm (excitation 455 nm) was noted for a degassed solution **C28**! This is intriguing, as the monomeric complex **C13B** showed no luminescent properties.

REFERENCES

1. Balzani, V. Supramolecular Photochem., Ed. Balzani, V., Nato ASI series, Series C, **214**, 187, 1987.
2. Blakely, R.L.; De Armond, M.K. J. Am. Chem. Soc., 4895, 1987.
3. Sadler. J.L.; Bard, A.J. J. Am. Chem. Soc., **90**, 1979, 1968.
4. Baizer, M.M. Electrochim. Acta., **20**, 33, 1975.
5. Bard, A.J.: Puglisi, V.J.; Kenkel, J.V.; Lomax, A. Disc. Faraday Soc., **56**, 353, 1973.
6. Goodwin, J.B.; Meyer, T.J. Inorg. Chem., **10**, 471, 1971.
7. Alford, P.C.; Cook, M.J.; Lewis, A.P.; McAuliffe, G.S.G.; Skarda, V.; Thomson, A.J.; Glasper, J.L.; Robbins, D.J. J. Chem. Soc. Perkin Trans. II., 705, 1985.
8. Giordano, P.J.; Book, C.R.; Wrighton, M.S. J. Am. Chem. Soc., **100**, 6960, 1978.
9. Jaris, A.; Balzani, V.; Barigelletti, F.; Campagna, S.; Belser, P.; von Zelewsky, A. Coord. Chem. Rev., **84**, 85, 1988.

5.0 SPECTRAL CHARACTERISATION AND PROPERTIES OF DERIVATISED RUTHENIUM(II) PHENANTHROLINE COMPLEXES.

5.1 Structural Characterisation of Ruthenium Complexes by NMR

Phenanthroline complexes, on the whole, represent quite a synthetic challenge to the chemist. It is not without reason that the majority of polyaza-cavity complexes of ruthenium(II) have been synthesised in the bipyridine series[1]. Firstly, access to the phenanthroline system is synthetically limited. Add to this a sensitivity of the heterocycle to reducing and oxidising agents, coupled with the relatively difficulty to isolate crystalline ruthenium complexes of functionalised derivatives and one begins to see why.

As we have seen earlier (Section 3.3), proton NMR, through baseline resolution, provides a powerful quality control system. As well as drawing attention to strongly adsorbed organics (frequently a problem by virtue of the amorphous precipitation of the product), the presence of reducing or oxidising impurities can be visualised through paramagnetic collapse signals.

Presented below are the full analyses of two spectra to illustrate just how NMR allows one to stroll around the complex.

The first, that of **C15**, provides an example of the dramatic perturbation to the 2,9-phenanthroline protons

resonances with substitution in the same ring at the 5,6-positions.

The second demonstrates this technique's versatility in more complicated instances, and is included also to help interpret the third spectrum, that of **C28.**

5.1.1. Bis(1,10-phenanthroline)(1,10-phenanthroline-5,6-quinone) ruthenium(II) bis(hexafluorophosphate), C15.

The ^{1}H NMR spectrum of the ~~centro-symmetric~~ complex **C15** (Figure 5.1), lends itself nicely to nine possible decoupling experiments. In practice however, only six were required for unambiguous interpretation.

There are two points worth noting when studying these spectra: 1) Recognising that the proximity of the 2,9-protons to the electron cloud system of the adjacent ligand affords them some shielding (Figure 5.2)[x], the interchange of the 2,9-4,7 resonances (relative to that observed in uncoordinated phenanthroline) becomes apparent; could the chemical shifts have more to do with the amount of electron donation from metal to ligand (ie. extent of back-bonding)?

Figure 5.2

Interaction of H_x and H_* with the aromatic ring of the adjacent ligand.

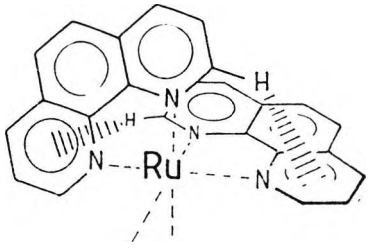

2) For metallic mono complexes NMR will not resolve the racemic form (Figure 5.3)[x].

Figure 5.3 Possible types of optically active chelate molecules for octahedral complexes with bidentate ligands, and the IUPAC nomenclature.

Using the nomenclature described in Scheme 5.1;

Scheme 5.1

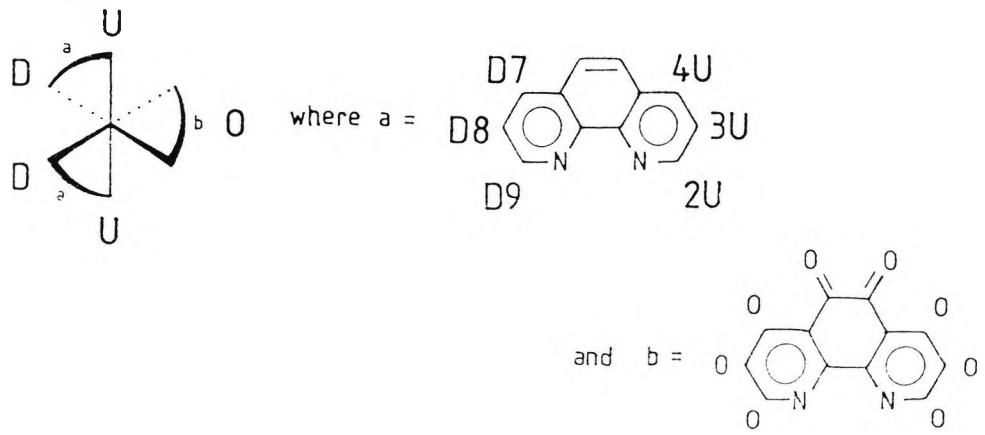

protons of the type O are distinguished by decoupling reactions at 8.6964ppm and 7.8206ppm; U at 8.5838ppm and 7.5936ppm; and D at 8.4772ppm and 7.4870ppm; giving the assignments in Table 5.1.

Table 5.1 Proton assignments for the 360 MHz 1H n.m.r. of (C15)

O	8.6970	dd	$J_{a,x}$ = 8.25 Hz $J_{a,z}$ = 1.22 Hz	2H
U	8.5844	dd	$J_{a,x}$ = 8.20 Hz $J_{a,z}$ = 1.26 Hz	2H
D	8.4785	dd	$J_{y,x}$ = 7.92 Hz $J_{y,z}$ = 1.30 Hz	2H
O	8.3378	dd	$J_{z,x}$ = 5.22 Hz $J_{z,a}$ = 1.22 Hz	2H

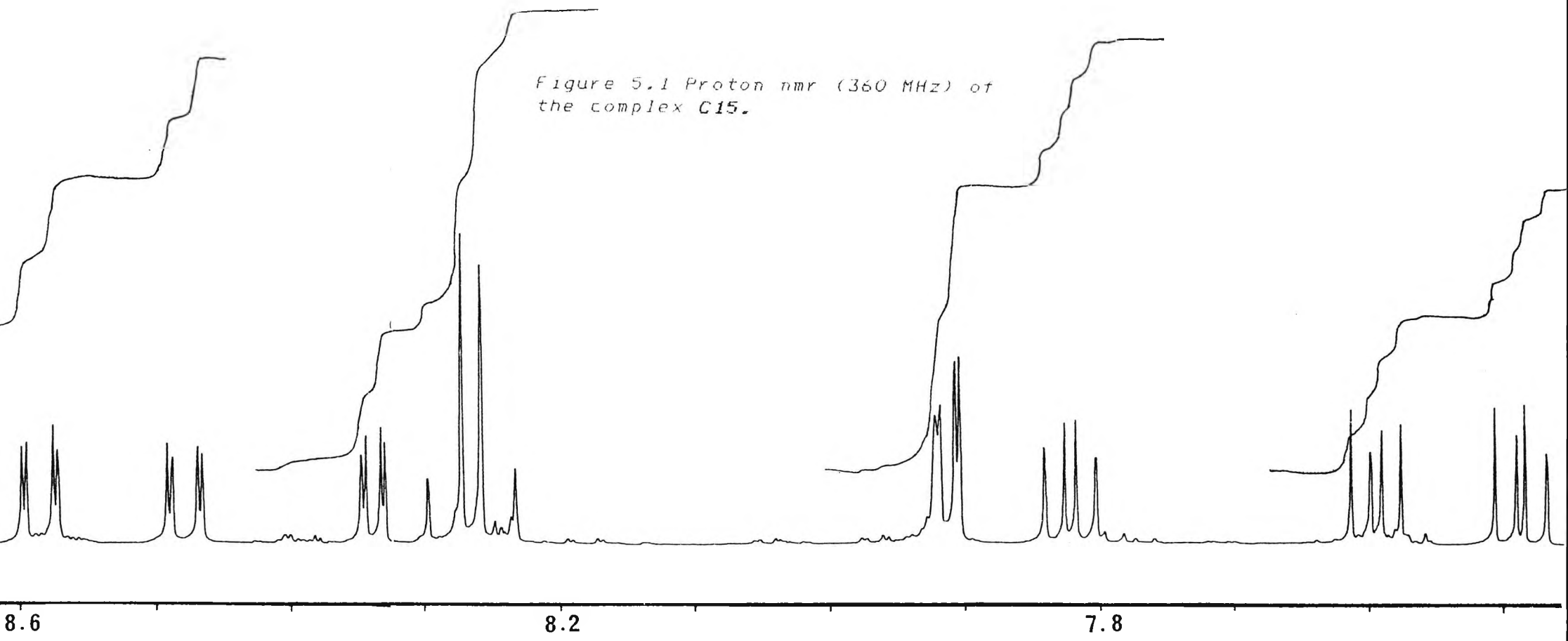

Figure 5.1 Proton nmr (360 MHz) of the complex **C15.**

	8.2838	d	$J_{5,6}$ = 8.97 Hz	4H
	8.2443	d	$J_{5,6}$ = 8.97 Hz	
UD	7.9118	dd	$J_{2,3}$ = 5.26 Hz $J_{2,4}$ = 1.22 Hz	4H
D	7.8207	dd	$J_{3,4}$ = 8.24 Hz $J_{3,2}$ = 5.26 Hz	2H
U	7.5937	dd	$J_{3,4}$ = 8.32 Hz $J_{3,2}$ = 5.22 Hz	2H
D	7.4869	dd	$J_{3,4}$ = 7.92 Hz $J_{3,2}$ = 5.69 Hz	2H

The difference in the assignments of two of the 1,10-phenanthroline 4,7- protons can be attributed to the remoteness of one on each ring from the anisotropic influence of the 1,10-phenanthroline 5,6-quinone. This is further evidenced as the 5-H, 6-H signals appear as an AB quartet.

5.1.2. Bis(1,10-phenanthroline)[3,6-bis(2'-pyridyl)4,5-dihydro-1,2,4,5-tetrazine] ruthenium(II) bis (hexafluorophosphate), C13 .

The proton NMR of this material (Figure 5.4) is of an order of magnitude more complicated than that of **C15**. However, with less simple experiments open to us (six), it is still possible to walk around the complex. It is fortunate that the pyridyl 3-H resonances are exposed. (The low field octets can be convincingly ascribed to a van der Waals de-shielding interaction. This is a result of steric crowding of the 3-H and 3'-H protons). Scheme 5.2 lists the nomenclature.

Scheme 5.2

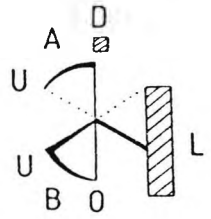

where A =

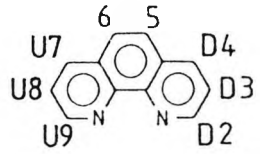

L =

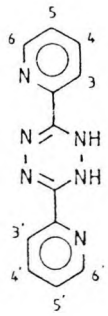

B =

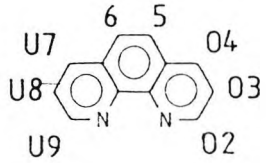

By decoupling at 8.9610ppm, protons **L4** (shifted as a result of ligation to a positive centre), **L5** and **L6** (back bonding counters anticipated shift to low field) are revealed (Table 5.2). Similarly, hitting 8.6727 leads us to **L5'**,**L6'** and **L4'**. However, the centre frequency of **L5'** is not clarified until decoupling of **L4'** (7.4904ppm), three experiments finding the heteroligand proton resonances.

Table 5.2 Proton assignments for the 360 MHz 1H n.m.r. of (C13)

L3	8.9601	ddd	$J_{3,4}$ = 8.00 Hz $J_{3,5}$ = 1.44 Hz $J_{3,6}$ = 0.77 Hz	1H
	8.7622	overlap	(dd 7UB) (dd 4DA)	3H
	8.7357	overlap	(dd 4OB)	
L3'	8.6722	ddd	$J_{3,4}$ = 4.72 Hz $J_{3,5}$ = 1.76 Hz $J_{3,6}$ = 0.93 Hz	1H
7UA	8.6259	dd	$J_{7,8}$ = 8.27 Hz $J_{7,9}$ = 1.28 Hz	1H
2DA	8.5648	dd	$J_{2,3}$ = 5.28 Hz $J_{2,4}$ = 1.24 Hz	1H
B	8.3254	s	(H_{5} + H_{6})	2H
9UB	8.2366	dd	$J_{9,8}$ = 5.27 Hz $J_{3,2}$ = 1.33 Hz	4H
A	8.2275	s	(H_{5} +H_{6})	
L4	8.2174	ddd	$J_{4,5}$ = 9.29 Hz $J_{4,3}$ = 7.89 Hz $J_{4,6}$ = 1.40 Hz	
2OB	8.1409	dd	$J_{2,3}$ = 5.24 Hz $J_{2,4}$ = 1.28 Hz	1H

Figure 5.4 Proton nmr (360 MHz) of the complex ***C13.***

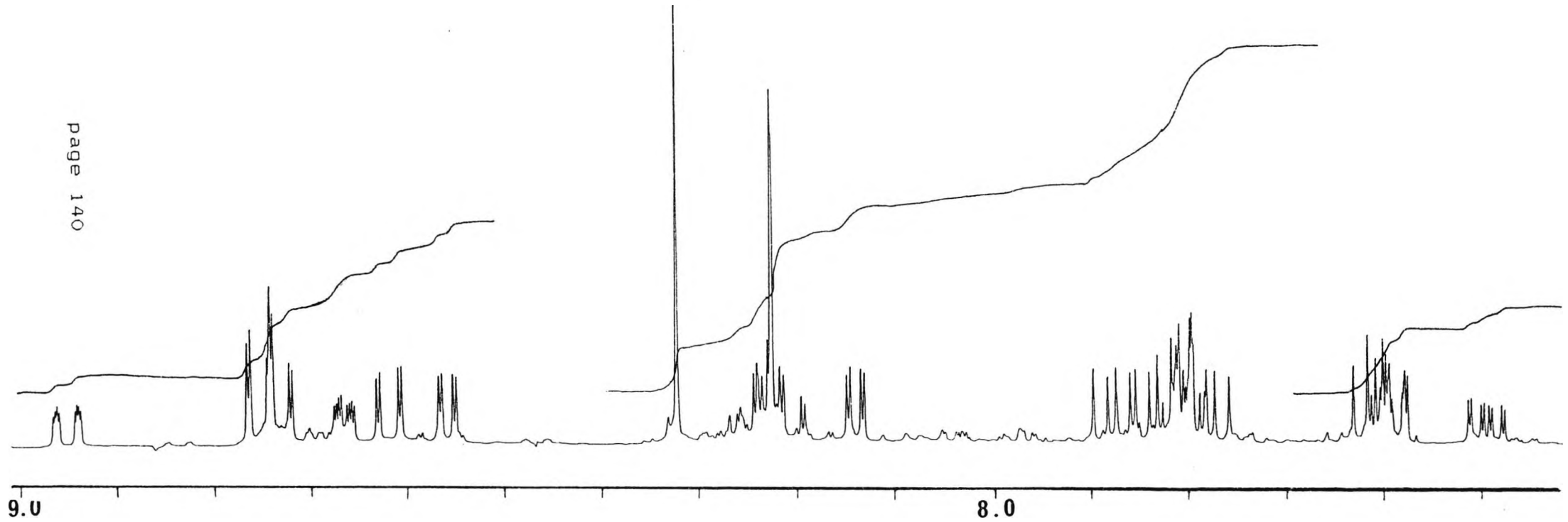

8uB	7.8785	dd	$J_{8,7}$ = 8.31 Hz $J_{8,9}$ = 5.27 Hz	1H
3DA	7.8352	dd	$J_{3,4}$ = 8.32 Hz $J_{3,2}$ = 5.23 Hz	5H
	7.8030	m	(center of L5 +L5')(9UA)	
3DB	7.7758	dd	$J_{3,4}$ = 8.32 Hz $J_{3,2}$ = 5.24 Hz	
8UA	7.6096	dd	$J_{8,7}$ = 8.27 Hz $J_{8,9}$ = 5.27 Hz	3H
	7.5910	m	(center of L6 +L6')	
L4	7.4905	ddd	$J_{4,5}$ = 7.65 Hz $J_{4,3}$ = 4.72 Hz $J_{4,6}$ = 1.18 Hz	
1H				

The remainder of the spectrum was deciphered through analysis of a model of the complex with the results of the following three experiments.

Decoupling at 8.6260ppm (assigned 7UA) found the protons on ligand A most remote from L (1UA and 7UA). The resonance centred at decoupling frequency 8.5641 has coupling constants identifying it as α-aza nitrogen. To experience such a dramatic shift, this proton must be influenced anisotropically by L. Indeed, modelling reveals that 2-H of ring A sits above the tetraaza moiety. This allows identification of 4DA and 3DA.

Hitting 8.1389ppm (pattern characteristic of an -aza proton in the phenanthroline system) identifies the other protons of ring B- in close proximity to L, 2OB being particularly shifted as a result of being over the coordinated pyridyl of L.

This leaves 7UB, 9UB and 8UB not detected directly by experiment, but clearly visible and identifiable by their coupling constants.

5.1.3. Tetrakis(1,10-phenanthroline)[-3,6-bis(2'-pyridyl)-tetrazine]diruthenium(II)tetra(hexafluorophosphate), C28.

Glancing at the proton NMR of **C28** (Figure 5.5) reveals that there are insufficient simple decoupling experiments open to us to begin to interpret the spectrum. For such a system, one must turn to the homonuclear correlation technique ^{1}H COSY (Figure 5.6).

Scheme 5.3 illustrates the diastereomers possible for **C28**. With these complicating factors in mind, a second look

---

Scheme 5.3 Pair of enantiomers (top) and meso form (bottom) of the dinuclear **L17** complex with $[Ru(phen)_2]^{2+}$ fragments.

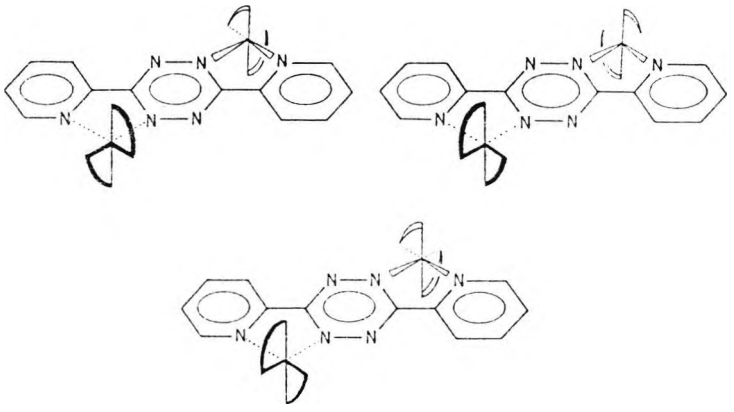

---

at Figure 5.5 reveals two pairs of interesting features. These are at 8.910 and 8.850 , also at 7.511 and 7.390, in case, the integrals being in the ratio 1:2 respectively. These latter resonances are quite clearly of a pyridyl pattern. In either the racemic mixture, or the meso form, a symmetry plane exists; however, inspection of the COSY plot

Figure 5.5 Proton nmr (360 MHz) of the complex **C28.**

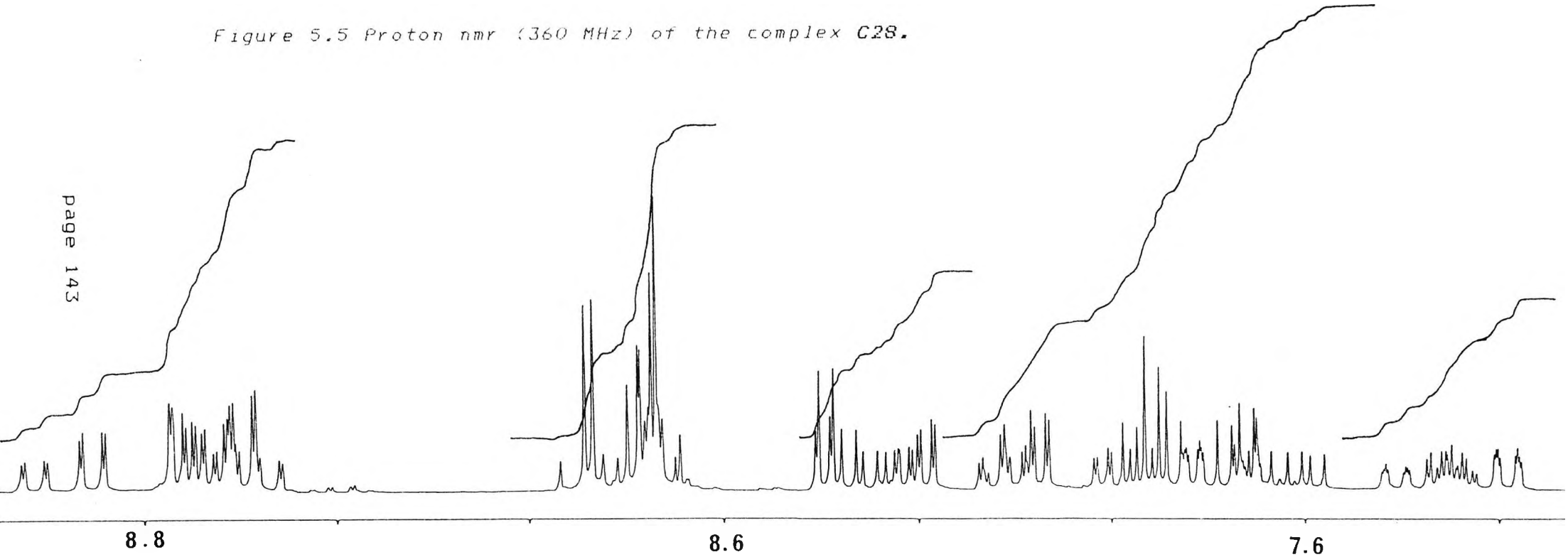

Figure 5.6 Proton-proton cosy experiment result for C28.

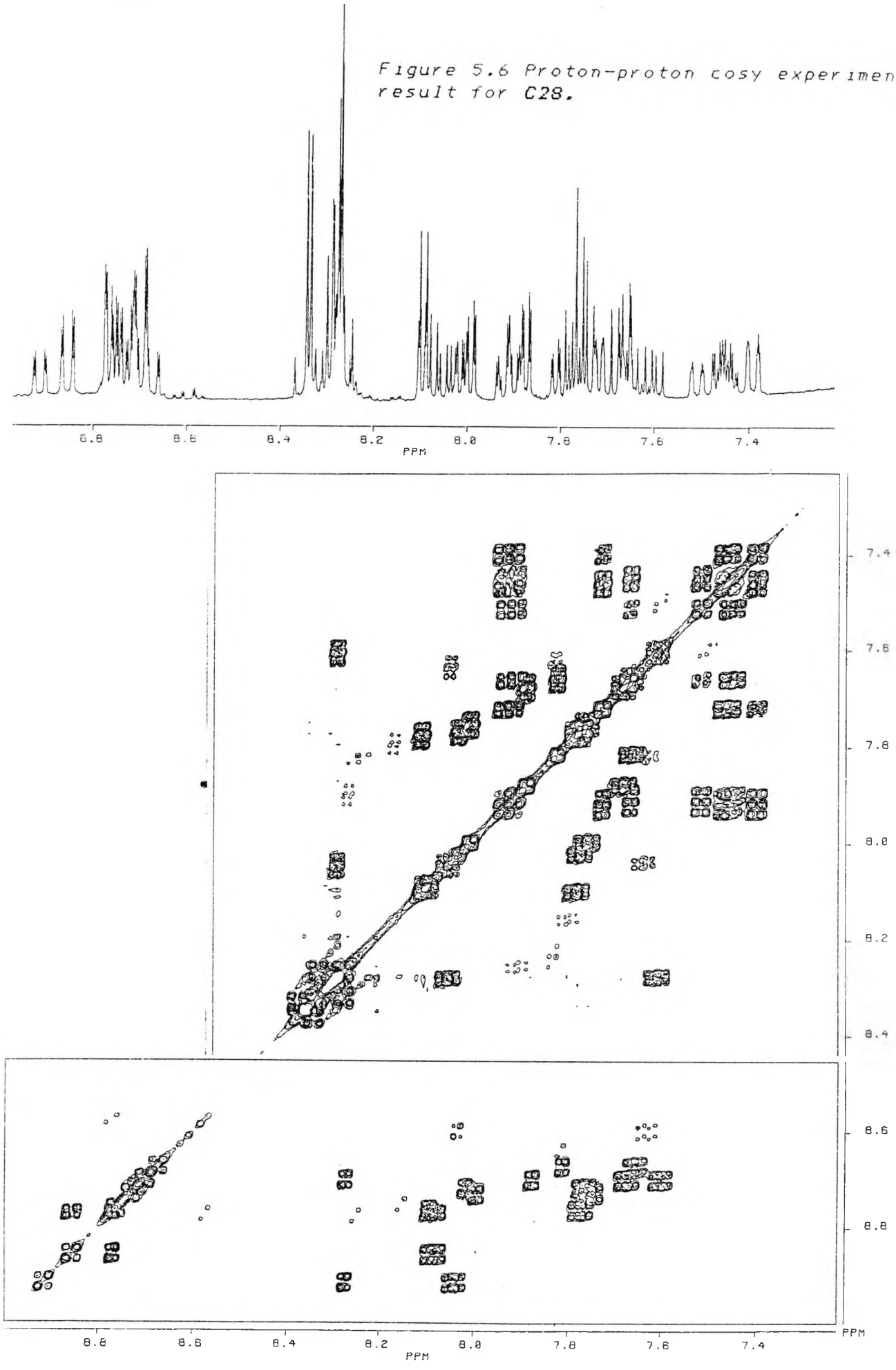

shows clearly that these two spectral features are not coupled. This was our first evidence that this was a 2:1 mixture of the diastereomers.

As to what predominates over what in the mixture, one must study Scheme 5.3. In each enantiomeric structure, a "bad interaction" exists as a result of two coordinated phenanthrolines pointing at one another. The result of this unusual geometry (steric crowding of an α-aza proton on each of the phenanthrolines) should result in a van der Waals de-shielding interaction. Indeed the COSY plot reveals that the doublet of doublets at 8.850 (4H protons) is coupled to the very next feature upfield (doublet of doublets, 8.763 δ). This drew us to the rather surprising conclusion that C28 formed in equal probability in the possible structures available to it, and not as expected of a material having two equivalent chiral centres a 1:1 mixture of meso and DL diastereomers (in fact the "bad interaction" would have us expecting near pure meso)!

We were unable to separate the components and hence unable to assign the spectrum.

5.2 FAB Mass Spectrometry - A Coordination Sphere Probe.

It was found that conventional mass spectrometry (MS) had limited application when it came to characterisation of our complexes. This was attributed primarily to their involatility. However, application of the technique of fast atom bombardment (FAB) MS proved remarkably informative.

Table 5.3 summarises the positive ion FAB of three hexacoordinate complexes.

Table 5.3 Positive ion FAB mass spectra of three Ru phen complexes

Complex	Fragment		Mass
(C15)	?		875
	(i)	M - PF_6 + H	819
	(ii)	(i) - PF_6	673
	(iii)	(ii) - phen + H	494
	(iv)	(ii) - L - H	462
	(v)	Ru phen	282
(C8)	(i)	M - PF_6 + 2H	1137
	(ii)	(i) - HCl	1101
	(iii)	(i) - SO_2Cl + 2H	1039
	(iv)	M - $2PF_6$	990(989)
	(v)	(i) - phen + H	958
	(vi)	(v) - Cl	923
	(vii)	Ru $phen_2$	462
	(viii)	Ru phen	282
(C28)	(i)	M - PF_6 + H	1596
	(ii)	(i) - PF_6	1449
	(iii)	(ii) - PF_6 + H	1305
	(iv)	Ru $phen_2$ L PF_6	843
	(v)	(iv) - PF_6	698
	(vi)	(v) - L	462
	(vii)	(vi) - phen	282

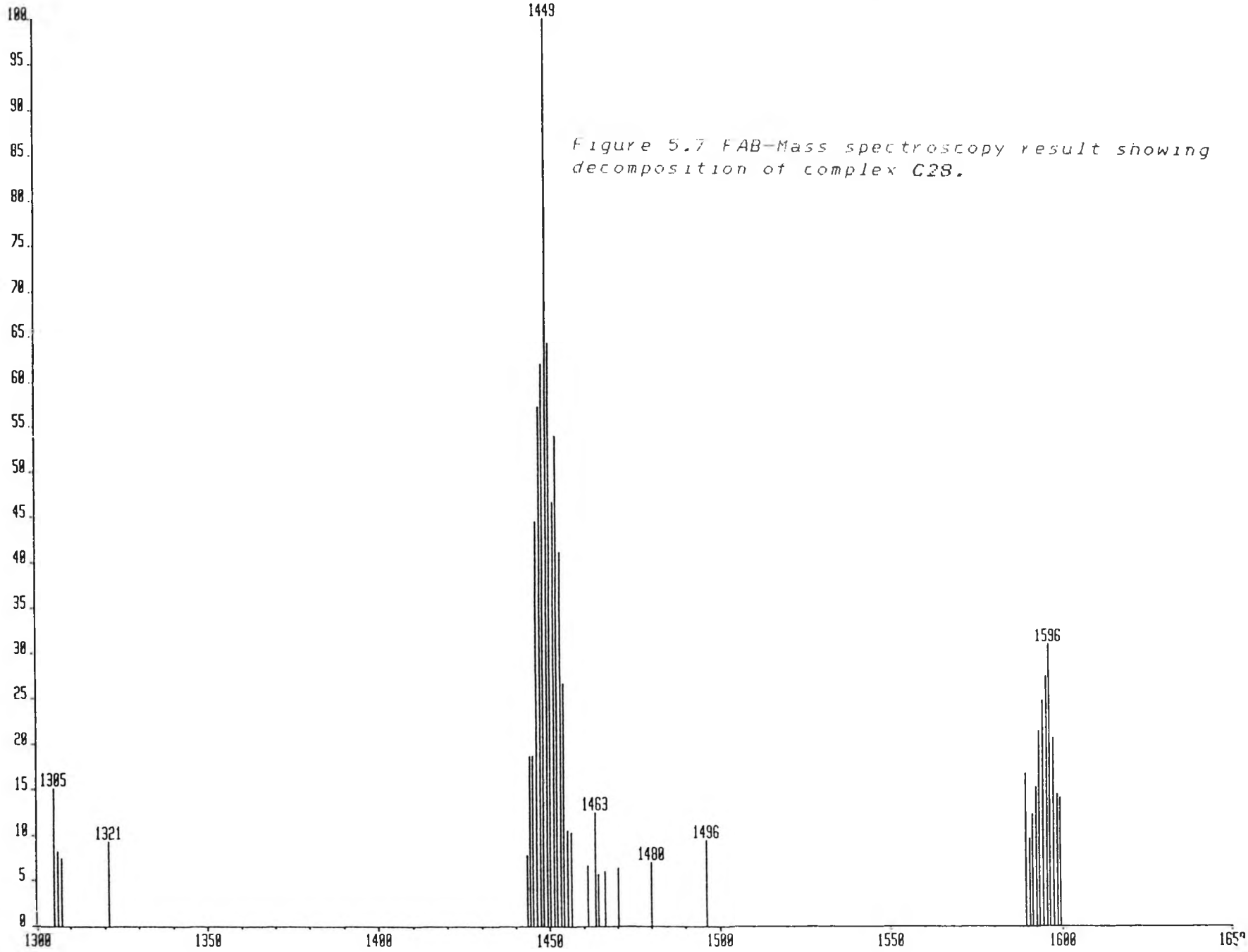

Figure 5.7 FAB-Mass spectroscopy result showing decomposition of complex **C28.**

The results clearly indicate a wealth of structural information. Ions for the complete coordination spheres of all the complexes are detected with or without attendant counter anions. The composition of these complexes can be confirmed from mass losses corresponding to those respective ligands (and counter ions, where applicable). As will be seen, hydride anion addition to fragments is a common feature. The sources of these species is likely to be the matrix employed (in this case, glycerol).

Figure 5.7 illustrates the decomposition of C28. Interpretation of the spectra is complicated as a consequence of the existence of five ruthenium isotopes [mass 99(13%), 100(13%), 101(17%), 102(39%) and 104(18%)].

5.3 Absorption Spectra

Table 5.4 lists data obtained for the absorption spectra of various complexes. Values correspond to the spectroscopic properties in the acetonitrile (recorded on a Philips PU 8720 UV/Vis spectrometer) at room temperature. They are normalised with respect to the intense ligand centred absorption at ~262nm (287nm in trispbipy Ru). A direct comparison of the extinction coefficient values with the literature is quite difficult, as where complexes have been made before (C1, C3, C7 and C25) it is usually with a different counter ion. However our value for C1 is remarkably high when compared to others (usually in the range 20000 $lmol^{-1}cm^{-1}$ and C4 is somewhat larger than that calculated by Cook and Thomson[4] for it's corresponding iodo salt. It is to be noted that the MLCT

band at ~440 nm is usually quite broad, and in cases indicated is actually flat over at the maximum for a considerable range (from 30 - 70 nm). It was communicated to us that the relaxation rate of acetonitrile is extremely rapid, suggesting that on the timescale of a UV experiment, there occurs a marked instantanious sensing of the formation of the dipolar excited state $[Ru^{3+}p_{\pi}(fp^{-})]^{2+*}$. Such an argument has been used for the solvent sensitivity of this transition[5].

That the position of the long wavelength MLCT band is rather insensitive to substitution in the phenanthroline ring is probably a reflection of the uniformity in splitting energy displayed by the d orbitals. Thus significant shifting (in the electron poor C13 and the blue shift in C23) can be attributed to a marked alteration in the ligand field.

Perturbations in the C2 and C17 complexes to the MLCT (progressive blue shift) can possibly be explained by the formation of an inter-ligand CT state (see Section 2.3.2). Such an effect is expected to be more pronounced in C17, as the bis amino ligand (L16) is unlikely to be able to adopt a planar geometry, resulting in a reduced frequency of interaction with the metal. This leads us to postulate that,

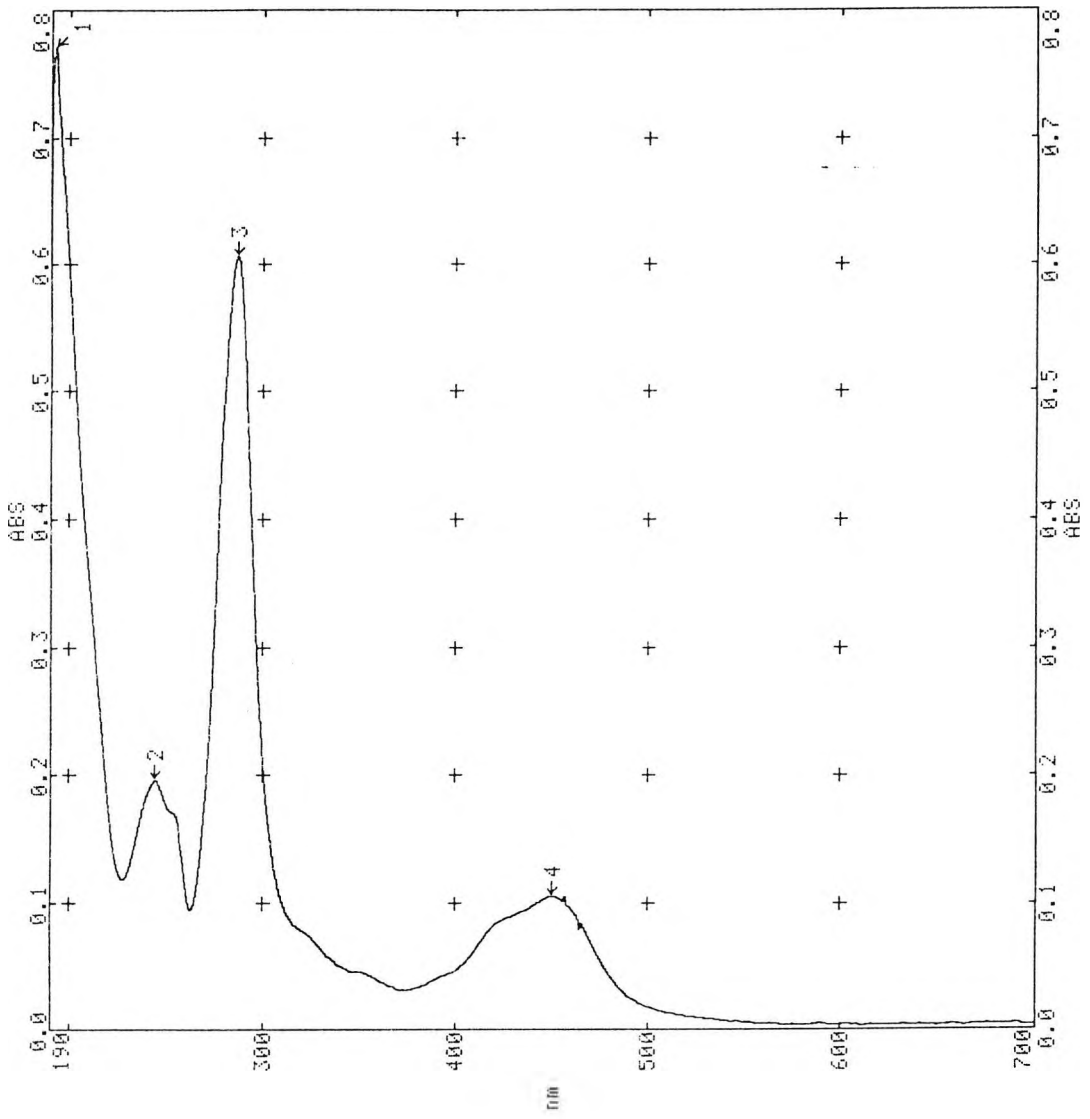

Figure 5.8 UV-Visible electronic spectrum of tris(bipyridyl) ruthenium(II) dichloride.

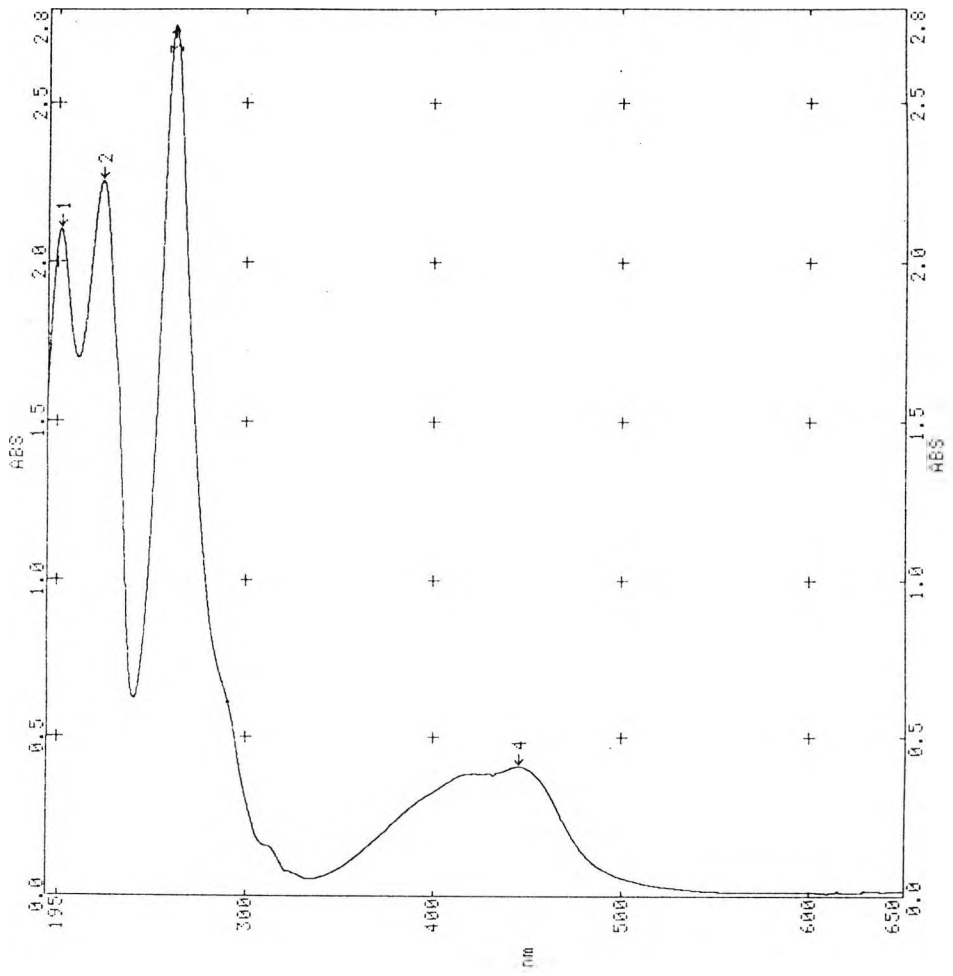

Figure 5.9 UV-Visible electronic spectrum of tris(1,10-phenanthroline)ruthenium(II) bis(hexafluorophosphate).

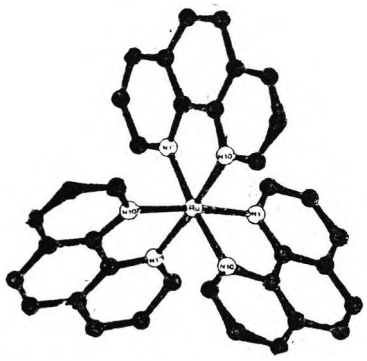

Figure 5.10 Structure of the tris(1,10-phenanthroline)ruthenium(II) complex.

Table 5.4 Electronic absorption data for some of the ruthenium(II) complexes prepared, in acetonitrile. The wavelength (λ_{max} / nm, **bold** type) values are presented with their intensity of absorption normalised with respect to the lower energy LC - band, thus [x], and the extinction coefficient presented as a subscript/ 10^{3} l $mol^{-1}cm^{-1}$.

TBRC	**192**[1.27] (**244**[0.31]-**254**h[0.26]) **287**s[1] (**323**[0.13]-**351**[0.06]) (**425**h[0.14]-**452**[0.17])
C1	**202**s[0.77] **223**s[0.87] (**263**s[1]-**277**h[0.70]-**309**h[0.13]-**324**[0.16]) **436**[0.19]$_{(29.7)}$
C2	(**203**h[0.70]-**222**s[0.77]) **264**s[1] (**400**h[0.15]-**425**h[0.16]-**450**[0.18]$_{(18.7)}$)
C3	(**206**h[0.81]-**223**s[0.90]) (**259**h[0.94]-**264**s[1]) **430**[0.20]$_{(17.1)}$
C4	(**213**[0.68]-**223**h[0.65]) (**263**s[1]-**285**h[0.25]-**303**h[0.11]) **434**[0.17]$_{(22.8)}$
C5	**202**s[0.73] **223**s[0.87] (**263**s[1]-**277**h[0.77]-**309**h[0.13]-**324**[0.06]) **436**[0.19]$_{(28.8)}$
C7	**199**s[1.10] **222**s[0.96] (**264**s[1]-**277**h[0.71]-**313**h[0.17]) (**429**s[0.21]-**450**[0.22]$_{(28.3)}$)
C8	**199**s[1.06] **223**s[0.90] (**264**s[1]-**276**h[0.72]-**310**h[0.17]) **446**[0.21]$_{(28.1)}$
C13	**201**s[0.91] **223**s[0.87] (**263**s[1]-**285**h[0.44]-**310**h[0.24]) (**419**h[0.14]-**459**[0.16]-**485**h[0.12])
C17	**204**s[0.93] **224**s[0.85] (**265**s[1]-**282**h[0.40]-**311**h[0.15]) **428**[0.21]-flat over 64nm
C21	**193**s[1.09] **200**s[1.03] **221**s[0.90] (**264**s[1]-**308**h[0.13]) **440**[0.18]-flat over 38nm
C24	**202**s[0.97] **222**s[0.79] (**263**s[1]-**286**h[0.25]-**308**h[0.07]) **433**[0.17]-flat over 38nm
C25	(**213**s[0.79]-**228**h[0.48]) (**266**s[1]-**303**h[0.15]-**317**h[0.09]-**329**h[0.05]) **349**[0.03] **447**[0.14]-flat over 38nm
C26	**223**s[0.84] (**280**s[1]-**309**h[0.32]-**324**h[0.17]-**336**h[0.08]) **437**[0.19]-flat over 30nm
C29	**202**s[1.00] **223**s[0.84] (**263**s[1]-**287**h[0.35]-**308**h[0.23]) (**370**h[0.17]-**381**s[0.18]-**398**s[0.19]-**416**h[0.12]) **602**[0.14]

primary charge separation in the E.S. would be expected to give a greater yield of the phenanthroline localised electron product. In turn, upon thermally activated coupling of L16, the metal centre could well be reduced (cf Moore *et al* in Section 1.0, Section 4.3.2 and Scheme 5.4).

Scheme 5.4

Possible mechanism fit accommodating data on **C17**

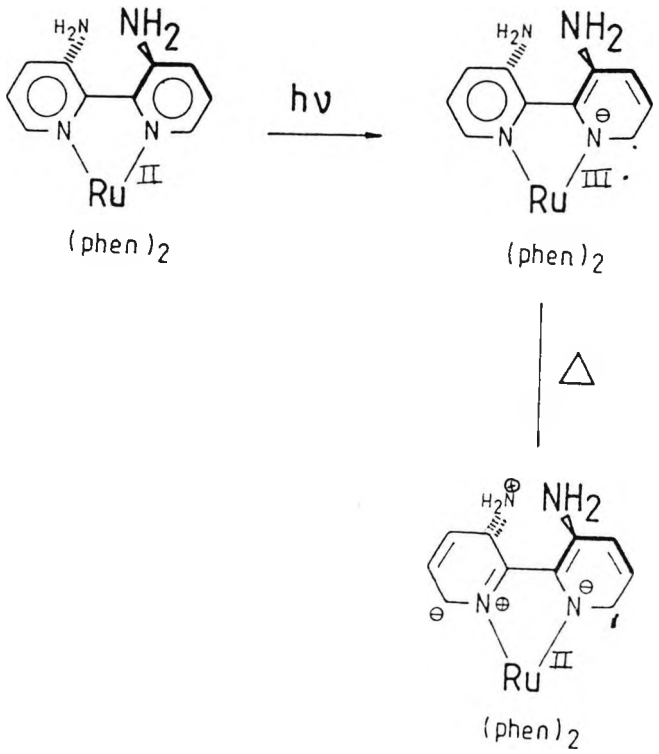

Precedent for such a mechanism as shown above (ie. independent deactivation pathways existing within the same molecule), is provided by De Almond *et al* [6,7,8]. Investigating spectroscopic properties of mixed ligand complexes with 2,2'-dipyridylamine, dual emission from a

ruthenium(II) complex are detailed.

The dinuclear complexes **C28** and **C29** show some very interesting photophysical behaviour. The appearance of low energy absorption maxima (690 and 602nm respectively) indicate enormous potential for tailored excited state properties. The complex **C28** proved to be solvent sensitive in a way not observed for these species.

Table 5.5 Anomalous solvent sensitivity displayed by complex **C28** (see Table 5.4 for layout)

Acetonitrile - deep green			
199s[0.95]	**220**s[0.85]	(**259**s[1]-**285**h[0.41]-**310**h[0.17]-**335**h[0.12]-**395**h[0.08]-**455**h[0.02])	(**570**h[0.03]-**690** [0.12])
Methanol - very light red			
(**210**h[0.79]-**223**s[0.87])		(**262**s[1]-**285**sh[0.35]-**312**h[0.14])	(**410**h[0.16]-**448**h[0.18]-**548**h[0.07-flat over 60 nm])

It should be noted that **C28** is obtained unchanged upon removal of the methanol.

REFERENCES

1. Jaris, A.; Balzani, V.; Barigelletti, F.; Campagna, S.; Belser, P.; von Zelewsky, A. Coord. Chem. Rev., 84, 85, 1988.
2. Seddon, S.A.; Seddon, K.R. The Chemistry of Ruthenium, Elsevier-Oxford, 1984.
3. Cotton, F.A.; Wilkinson, G. Adv. Inorg. Chem., 5th Edit., J. Wiley, 1988.
4. Cook, M.J.; Thomøson, A.J. Chem. Br., 914, 1984.
5. Kober, E.M.; Sullivan, B.P.; Meyer, T.J.; Inorg. Chem., **23**, 2098. 1984.
6. Blakely, R.L.; De Armond, M.K. J. Am. Chem. Soc., **109**, 4895, 1987.
7. Blakely, R.L.; Myrick, M.L.; De Armond, M.K. J. Am. Chem. Soc., **108**, 7843, 1986.
8. Morris, D.E.; Ohswa, Y.; Segers, D.P.; De Armond, M.K.; Hanck, K.W. Inorg. Chem., **23**, 3010, 1984.

6.0 CONJUGATION STUDIES

6.1 Labelling Myoglobin - Attempts to Singularly Modify a Structurally Characterised Heme-protein.

Our initial requirements for a hardy, compact, structurally characterised heme protein were met by sperm whale myoglobin (Figure 6.1). Myoglobin represents a particularly good model for the effects of our semisynthetic methodology upon protein structure, by virtue of solution-crystal state comparisons having been made for it[1,2]. We considered it advantageous to target reactivity at the N-terminus of the protein sequence for three reasons. 1) The pK values for myoglobins containing natural NH_2-terminal valine and glycine residues has been determined by chemical kinetics[3]. 2) It has been implicated as a potential metal chelating site[4,5] and, 3) the importance of the hemoglobin NH_2-terminals in regulating control of ligand binding[6-9].

To obtain optimum labelling levels, fluorescein isothiocyanate (FITC) was employed as a probe molecule. Thus, as a standard, FITC (2 mg, 5 uM) would be stirred with ammonium acetate (2 g in 100 cm^3) for the duration of the series of labelling reaction, the standard procedure for which was to treating sperm whale myoglobin (1 mg/cm^{-3}, Sigma) with a known excess of FITC in phosphate buffered saline PBS (0.1 M, pH = 7.8) at 4°C overnight.

The excess reagents were removed by gel filtration on a Sephadex G-25 column (5 x 0.5 cm), equilibrated with PBS. The

THE TERTIARY STRUCTURE OF MYOGLOBIN

labelled solutions and the standard (1 cm^3) were diluted to 5 cm^3, degassed with a gentle steam of nitrogen and their fluorescence spectra recorded. Samples which gave a fluorescent yield close to that of the standard were adjudicated to have achieved a level of labelling close to unity.

It was on this basis that a 10 fold excess of bis(1,10-phenanthroline)(bathophenanthrolinedisulphonylchloride) ruthenium(II) bishexafluorophosphate **(C8)** was employed for conjugation studies. Initially, after labelling the conjugate was subjected to only the one gel filtration step and life time studies conducted on this sample.

Photophysical data were determined on the Fluorescence Microscope modular work bench described in Section 4.1 and illustrated below (Figure 6.2).

Figure 6.2 Fluorescence Microscope

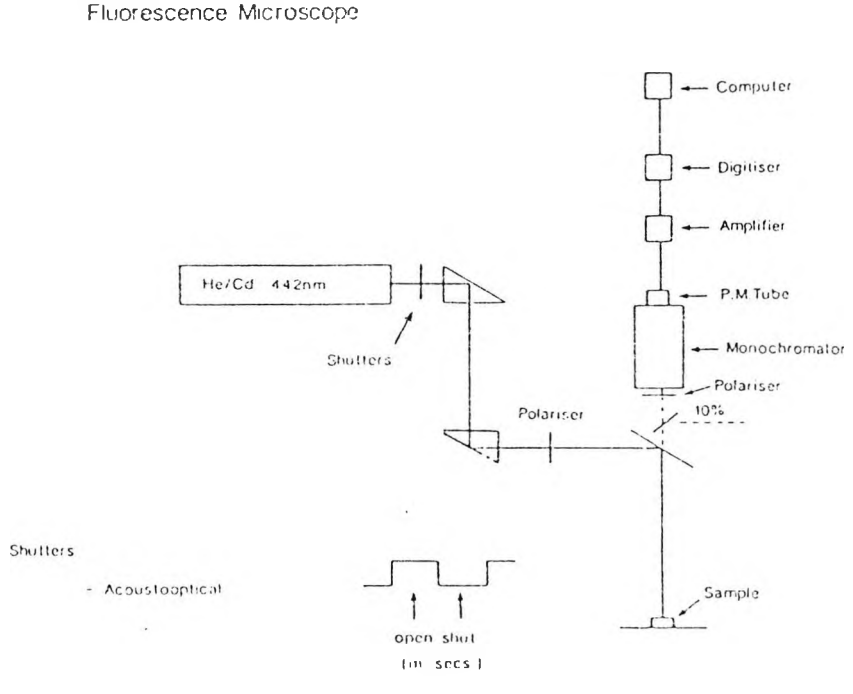

Initially, samples were studied by degassing with a steady stream of argon, placing the sample on a dimpled microscope slide and then covering it with a cover slip (0.17 mm thick); this configuration proved unsatisfactory. An improved sample holder offering better protection from the atmosphere was needed. Thus, a 1mm (thickness) fluorescence cell was employed, it being charged with sample in a nitrogen purged inert-atmosphere box.

Investigation of this system lead to the following averaged lifetimes being recorded: 0.58 μs(10%), 1.15 μs(50%) and 3.58 μs(40%). The latter value has been shown to correspond to that of free probe in solution (see Section 4.3).

The high concentration of free complex suggested that there was an electrostatic interaction with the protein, allowing unbound probe to be transported through the molecular exclusion column. Also, the possibility of multiple labelling had not been addressed.

Some separation was observed on Sephadex DEAE-A50 (5x0.5 cm). Using a freshly coupled conjugate, gel filtered (and concentrated using G25) two bands were obtained on DEAE-A50, monitoring elution pattern at 280nm and eluting in 0.05M Tris buffer. Only the first band showed ruthenium luminescence. Spectroscopic evaluation gave the same results as before. However, for the first time, it was noted that a dark fading process was occurring. Decreasing the labelling ratio, increasing the size of the columns and more rigorous

purification of C8 all failed to improve the situation. Gray et al after gel filtration utilised preparative isoelectric focusing prior to ion exchange chromatography. However the dark reaction tended to point to something unsuitable about (C8) as a probe. It should be pointed out that Sykes *et al.* [11,12] have had difficulties in obtaining reprducible data and in interpreting results in a self-consistent manner with other metallo-complexes of this class.

In the face of mounting evidence that (C8) was over functionalised and our continued problems of obtaining isomeric purity of this complex, we synthesised bis(1,10-phenanthroline)[4-(4-chlorosulphonylphenyl)-1,10-phenanthroline]ruthenium(II) dichloride (C27).

A scale model of sperm whale myoglobin was constructed[13-16] to better visualise the enormity of the site specificity problem (Appendix III). The model revealed that all nineteen lysine residues in the 153 residue polypeptide chain, were residing on the outside surface of the protein- along with all other polar substituents! Whilst not having a surface charge distribution map, it was clear sites of negative charge existed ~~about~~ near many of the lysine ε - amino groups. As a consequence of the electrostatic interaction between the protein and the complex (creating in affect an abnormal concentration effect) their presence could not be considered trivial.

Table 6.1 LIFETIME DATA FOR MYOGLOBIN RUTHENATED WITH C28

PROTEIN LABELLED WITH C27	OBSERVED LIFETIMES (μs)	RATIO
Apomyoglobin[a],17	2.078	
Myoglobin[a]	1.65-1.55-1.56	12
	1.16-1.36-1.20	12
	0.24-0.39-0.29	67
Myoglobin[b]	2.60-2.80-2.40	1
	0.30-0.35-0.38	2

(a) Deoxygenated system

(b) Oxygenated system

Conjugation of myoglobin with the probe C27 cured the dark reaction problem. Multiexponential simulation allowed us to obtain the following data for luminescence decays (Table 6.1). Assuming these derive from a single species system as a consequence of dynamic molecular processes (such as conformational isomerisation) then the shortest lifetime in the deoxygenated system can be assumed as deriving from optimal observed coupling between C27 and the heme. The electron transfer rate for this reaction would be:-

$$k_{et} = \frac{1}{\tau} - \frac{1}{\tau_o}$$

where, τ = lifetime of conjugate,

τ_o = lifetime of apomyoglobin derivative.

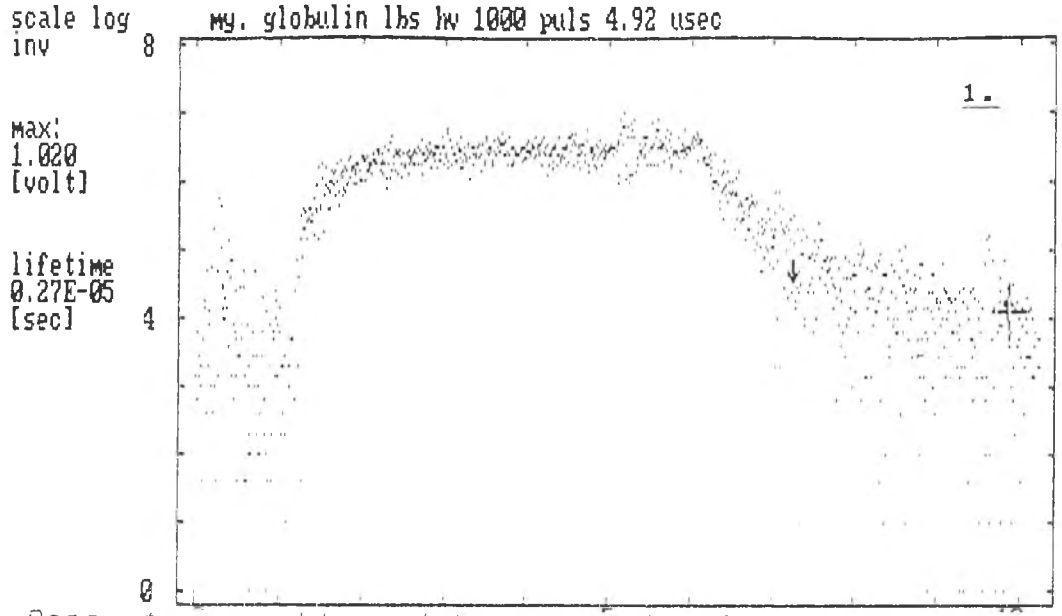

Decay traces obtained for oxgenated labelled myoglobin (Table 6.1) showing 1. result from excitation 2. analysis for slow component 3. analysis for fast decay.

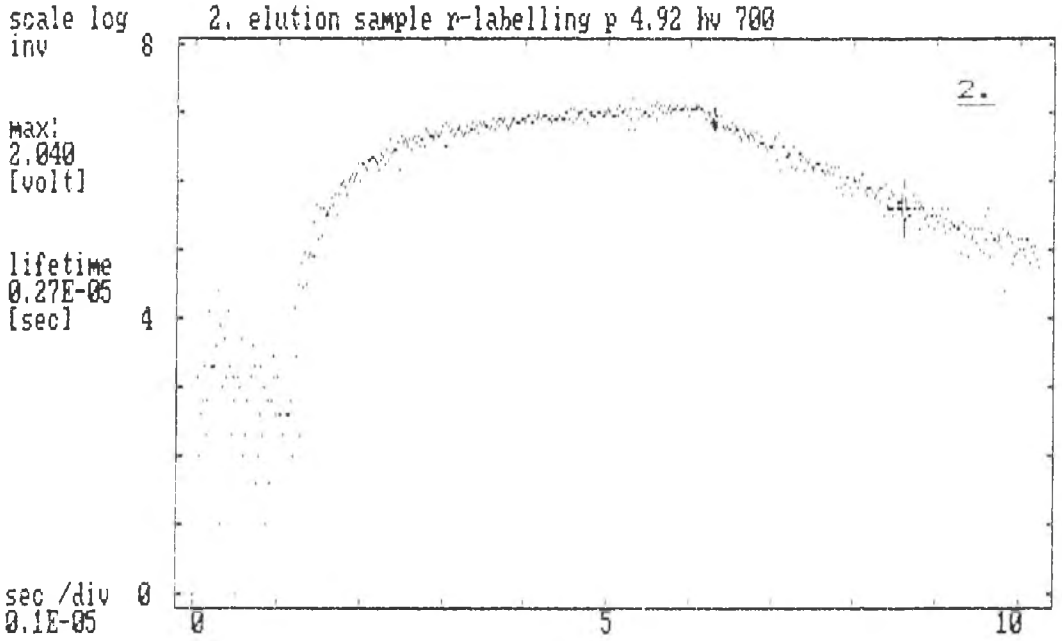

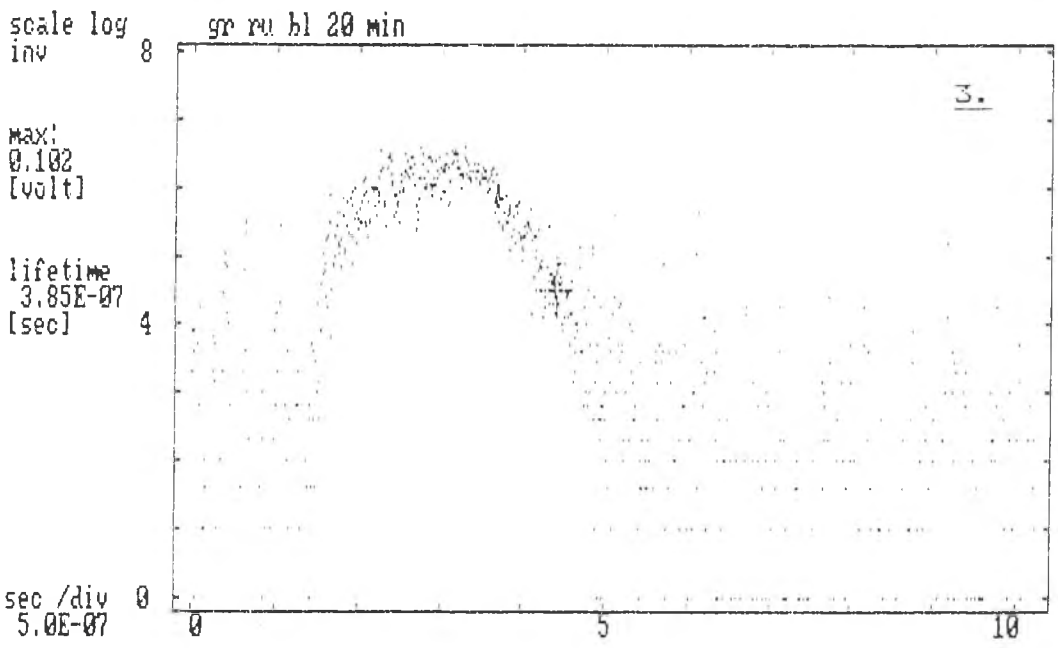

therefore, $k_{et} = \frac{1}{3.06\times10^{-7}} - \frac{1}{2.78\times10^{-6}}$

$k_{et} = 2.91\times10^{6}\ s^{-1}$

Assuming that the redox couple of C27 is the same as that of *tris* (4,7-diphenyl-1,10-phenanthroline)ruthenium(II) (Table 2.2) and that of sperm whale myoglobin, E (Fe^{3+}/Fe^{2+}) = 0.059 V[18], then the driving force of the reaction is:-

$$\Delta G = -\nu F \Delta E$$

where ν = number of electrons involved

$F = 9.648\times10^{4}\ C\ mol^{-1}$

giving, $\Delta G = 92.4\ kJmol^{-1}$

Substitution into the standard theoretical expression for the electron transfer rate constant[20].

$$k = 10^{13}\exp[-(\lambda + \Delta G)^2/4\lambda RT]\exp[-\beta(d-3)]$$

where λ = vertical reorganisational energy

= reorganisation at the heme

$= 83.9\ kJmol^{-1}$

$$k = 13\ln10 - (\lambda + \Delta G)^2/4\lambda RT + \beta(d-3)$$

$$14.88 = 29.93 - 37.36 + \beta(d-3)$$

$$22.31 = \beta(d-3)$$

Assuming $d = 25\pm2$ Å,

$\beta = 0.89$

From the model, an estimate of the distance (edge to edge) (d 25 Å) gives a value much less than the normally assumed values ($1.2-1.4 Å^{-1}$), indicating enhancement of the

donor-acceptor coupling.

Whilst these figures correlated fairly well with the findings by Gray *et al* [10], for the reasons discussed, it is dangerous for us to make any quantitative statements regarding this distance dependence of electron transfer in this system.

6.2 Affinity Labelling: A Route to Mono-Modification

Our strategy to the synthesis of a new metallo-protein required the site-specific, irreversible inhibition of a structurally characterised enzyme. Analysis of its electron transfer reactivity was envisaged as being achieved (initially) by the method of Sykes *et al* [11]. Chymotrypsin fit our requirements perfectly (see Figure 6.3)[23]. Thus, tosyl-L-phenylalanine chloromethyl ketone (TPCK, Figure 6.4) binds specifically to the active site in the enzyme, because it resembles a substrate. Its mode of action, is to react (with total regiospecifity) at histidine 57, which is alkylated at one of its ring nitrogens.

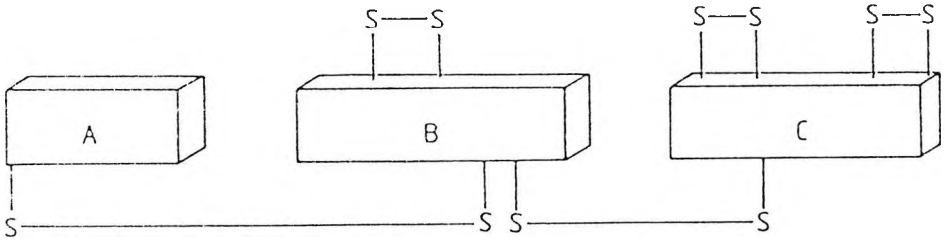

Figure 6.3 Schematic diagram illustrating structural elements of the α-chymotrypsin protease.

Incorporation of these design elements into a ruthenium(II) complex was realised through the synthesis of

bis(1,10-phenanthro-line)(4-[N-(2-phenylethyl chloromethyl ketone)sulphamoylpheny]-1,10-phenanthroline)ruthenium(II) bishexafluorophophate **(C24A)**.

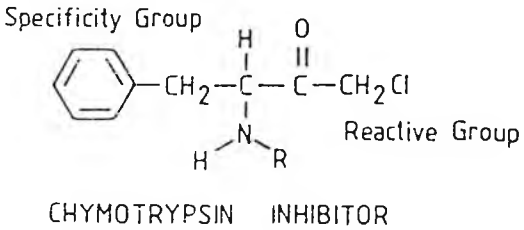

CHYMOTRYPSIN INHIBITOR

Figure 6.4 Structure of the chymtrypsin inhibitor molecule.

Labelling of chymotrypsin was affected by treatment in a 0.1 M Hepes buffer, 0.1 M sodium chloride pH 7.50 solution with **(C24A)** (20 fold excess) in a 4% by volume amount of DMSO, at room temperature for thirty minutes. Separation from reactants was achieved on a Sephadex G25 column, followed by a Sephadex DEAE-A50 column (eluted with 0.05 M PBS) with concentration by addition of dry G25 beads.

Qualitative confirmation of formation was provided by a negative reaction of the conjugate with N-succinyl-Ala-Ala-Pro-Phe p-nitroanilide (no hydrolysis to p-nitrophenol detected).

Photophysical data for the conjugate is presented in the Table 6.2. The perturbation observed for the bound ruthenium is very interesting. Normally conjugation results in longer lifetime (see Section 6.1), yet quite clearly, some form of quenching is evidenced.

Table 6.2 LIFETIME DATA FOR **C24A** RECORDED IN PHOSPHATE BUFFERED SALINE, AT 25°C.

COMPLEX/CONJUGATE	OBSERVED LIFETIME (s)
C24(a)	3.60-3.70
C24(b)	1.15-1.00
Chymotrypsin(a)	1.55-1.58
Chymotrypsin(b)	0.70

(a) deoxygenated
(b) oxygenated

Utilisation of this novel metallo-protein system to study electron transfer as a function of distance was visualised as proceeding through outer-sphere association with a suitable inorganic complex[21,22].

At physiological pH (~ pH 7), aspartic and glutamic acid residues are dissociated and have single negative charges; arginine, uncoordinated histidine and lysine are protonated and carry single positive charges (it is accepted that this is an over-simplification, and in reality local effects such as H-bonding to proximal groups will give abnormal pK_a values). These charged regions give rise to possible electrostatic binding sites for association of a charged redox partner, allowing possible electron transfer.

The position of the binding site can be explored by use of NMR[85]. Thus, a complex of similar dimensions and charge to the redox partner, but which is redox inactive and paramagnetic may reveal the position of the binding site by analysis of NMR line broadening experiments.

REFERENCES

1. Hugli, T.E.; Gurd, F.R.N. J. Biol. Chem., **245**, 1930, 1970.
2. Hugli, T.E.; Gurd, F.R.N. J. Biol. Chem., 245, 1939, 1970.
3. Garner, M.H.; Garner, W.H.; Gurd, F.R.N. J. Biol. Chem., **248**, 5451, 1973.
4. Hartzell, C.R.; Bradshaw, R.A.; Hapner, R.D.; Gurd, F.R.N. J. Biol. Chem., **243**, 690, 1968.
5. Hartzell, C.R..; Gurd, F.R.N. J. Biol. Chem., **244**, 147, 1969.
6. Garner, M.H.; Bogardt, R.A.; Gurd, F.R.N. J. Biol. Chem., **250**, 4398, 1975.
7. Morrow, J.S.; Keim, P.; Visscher, R.B.; Marshall, R.C.; Gurd, F.R.N. Proc. Natl. Acad. Sci. U.S.A., **70**, 1414, 1973.
8. Benesch, R.E.; Benesch, R.; Yu, C.I. Biochem, 8, 2567, 1969.
9. Kilmartin, J.V.; Rossi-Bernardi, L. Nature, **222**, 1243, 1969.
10. Axup, A.W.; Albin, M.; Mayo, S.L.; Crutchley, R.J.; Gray, H.B. J. Am. Chem. Soc., **110**, 435, 1988.
11. Sykes, A.G. Chem. Soc. Rev., **14**, 283, 1985.
12. Lappin, A.G.; Segal, M.G.; Weatherbum, D.C.; Sykes, A.G. J. Am. Chem. Soc., **101**, 2297, 1978.
13. Dickerson, R.E. The Proteins, 2, Ed. Neurath, H., 2nd Edit., Academic Press, 1964.

14. Edmundson, A.E. Nature, 205, 883, 1965.

15. Kendrew, J.C. Sci. Amer., 205, 96, 1961.

16. Kendrew, J.C. Science., 139, 1259, 1963.

17. Supplied by D. Chapple.

18. Crutchley, R.J.; Ellis, W.R.; Gray, H.B. J. Am. Chem. Soc., 107, 5002, 1985.

19. Atkins, P.W. Physical Chemistry, 2nd Edit., Oxford University Press, 1982.

20. Marcus, R.A.; Sutin, N.J. Biochim. Biophys. Acta., 811, 265, 1985.

21. Holwerda, R.A.; Wherland, S; Gray, H.B. Annu. Rev. Biophys. Bioeng., 5, 363, 1976.

22. Lappin, A.G. Metal Ions in Biological Systems, ed. Sigel, H., M. Dekker, New York, 13, 1981.

23. Stryer, L. Biochemistry, 3rd Edit., W.H. Freeman and Co., New York, 1988.

24. Williams, G.; Claydon, N.J.; Moore, G.R.; Williams, R.J.P. J. Mol. Biol., 183, 447, 1985.

7.0 CONCLUSION

The objective of this project was to elucidate the parameters influencing electron transfer between an electron donor and acceptor, spatially separated and rigidly held by a bridging medium.

$$D\text{——}A \xrightarrow{h\nu} D^{*}\text{——}A \xrightarrow{ET} D^{\pm}\text{——}A^{-} \quad (1)$$

In our approach to the elucidation of pertinent parameters governing event (1), the donor component of the molecular rectifier [of the form donor-insulator-acceptor-system (DIAS)] had to possess:

i) a long lived photon populated excited state and,

ii) stability/solubility in a range of solvents.

This project has primarily focused on the design of reaction conditions to yield pure ruthenium complexes which satisfied these criteria. This has led to the development of a synthesis to an isolatable reactive novel ruthenium complex, bis(1,10-phenanthroline)bis(trifluoromethane-sulphonato)ruthenium(II) (CTf).

From the 29 new ruthenium(II) polyaza-cavity complexes reported, it is found that maximisation of desired donor properties are conferred upon mono-nuclear ruthenium species. Partiularly when two of the ligands are 1,10-phenanthroline, and the third is a 1,10-phenanthroline ligand functionalised in the 4 and/or 7 positions with aryl substituents.

Analysis of the luminescence photochemical data shows no trend for tuning of the excited state in most of the

mononuclear metallo-complexes. Substitution to the parent tris(1,10-phenanthroline) coordination sphere merely alters non-radiative decay rates. Tuning of the excited state is only observed upon a) alteration of the ligators' magnitude of d level splitting (as for C12) and b) large perturbation of the ligands π^*-levels.

The dinuclear complexes C28 and C29 show exciting characteristics required of tailored excited state species. This is through the appearance of low energy (> 500 nm) absorption spectral features. However, more examples of these species are required to identify a trend.

The three fundamental questions we wished to address by analysis of DIAS's were;

I) Over what range can an electron be transferred ?

II) To what extent are solvent molecules involved ?

III) Can a protein act as a solvent or as a conduit for an electron ?

It became obvious that our initial strategy to answer these questions would require more man years then available. The aims were re-focused to address questions I) and III).

Conjugation of bis(1,10-phenanthroline)[4-*p*- chloro-sulphonyl)phenyl-1,10-phenanthroline]ruthenium(II) to sperm whale myoglobin gave reproducible quenching (three experiments presented) consistent with mono-modification.

Analysis of the data assuming N-terminal protein modification correlates with arguments for which precedent is provided in the literature (namely the existence of through

space coupling enhancement between a donor and acceptor and long distance electron transfer).

Functionalisation of a ruthenium complex with L-chloro-methylketone (C24A), provided a route to mono modification of α-chymotrypsin. Analysis of the data from the affinity labelled conjugate (reproducible) show inner-sphere quenching of the ruthenium(II) complex excited state. By comparison with results obtained for apomyoglobin conjugates, the disulphide residues in α-chymotrypsin are thought to be responsible for this observation.

The results demonstrate the suitability and usefulness of ruthenium polyaza-cavity complexes in the approach to answering I) and III).

However, our application of this interdisciplinary technology serves to illustrate that more sophisticated resources and facilities are necessary to carry out experiments of sufficient number and quality to quantitatively address such fundamental questions.

8.0 EXPERIMENTAL SECTION

All synthetic reactions were performed under a nitrogen atmosphere. All solvents used for preparations were dried and distilled prior to use , unless otherwise stated. Starting organic materials were obtained commercially and were purified to accepted levels of elemental analysis when necessary. All compounds synthesised were isolated by column chromatography. The solid phase tended to be neutral alumina, and eluent systems were usually (water/chloroform/methanol), (acetic acid/toluene/dichloromethane), (acetonitrile) and (0,5 M tetraethylammonium tetrafluoroborate in methanol) choices. Infra-red spectra were recorded on a Perkin-Elmer 983G (-indicates very strong peak), and proton n.m.r. on a Jeol JNM-MH-100(f-relates to resonances from functionalised phenanthroline, *-relates to voyeur phenanthroline pair). CHN Analysis were obtained on a Carlo-Erba instrument.*

Preparation of 3,6-bis(2'-pyridyl)-4,5-dihydro-1,2,4,5-tetrazine, (L18).

A solution of 2-cyanopyridine (5.2 g, 0.05 mol) and hydrazine monohydrate (14.28 cm^3, 0.20 mol) in 50 cm^3 ethanol was refluxed gently for seven hours. The orange mixture (suspension) was kept at 0 °C overnight, and the resulting orange precipitate collected and recrystallised from ethanol (2.50 g ~42% yield based on 2-cyanopyridine), m.p. 193 °C (lit., m.p. 194.2 °, 193-194 °C). Fine yellow needles.

δ ($CDCl_3$) 8.65 (2 H, bs, 3-H; NH), 8.15 (1 H, d, J = 8 Hz, 6-H), 7.80 (1 H, ddd, $J_{4,5} = J_{4,3} = 8$ Hz; $J_{4,2} = 2$ Hz, 4-H), 7.45 (1 H, $J_{5,6} = J_{5,4} = 8$Hz, 5-H)

Anal. Calcd for $C_{12}H_8N_6$: C, 60.50; H, 4.23; N, 35.27. Found: C, 60.37; H, 4.10; N, 35.25.

Preparation of 3,6-bis(2'-pyridyl)-1,2,4,5-tetrazine, **(L17)**.

The dihydrobase **(L18)** (1.0 g,0.0042 mol) was dissolved in 50 cm3 of glacial acetic acid, with heating to 70 °C. Concentrated nitric acid (8 cm^3) was added dropwise with cooling (yellow solution turns deep red). An excess of crushed ice was added and the mixture made distinctly alkaline by addition of saturated sodium bicarbonate solution. The crystalline precipitate was separated [0.65 g ~65% yield based on **(L18)**], m.p. 221 °C (lit., m.p. 224.5°, 222° C dec.). Purple-red solid.

δ ($CDCl_3$) 9.00 (1 H, d, J = 4 Hz, 3-H), 8.75d (1 H, d, J = 8 Hz, 6-H), 8.04 (1 H, ddd, $J_{5,6} = J_{5,4} = 8$ Hz; $J_{5,3} = 2$ Hz, 4-H), 7.60 (1 H, dd, $J_{4,5} = 8$Hz; $J_{4,3} = 4$ Hz, 3-H)

Anal. Calcd for $C_{12}H_8N_6$: C, 61.07; H, 3.41; N, 35.57. Found: C, 60.17; H, 3.21; N, 34.72.

ν_{max}: 3440, 3095-3059, 1630, 1583*, 1443, 1390*, 1259, 1131*, 1092, 994, 920, 799*, 745*-733 and 620-598* cm^{-1}

Preparation of 2,3,5,6-tetrakis(2'-pyridyl)pyrazine **(L19)**.

α-Pyridoin (5.0 g, 0.023 mol) and ammonium acetate (22.5 g, 0.292 mol) were mixed in a 100 cm^3 Quick-fit boiling tube, fitted with a reflux condenser and slowly heated to 180 °C in

an oil bath. The mixture became molten, and a very dark brown-green colour developed. The heating was continued for two and a half hours with continuous stirring. The yellow crude product was isolated and washed with ethanol, then recrystallised from pyridine (leaving a fluorescent yellow mother liquor). The product was again washed with ethanol, and dried at reduced pressure (1.0 g ~22% yield based on - pyridoin), m.p. 282 °C (lit., 284 °C). Colourless fine platelet crystals.

d (DMSO-d6) 8.40 (1 H, d, J = 6 Hz, 3-H), 8.05 (1 H, d, J = 10 Hz,6-H), 7.78 (1 H, dd, $J_{4,5}$ = 8 Hz; $J_{4,3}$ = 6 Hz, 4-H) 7.20 (1 H, dd, $J_{5,6}$ = 10 Hz; $J_{5,4}$ = 8 Hz, 5-H)

Anal. Calcd for $C_{24}H_{16}N_6$: C, 74.21; H, 4.15; N, 21.64. Found: C, 74.07; H, 4.20; N, 21.56

ν_{max}: 3441, 3084-3050-3017, 1608, 1588*-1566*, 1484, 1434, 1391*, 1151-1130*, 1095, 1037, 989, 808-785*-754 and 552 cm^{-1}

Preparation of 4,5-diazafluoren-9-one (L20).

1,10-Phenanthroline (8.0 g, 0.044 mol) was dissolved slowly (added over ~15 minutes) in 25 cm^3 of fuming sulphuric acid with continuous stirring; in a 250 cm^3 three-necked flask, fitted with a thermometer; ensuring the temperature in the flask did not rise above 60 °C so as to minimise attendant carbonisation.

Fuming nitric acid (22 cm^3) was added dropwise with caution to avoid violent splattering and also to ensure that the temperature did not exceed 120 °C.

Following the addition of fuming nitric acid, the reaction

mixture was heated under reflux in an oil bath at 175 °C, with stirring, for thirty minutes.

The reaction mixture was allowed to cool, then poured onto 200 g of crushed ice. The strongly acidic solution was then cautiously neutralised with a 30% sodium hydroxide solution (keeping the mixture below 10 °C) (colour change-white copious precipitate goes to green solution). Sufficient dilute nitric acid was added to make the contents of the beaker just acidic to litmus. The precipitate (of 5-nitro-1,10-phenanthroline, L2) was collected.

a) The filtrate was then made just basic with sodium hydroxide solution, and then evaporated to half of its volume (300 cm^3) on a hot plate.

The black solid obtained by filtration was dried, crushed, washed with water to remove co-precipitated inorganic salts, dried and then boiled in 200 cm^3 of ethanol. This suspension was cooled and filtered through filter-aid

The orange solid (obtained by isolation on rotavapor) was loaded onto a vacuum column and eluted with ethanol to yield a silvery-yellow solid on evaporation. Recrystallisation from water gave long silver-yellow needles [**(L2)**, 8.00 g ~80% yield; **(L20)**, 0.60 g ~7% yield; based on 1,10-phenanthroline].

b) The strongly acidic solution was adjusted to pH 6 with 10M aqueous sodium hydroxide, and the solution extracted with chloroform. The dried organic phase was stripped of solvent and the residue crystallised from methanol.[**(L21)**, 1.20 g ~

12% yield; based on 1,10-phenanthroline]

(L2) Anal. Calcd for $C_{12}H_7N_3O_2$: C, 64.00; H, 3.13; N, 18.66. Found: C, 63.97; H, 3.10; N, 18.58.

d ($CDCl_3$) 9.43 (1 H, dd, $J_{9,8}$ = 4.5 Hz; $J_{9,8}$ = 1.9 Hz, 9-H), 9.38 (1 H, dd, $J_{2,3}$ = 3.7 Hz; $J_{2,4}$ = 1.9 Hz, 2-H), 9.04d (1 H, dd, $J_{7,8}$ = 8.6 Hz; $J_{7,9}$ = 1.9 Hz, 7-H), 8.68 (1 H, s, 6-H), 8.46 (1 H, dd, $J_{4,3}$ = 7.5 Hz; $J_{4,2}$ = 1.9 Hz, 4-H), 7.86d (1 H, $J_{8,7}$ = 8.6 Hz; $J_{8,9}$ = 4.5 Hz, 8-H), 7.82 (1 H, dd, $J_{3,4}$ = 7.5 Hz; $J_{3,2}$ = 3.7 Hz, 3-H)

ν_{max}: 3419, 3079, 1619-1602-1589, 1519*, 1446, 1419*, 1383, 1357*, 1310, 1287, 1202, 1145, 905, 833*-807*, 745-734*-714 and 622 cm^{-1}

(L20) Anal. Calcd for $C_{11}H_6N_2O$: C, 72.52; H, 3.13; N, 15.37. Found: C, 72.55; H, 3.13; N, 15.33.

d ($CDCl_3$) 8.80 (2 H, d, J = 5.0 Hz, 2-H; 9-H), 8.00 (2 H, d, J = 8.0 Hz, 4-H; 7-H), 7.30 (2 H, dd, $J_{3,4}$ = 8.0 Hz; $J_{3,2}$ = 5.0 Hz, 3-H; 8-H)

m/z (EI) 183 (M + 1) and 182 (M^+, 100%).

(L21) Anal. Calcd for $C_{12}H_6N_2O_2$: C, 68.57; H, 2.88; N, 13.33. Found: C, 68.60; H, 2.77; N, 13.16.

d ($CDCl_3$) 9.12 (1 H, dd, $J_{2,3}$ = 4.7 Hz; $J_{2,4}$ = 1.7 Hz, 2-H), 8.45 (1 H, dd, $J_{4,3}$ = 7.5 Hz; $J_{4,2}$ = 1.7 Hz, 4-H), 7.60 (1 H, dd, $J_{3,4}$ = 7.5 Hz; $J_{3,2}$ = 4.7 Hz, 3-H)

ν_{max}: 3581*, 2923*, 1686*, 1566*, 1461*, 1481*, 1317*, 1300*, 1286*, 1209*, 1121*, 1091*, 1062*, 1018*, 929* and 739* cm^{-1}

m/z (EI) 210 (M^+, 6%), 183 (13%) and 182 (100%).

Preparation of 5-amino -1,10-phenanthroline L3.

To (L2) (1.0 g, 0.0044 mol) was dissolved in 125 cm^3 of ethanol and the mixture set refluxing. To this mixture was added hydrazine monohydrate (4 cm^3, ~0.08 mol) followed by activated palladium (~1.5 g). Upon addition, the mixture fizzes wildly. Reflux was continued for ten minutes and the addition of activated palladium then repeated, this process was repeated until no further fizzing was noted - usually only three additions required. After refluxing for a final ten minutes, the reaction mixture was cooled, filtered with care, and the ethanol removed. The residue was dissolved in dilute hydrochloric acid and the product precipitated by making the solution (100 cm^3) alkaline. The product was recrystallised from 100 cm^3 of water (0.70 g ~80% based on L2). Yellow fine needles.

Anal. Calcd for $C_{12}H_9N_3$: C, 73.83; H,4.65; N, 21.52. Found: C, 73.69; H, 4.63; N, 21.60.

d (DMSO-d6) 8.82 (1 H, dd, $J_{2,3}$ = 3.7 Hz; $J_{2,4}$ = 1.5 Hz, 2-H) 8.50 (1 H, dd, $J_{4,3}$ = 8.3 Hz; $J_{4,2}$ = 1.5 Hz, 4-H), 8.46 (1 H, dd, $J_{9,8}$ = 4.5 Hz; $J_{9,7}$ = 1.5 Hz, 9-H), 7.85 (1 H, dd, $J_{7,8}$ = 7.5 Hz; $J_{7,9}$ = 1.5 Hz, 7-H), 7.56d (1 H, dd, $J_{8,7}$ = 8.3 Hz; $J_{8,9}$ = 4.5 Hz, 8-H), 7.32 (1 H, dd, $J_{3,4}$ = 7.5 Hz; $J_{3,2}$ = 3.7 Hz, 3-H), 6.76 (1 H, s, 6-H)

d (MeOD-d3) 8.82 (1 H, dd, $J_{2,3}$ = 4.1 Hz; $J_{2,4}$ = 1.5 Hz, 2-H) 8.50 (1 H, dd, $J_{9,8}$ = 4.1 Hz; $J_{9,7}$ = 1.5 Hz, 9-H), 8.37 (1 H, dd, $J_{4,3}$ = 7.9 Hz; $J_{4,2}$ = 1.5 Hz, 4-H), 7.84 (1 H, dd, $J_{7,8}$ = 7.9 Hz; $J_{7,9}$ = 1.5 Hz, 7-H), 7.52 (1 H, dd, $J_{3,4}$ =

7.9 Hz; $J_{5,6}$ = 4.1 Hz, 3-H), 7.32 (1 H, dd, $J_{8,7}$ = 7.9 Hz; $J_{8,6}$ = 4.1 Hz, 8-H), 6.80d (1 H, s, 6-H)

ν_{max}: 3417*-3324*-3229*, 1637*-1612*-1595*-1560, 1503-1488*, 1454, 1429*-1408*, 1341-1304, 1273, 1220, 1129-1108, 1068, 1035, 885, 843*-826-814-792, 741*,711, 652 and 628 cm^{-1}

m/z (EI) 196 (M + 1, 14%) and 195 (M^{+}, 100%).

Preparation of o-bis(ß-dicarbethoxyvinylamino)benzene A.

A mixture of o-phenylenediamine (5.00 g, 0.0463 mol) and ethoxymethylenemalonic ester (20.0 g, 0.0463 mol) was heated for four hours at 100 °C. When cooled, the solidified reaction mixture was dissolved in 40 cm^{3} of boiling methanol. The brown solution was cooled to 0 °C, where upon a white crystalline solid was deposited.

The solid was dissolved in 300 cm^{3} of ethylacetate, and washed with dilute hydrochloric acid (300 cm^{3}), saturated sodium bicarbonate, and finally with water. The dried organic phase was stripped of solvent and the resulting oil taken up in 40 cm^{3} of boiling methanol. On cooling to 0 °C, a white mass was obtained, which was dried at reduced pressure (21.07 g ~100% based on o-phenylenediamine).

Anal. Calcd for $C_{22}H_{28}N_{2}O_{8}$: C, 58.92; H, 6.29; N, 6.25. Found: C, 58.68; H, 6.42; N, 6.01.

d ($CDCl_{3}$) 10.70 (1 H, broad d, J = 12.9 Hz, -NH-), 8.17 (1 H, d, J = 12.9 Hz, -CH=), 7.07 (2 H, s, Ar-H), 4.22d (2 H, q, J = 6.6 Hz, $-CH_{2}-$), 4.13 (2 H, q, J = 6.0 Hz, $-CH_{2}-$),

1.30 (6 H, m, $-CH_3$)

ν_{max}: 3414, 3146, 2978*, 2932*, 2932*, 1718*, 1693*, 1657*, 1619*, 1582*, [1500-1000 * peaks] 797* and 758* cm^{-1}

Preparation of 3,8-dicarbethoxy-4,7-dihydroxy-1,10-phenanthroline L10.

To 75 cm^3 of refluxing diphenyl was added (A) (2.5 g, 0.006 mol) over a period of five minutes. The mixture was refluxed for an additional twenty-five minutes and then allowed to cool to room temperature. To the semi-solid mass was added 25 cm^3 of (80-100) petroleum ether, the mixture stirred vigorously and then filtered. The precipitate was triturated with 50 cm^3 of petroleum ether; the mixture was filtered and the solid (off-white) was washed with ethylacetate [1.22 g ~57% based on (A)]

Anal. Calcd for $C_{18}H_{16}N_2O_6$: C, 60.67; H, 4.53; N, 7.86. Found: C, 60.49; H, 4.52; N, 7.91.

ν_{max}: 3428, 3179, 2983*, 1715*, 1673*, 1610*, 1535 [1500-800 * peaks] and 790* cm^{-1}

m/z (EI) 356 (M^+, 13%), 284 (81%), 265 (25%) and 238 (100%).

Preparation of 3,8-dicarboxy-4,7-dihydroxy-1,10-phenanthroline L11.

A mixture of (L10) (1.25 g, 0.004 mol) and 150 cm^3 of 20% potassium hydroxide solution was refluxed for three hours. The reaction mixture was filtered while hot, cooled and extracted with (60-80) petroleum ether, then neutralised with 30% hydrochloric acid. The white precipitate was isolated,

washed with a large volume of water, and dried at reduced pressure [1.00 g ~90% yield based on (**L10**)].

Anal. Calcd for $C_{14}H_8O_6N_2$: C, 56.01; H, 2.69; N, 10.66. Found: C, 52.87; H, 3.03; N, 8.72.

d (NaOD) 8.50 (2 H, s, 2-H; 9-H), 7.90 (2 H, s, 5-H; 6-H)

ν_{max}: 3580*, 3236, 3079*, 1712*b, 1622*, 1535*, 1461, 1390*, 1322*, 1279*, 1208*, 948*, [peak at 906 characteristic of S.M. impurity] 796* and 399* cm^{-1}

Preparation of 4,7-dihydroxy-1,10-phenanthroline **L4.**

Into a 10 cm^3 R.B. flask, (**L11**) (0.40 g, 0.0013 mol) was placed. The flask was immersed in a Wood's metal bath maintained at ~320 oC. The time required for decarboxylation was fifty minutes.

No solvent could be found for the product, though partial solubility was noted in DMSO [0.23 g ~81% based on (**L11**)]. Yellow powder.

Anal. Calcd for $C_{12}H_8N_2O_2$: C, 67.92; H, 3.80; N, 13.80. Found. C, 66.78; H, 3.59; N, 12.80.

ν_{max}: 3368, 3239, 3185, 3034-2979-2915, 1679, 1643, 1598*-1552*-1501*, 1449*-1434*-1413-1385, 1255*, 1213*-1190*, 1130, 909, 856-806*, 723, 677-663, 548-509 and 365 cm^{-1}

m/z (EI) 213 (M + 1, 13%), 212 (M^+, 100%), 184 (54%), 156 (13%) and 155 (13%)

Preparation of 4,7-dichloro-1,10-phenanthroline (**L5**).

In a 50 cm^3 R.B. flask, equiped with magnetic stirrer and reflux condenser, a mixture of phosphorous pentachloride

(2.0 g, 9.6×10^{-3} mol) and phosphorous oxychloride (3.2 g, $21 * 10^{-3}$ mol) was heated to 90 °C. To this mixture was added as quickly as possible, (L4) (1.0 g, 4.7×10^{-3} mol). The temperature of the mixture was then raised to 130 °C and maintained there for one hour.

The mixture was poured (after allowing to cool to room temperature) onto ice. The suspension was stirred overnight, and then filtered. The filtrate was made alkaline with a 15% sodium hydroxide solution, the white precipitate collected, and dried in an oven at 80 °C.

The dried product was dissolved in ~150 cm^3 of boiling methanol. The alcohol solution was filtered through 60H kieselgel and concentrated to half its volume. To this was added 5 cm^3 of water and the mixture was then cooled in ice and filtered [0.88 g ~76% based on (L4)]. Buff coloured compound.

Anal. Calcd for $C_{12}H_6N_2Cl_2$: C, 57.86; H, 2.43; N, 11.25. Found: C, 57.03; H, 2.25; N, 10.89.

d ($CDCl_3/Cl_3CCO_2H$) 9.25 (2 H, d, J = 5.0 Hz, 2-H; 9-H), 8.43 (2 H, s, 5-H; 6-H), 8.05 (2 H, d, J = 5.0 Hz, 3-H; 8-H)

ν_{max}: 3418, 2923*, 1644, 1609*, 1573*, 1549*, 1495*, 1432*, 1413*, 1213*, 1080*, 840*, 813*, 781* and 721* cm^{-1}

m/z (EI) 252 (M + 4, 10%), 250 (M + 2, 65%), 248 (M^+, 100%), 215 (17%) and 213 (52%).

Preparation of 1,10-phenanthroline-5,6-quinone (L21).

In a R.B. flask (L3) (0.35 g, 0.0018 mol) was mixed with cold concentrated sulphuric acid (2 cm^3). Fuming nitric acid (~1.2 cm^3) was added dropwise with stirring (causing solution of suspension). The mixture was heated to 120 °C for two hours, cooled and poured onto ice (10 g). The pH was adjusted to ~6 With 10 M aqueous sodium hydroxide, and the solution extracted with chloroform. The dried organic phase was stripped of solvent and the residue recrystallised from methanol to afford the product [0.05 g ~13% based on (L3)]. Bright orange crystals.

Anal. Calcd for $C_{12}H_6N_2O_2$: C, 68.57; H, 2.88; N, 13.33. Found: C, 68.50; H, 2.79; N, 13.07

d ($CDCl_3$) 9.12 (1 H, dd, $J_{2,3}$ = 4.7 Hz; $J_{2,4}$ = 1.7 Hz, 2-H), 8.45 (1 H, dd, $J_{4,3}$ = 7.5 Hz; $J_{4,2}$ = 1.7 Hz, 4-H), 7.60 (1 H, dd, $J_{3,4}$ = 7.5 Hz; $J_{3,2}$ = 4.7 Hz, 3-H)

m/z (EI) 210 (M^+, 6%), 183 (13%) and 182 (100%)

Preparation of 4,7-dibromo-1,10-phenanthroline L6.

Prepared as described for L5 but using;

Phosphorous oxybromide	4.00 g, 14 mmol
L4	0.1887 g, 0.9 mmol

The phosphorous oxybromide required purification by distillation prior to use. This gave 0.1517 g ~50% based on L4. Buff powder.

Anal. Calc. for $C_{12}H_6N_2Br_2$: C, 42.64; H, 1.78; N, 8.28. Found: C, 42.50; H, 1.81; N, 8.20.

d (TFA) 9.65 (1 H, d, J = 6.0 Hz, 2-H; 9-H), 9.25 (1 H, s, 5-H; 6-H), 9.04 (1 H, d, J = 6.0 Hz, 3-H; 8-H)

ν_{max}: 3410*, 1606, 1567-1547, 1489*, 1408*-1369, 1207-1183, 1061, 840, 784-762, 722 and 532 cm^{-1}

Preparation of 4,7-bisthiophenoxy-1,10-phenanthroline L7.

A mixture of **L5** (0.30 g), thiophenol (4 cm^3) and potassium hydroxide (0.3 g) was heated to 100 °C for 10h. The mixture was digested with 30% aqueous potassium hydroxide solution (40 cm^3) and the mixture filtered. The residue was washed with water and crystallised from aqueous methanol to afford the thiophenoxy derivative (0.24 g ~51%)

Anal. Calcd. for $C_{24}H_{14}N_2S_2$: C; 73.14, H; 3.58, N;7.10. Found: C; 73.02, H; 3.48, N; 7.22.

d (AcOD-d3) 8.60 (2 H, d, J = 5.3 Hz, 2-H), 8.18 (2 H, s, 5-H), 7.44 (5 H, broad s, Ar-H) 7.04 (2 H, d, J = 5.3 Hz, 3-H).

Preparation of 3,8-dicarbethoxy-4,7-dichloro-1,10-phenanthroline L12.

To a stirred suspension of chilled **L10** (1.0 g, 2.8 mmol) in triethylamine (0.57 g, 5.6 mmol) was added (cautiously) phosphorous oxychloride (10 cm^3), whereupon the temperature was raised to 130 °C and maintained there for one hour. The reaction mixture was worked up as for **L5**, but on making alkaline, the filtrate was extracted with dichloromethane (0.76 g ~69%).

Anal. Calcd. for $C_{16}H_{14}N_2O_4Cl_2$: C, 54.98; H, 3.58; N, 7.12. Found: C, 54.98; H,3.47; N, 7.14.

d ($CDCl_3$) 9.40 (1 H, s, 2-H; 9-H), 8.40 (1 H, s, 5-H; 6-H), 4.67 (2 H, q, J = 7.0 Hz, $-CH_2-$), 1.50 (3 H, t, J = 7.0 Hz, $-CH_3$)

ν_{max}: 3436, 1725, 1604, 1549*, 1479*, 1430*, 1368*-1335*, 1291-1258, 1213, 1086, 1002*, 835*-806*-793*-773*, 685, 605-576-543 and 476 cm^{-1}.

Preparation of 3,8-dicarbethoxy-4,7-dioxy-p-cyanobenzyl-1,10-phenanthroline **L13.**

To a dry acetone slurry of **L10** (1.0 g, 2.8 mmol) and excess potassium carbonate, was added 4-cyanobenzyl chloride (0.85 g, 5.6 mmol). The mixture was refluxed for 2h. Removal of the solvent followed by extraction with dichloromethane gave the product (1.37 g, ~83%)

d $CDCl_3$ 8.66 (2 H, s, 2-H; 9-H), 8.36 (1 H, d, J = 8.3 Hz, 5-H), 8.00 (1 H, d, J = 8.3 Hz, 6-H), 7.38 (4 H, d, J = 7.5 Hz, Ar-H), 7.08 (4 H, d, J = 7.5Hz, Ar-H), 6.40 (4 H, s, $-CH_2Ar$), 4.40 (4 H, m, $-CH_2-$), 1.40 (6 H, m, $-CH_3$)

Preparation of 3,3'-dinitro-2,2'-bipyridyl **L15.**

Method a) 2-Chloro-3-nitropyridine (5.00 g, 0.032 mol), DMF (30 cm^3) and copper powder (copper bronze for organic synthesis; 5.00 g, 0.079 g atom) were stirred and heated at 100 °C for fifteen hours. The reaction mixture was cooled and poured into 300 cm^3 of water and the precipitate separated onto a no. 4 sintered glass funnel, and washed with water.

The solid was triturated on the filter with concentrated ammonia (3 x 35 cm^3), washed with ice cold ethanol (2 x 30

cm^3) and extracted with boiling dioxan (4 x 30 cm^3). The product was recrystallised from dioxan (0.99 g ~12% based on 2-chloro-3-nitropyridine). Buff coloured orthorhombic crystals. Mpt. 210 °C

Anal. Calcd for $C_{10}H_6N_4O_4$: C, 48.78; H, 2.45; N, 22.75. Found: C, 48.83; H, 2.35; N, 22.77.

d (DMSO-d6) 8.87 (1 H, dd, $J_{6,4}$ = 1.5 Hz; $J_{6,5}$ = 4.5 Hz, 6-H), 8.66 (1 H, dd, $J_{4,5}$ = 7.5 Hz; $J_{4,6}$ = 1.5 Hz, 4-H), 7.90 (1 H, dd, $J_{5,4}$ = 7.5 Hz; $J_{5,6}$ = 4.5 Hz, 5-H)

ν_{max}: 1590, 1559-1529*, 1440, 1415, 1365*, 1049-1038, 865-855, 821, 790, 751, 703, 621 and 529 cm^{-1}

m/z (EI) 246 (M^+, 1%), 200 (78%), 91 (70%), and 63 (100%)

Method b) Powdered lithium (0.048 g, 6.9 mmol) was sonocated in dioxane (50 cm^3) for 5 minutes in a conical flask (250 cm^3). To this suspension was added 2-chloro-3-nitropyridine (1.00 g, 6.3 mmol) and sonocation resumed and continued for 6 hrs. The hot reaction mixture was cooled and water (5 cm^3) added dropwise. The solvent was then removed and the solid residue soxlet extracted with dichloromethane. Separation on alumina (chloroform) gave 360 mg **L15**. Mpt. 210 °C

Anal. Calcd for $C_{10}H_6N_4O_4$: C, 48.78; H, 2.45; N, 22.75. Found: C, 48.80; H, 2.46; N, 22.79

5,6-Diaza-1,10-phenanthroline **L14**.

To a suspension of powdered (**L15**) (5.00 g, 0.032 mol) in 200 cm^3 water, was added sodium sulphide nonahydrate (45.00 g, 0.19 mol) and the resulting solution stirred at room

temperature for five hours. The solution was extracted with chloroform (3 * 100 cm^3). The extract was then washed with water, dried, and stripped of solvent; the bright yellow residue was recrystallised from ethanol to give bright yellow needles (2.77 g, 97%).

Anal. Calcd for $C_{10}H_6N_4$: C, 65.93; H, 3.32; N, 30.75

Found: C, 66.00; H, 3.37; N, 30.90

d ($CDCl_3$) 9.43 (2 H, dd, $J_{2,3}$ = 5 Hz; J2,4 = 1.5 Hz, 2-H; 9-H), 9.13 (2 H, dd, $J_{4,3}$ = 8.0 Hz; $J_{4,2}$ = 1.5 Hz, 4-H; 7-H), 8.02 (2 H, dd, $J_{3,4}$ = 8.0 Hz; $J_{3,2}$ = 5.0 Hz, 3-H; 8-H)

3,3-Diamino-2,2-bipyridyl **L16.**

To **L14** (50 mg, 0.27 mmol) dissolved in acetic acid (2cm^3)was added zinc dust (325 mg, 5.0 mmol). After the initial vigorous reaction the mixture was heated to ~70°C for 5 min., and then allowed to cool to room temperature, filtered and solvent removed. The residue was dissolved in water (2 cm^3) and made alkaline with ammonia to give a precipitate of the diamine (30 mg, 58%).

Anal. Calcd for $C_{10}H_{10}N_4$: C, 64.50; H, 5.41; N, 30.09

Found: C, 64.60; H, 4.78; N, 29.87

1,2,3,4-Di(2,3-pyrido)phenazine **L30.**

To a solution of **L21** (0.1 g, 0.00048 mol) in boiling methanol (5 cm^3) was added 1,2-phenylenediamine (0.057 g, 0.00052 mol). A trace of trifluoroacetic acid was added, and heating continued for five mins. Toluene (1 cm^3) was added and the solution cooled in ice, an almost colourless solid

solid being isolated (0.11 g, 82%).

Anal. Calcd., for $C_{16}H_{10}N_4$: C, 76.58; H, 3.57; N, 19.85.

Found: C, 76.28; H, 3.64; 19.74

d (AcOD-d3) 8.99 (1 H, dd, $J_{3,2}$ = 16.5 Hz; $J_{3,1}$ = 3.0 Hz, 3-H), 8.84 (1 H, dd, $J_{1,2}$ = 8.3 Hz; $J_{1,3}$ = 7.5 Hz, 1-H), 7.82 (1 H, dd, $J_{4,5}$ = 12.0 Hz; $J_{4,5'}$ = 7.5 Hz, 4-H), 7.60 (2 H, m, 2-H; 5-H)

ν_{max}: 1632, 1574, 1488*, 1413*, 1361*, 1338, 1135, 1075*, 814, 764, 740* and 414 cm^{-1}

7-Nitro-1,2,3,4-di(2,3-pyrido)phenazine **L31**.

Synthesis as for **L30**, but using:

L21 (0.1 g, 0.00048 mol)

4-Nitro-1,2-phenylenediamine (0.084 g, 0.00055 mol)

The solid product was recrystallised from acetic acid to yield a light yellow product (0.13 g, 83%).

Anal. Calcd., for $C_{16}H_7N_5O_2$: C, 66.05; H, 2.77; N, 21.40.

Found: C, 66.03; H, 2.71; 21.38.

d (AcOD-d3) 8.76 (2 H, d, J = 7.5 Hz, 3-H), 8.46 (2 H, d, J = 4.5 Hz, 1-H), 8.31 (1 H, d, J = 2.4 Hz, 4-H), 7.90 (1 H, dd, $J_{5,6}$ = 9.0 Hz; $J_{5,4}$ = 2.4 Hz, 5-H), 7.66 (1 H, d, J = 9.0 Hz, 6-H), 7.22 (2 H, dd, $J_{2,3}$ = 7.5 Hz; $J_{2,1}$ = 4.5 Hz, 2-H)

ν_{max}: 1619, 1577, 1520*, 1481, 1408, 1343*, 1067*, 849*-831*-813*, 739*-725* and 618 cm^{-1}

4,5-Diazafluoren-9-one oxime **B**.

Added into a conical flask (50 cm^3) containing water (10 cm^3) was added **L20** (1.0 g, 0.0055 mol), hydroxylamine

hydrochloride (0.46 g, 0.0066 mol), and sodium acetate (0.54 g, 0.0066 mol); the contents of the flask were swirled until the solids dissolved, sufficient ethanol being added to ensure a clear solution. The solution was heated on a steam-bath for twenty mins., and then cooled to 0°C. The resulting precipitate was recrystallised from water (0.72 g, 66%).

Anal. Calcd. for $C_{11}H_7N_3O$: C, 67.00; H, 3.58; N, 21.31.

Found: C, 67.01; H, 35.5; N, 21.30

5-Aza-6-hydroxy-1,10-phenanthroline **L28.**

Concentrated sulphuric acid (2 cm^3) was heated in a conical flask (50 cm^3) until the temperature of the acid was atleast 90°C. In small portions **B** (0.5 g, 0.0025 mol) was added with swirling (aliquots being added after the previous vigorous reaction had subsided). The flask was maintained at 100°C for an additional fifteen mins., and then pipetted onto ice (50 g). The solution was neutralised with solid sodium bicarbonate and the product isolated by filtration (0.27 g, 54%).

Anal. Calcd. for $C_{11}H_7N_3O$: C, 67.00; H, 3.58; N, 21.31.

Found: C, 66.86; 3.67; N, 21.22.

d (DMSO-d6) 9.00 (3 H, m, 2-H; 9-H; 4-H), 8.46 (1 H, dd, $J_{7,8}$ = 7.5 Hz; $J_{7,9}$ = 0.9 Hz, 7-H), 7.80 (2 H, m, 3-H; 8-H)

ν_{max}: 3139*, 3033*, 2761*, 1725, 1593*, 1563*, 1491*-1467*, 1396*, 1172*-1158*, 1007*, 948*, 817* and 750* cm^{-1}

m/z (EI) 198 (M + 1, 13%) and 197 (M^+, 100%)

1,10-Phenanthroline-2,9-dicarboxaldehyde L22.

To a solution of 2,9-dimethyl-1,10-phenanthroline (3.00 g, 0.014 mol) in dioxan containing 4% water (200 cm^3) was added selenium dioxide (7.5 g, 0.068 mol). The solution was heated under reflux for two hours and then filtered through filter aid while still hot. The dialdehyde separated from the cold filtrate as silvery crystals (2.00 g, 59%).

Anal. Calcd. for $C_{14}H_8N_2O_2$: C, 71.18; H, 3.41; N, 11.86. Found: C, 71.10; H, 3.40; N, 11.86

d (DMSO-d6) 10.57 (1 H, s, CHO), 8.98 (1 H, d, J = 7.5 Hz, 4-H), 8.58 (2 H, m, 3-H; 5-H)

ν_{max}: 3457, 3062, 2853, 1701*, 1595, 1552, 1281, 1238, 869, 815 and 767-740 cm^{-1}

2,9-(Bishydroxymethyl)-1,10-phenanthroline L23.

A solution of L22 (0.5 g, 0.0021 mol) and sodium borohydride (0.1 g, 0.0026 mol) in ethanol (25 cm^3) was heated under reflux for two hours. The mixture was concentrated and the residue recrystallised from water to give the diol (0.38 g, 74%). Buff needles.

Anal. Calcd for $C_{14}H_{12}N_2O_2$: C, 69.99; H, 5.03; N, 11.66. Found: C, 70.00; H, 5.00; N, 11.48

d (AcOD-d3) 8.45 (1 H, d, J = 7.8 Hz, 4-H), 7.62 (2 H, m, 3-H, 5-H) 5.05 (2 H, s, $-CH_2-OH$)

2,9-(Bisbromomethyl)-1,10-phenanthroline L25.

A solution of L23 (0.2 g, 0.010 mol) and hydrobromic acid (20 cm^3) was heated under reflux for two hours and then

cooled on ice. The solution was treated with solid sodium bicarbonate until precipitation was complete. Column chromatography on silica gel [CH2Cl2/EtOAc (5:1)] gave the bromo compound as a pale yellow solid (0.22 g, 71%).

Anal. Calcd. for $C_{14}H_{10}N_2Br_2$: C, 45.94; H, 2.75; N, 7.65. Found: C, 45.78; H, 2.70; N, 7.54.

d (DMSO-d6) 8.34 (1 H, d, J = 7.2 Hz, 4-H), 7.84 (2 H, m, 3-H, 5-H), 5.40 (2 H, s, $-CH_2Br$)

Preparation of di(O-carboxymethyl)-1,10-Phenanthroline-2,9-dicarboxaldehyde oxime **L24.**

Sodium acetate (300 mg) and carboxymethoxylamine hemihydrochloride (350 mg, 1.6 mmol) were dissolved in 1 cm^3 water. The dialdehde **L22** (180 mg, 0.76mmol) was added and the reaction mixture heated to reflux for 1h. The course of the reaction was followed by tlc $CHCl_3$/MeOH/AcOH(7:2:1). The mixture was diluted with 1 cm^3 water, and extracted with dichloromethane (195 mg ~67%).

d (DMSO-d6) 8.30 (1 H, s, $-CO_2H$), 8.25 (1 H, d, J = 7.8 Hz, 4-H), 7.94 (1 H, d, J = 7.8 Hz, 3-H), 7.82 (1 H, s, 5-H), 4.74 (1 H, s, -CH=), 3.50 (1 H, s, $-CH_2-$)

2,9-Bis(tribromomethyl)-1,10-phenanthroline **L26.**

A solution of 2,9-dimethyl-1,10-phenanthroline (1.0 g, 0.0048 mol) and anhydrous sodium acetate (4.4 g, 0.054 mol) in acetic acid (150 cm^3) at 70°C was added bromine (4.4 g, 0.055 mol) in acetic acid (20 cm^3) over half an hour. The reaction mixture was kept at 70°C for a further two hours and then

cooled. Water was added and the resultant solid recrystallised from methanol (2.3 g, 70%). Buff coloured solid.

d (TFA) 8.80 (1 H, d, J = 8.6 Hz, 4-H), 8.61 (1 H, d, J = 8.6 Hz, 3-H), 8.12 (1 H, s, 5-H)

Preparation of 1,10-phenanthroline-2,6-dicarboxylic acid **L27**

L26 (0.5g) and 10% sulphuric acid (20 cm^3) for 17h. The cooled mixture was filtered and neutralised with solid sodium bicarbonate. The white precipitate was washed with tetrahydrofuran and dried (0.75g ~60%)

d (DMSO-d6) 8.63 (1 H, d, J = 8.1 Hz, 4-H), 8.29 (1 H, m, 3-H, 5-H)

4-Phenyl-1,10-phenanthroline **L32.**

To phosphoric acid (85%, 11.5 cm3) was added 8-aminoquinoline (2.5 g, 0.017 mol), and the mixture heated to 120°C to effect solution. Introduced into the mixture was colloidal arsenic acid (80%, 3.3 cm3). Added thereto over a period of five mins., was 3-chloropropiophenone [3.72 g, 0.022 mol (rx EtOH)]. The reaction mixture was subsequently heated to 140°C and left at this temperature for a further one hour. The reaction mixture was cooled, neutralised and extracted with chloroform. The residue was dissolved in acid, neutralised with ammonia, and then chromatographed on alumina (neutral, MeOH/$CHCl_3$::1:9). Mpt 73-77 °C (Lit. 105-106 °C).

d ($CDCl_3$) 8.96 (2 H, m, 2-H; 9-H), 7.80 (1 H, dd, J7,8 = 8.3 Hz; J7,9 = 1.5 Hz, 7-H), 7.56 (1 H, d, J = 9.0 Hz, 5-H), 7.24 (8 H, m, Ph-H; 3-H; 8-H; 6-H)

m/z (EI) 257 (M + 1, 20%), 256 (M^+, 100%) and 255 (M - 1, 50%).

Reaction of 4,7-dimethyl-1,10-phenanthroline with terephthalaldehyde L9

A mixture of terephthalaldehyde (0.91 g, 6.8 mmol) and dimethylphenanthroline (0.42 g, 2 mmol) was heated in a mixed solvent of acetic anhydride (0.53 cm^3, 4.8 mmol) and acetic acid (0.25 cm^3, 4 mmol) under reflux for 6h. The reaction mixture was quenched in 5 M hydrochloric acid and repeatedly extracted with dichloromethane. Neutralisation afforded a buff coloured solid which was further purified by column chromatography (alumina,neutral).

Anal. Calcd. for $C_{30}H_{20}N_2O_2$: C, 81.80; H, 4.58; N, 6.36. Found: C, 81.79; H, 4.50; N, 6.36.

d (DMSO-d6) 9.80 (2 H, s, -CHO), 9.24 (2 H, d, J = 3.5 Hz, 2-H; 9-H), 8.80 (2 H, d, J = 4.5 Hz, -NAr-CH=), 8.32 (2 H, d, J = 4.5 Hz, =CH-Ar), 8.20-7.70 (12 H, m, Ar-H; 3-H; 8-H; 5-H; 6-H)

Preparation of hexamethyldisilane C.

Sodium-potassium alloy was prepared in situ in a 1000 cm^3 flask by heating sodium (7.30 g, 0.32 mol) and potassium (50.0 g, 1.28 mol) covered with 75 cm^3 of xylene to 100 °C with vigorous stirring (egg-shaped magnetic stirrer). The mixture was allowed to cool to room temperature. While the alloy was stirred slowly, trimethylchlorosilane (200 cm^3 ~171 g, ~1.6 mol) was added dropwise. Reaction was slow to start, eventually generating slight exotherm, accompanied by the formation of a characteristic purple colour. As the reaction proceeded, dilution with more solvent (ca. 200 cm^3)

was necessary to facilitate stirring, and the addition of the silane required one and a half hours. After an additional two and half hour reflux period, the mixture was diluted with 200 cm^3 of xylene, and the mixture distilled through a fractionating column until the vapour temperature reached 130 °C. Distillation followed by two repeated fractionations yielded the product (35.5 g, ~30% based on trimethylchlorodisilane). Colourless liquid, b.p. 112.5 °C (lit. 112 °C).

Anal. Calcd. for $C_6H_{18}Si_2$: C, 49.23; H, 12.39; N 0.00. Found: C, 49.13; H, 12.22; N, 0.00.

Preparation of pentamethylchlorodisilane L34

A 250 cm^3 three-necked flask fitted with thermometer, and reflux condenser, was connected to an apparatus for collecting gas. Hexamethyldisilane (5.0 g, 0.343 mol) and concentrated sulphuric acid (17 g, sp.gr. 1.84) were combined. The mixture was vigorously stirred at room temperature. After three and a half hours ~1.6 L of methane had been collected and the reaction mixture appeared to be homogeneous. The mixture was cooled in an ice bath and ammonium chloride (2.7 g, 0.0505 mol) was added to the mixture over 30 minutes.

Stirring was continued for an additional 30 minutes. Separation by vaccuum distillation of the reaction mixture, followed by two distillations of the distillate gave the product. Yield 4.85 g (85 %).

d ($CDCl_3$) 0.17 (2 H, s, $-Si(CH_3)_2Cl$), 0.07 (3 H, s, $(CH_3)_3Si-$

Preparation of bis(1,10-phenanthroline)dichloride ruthenate(II) hydrate (CDC)

Ruthenium trichloride trihydrate (2.5 g, 0.0096 mol), 1,10-phenathroline (3.5 g, 0.194 mol) and lithium chloride (5.0 g) were heated together under reflux in dry dmf (50 cm^3), with efficient stirring for seven hours. The purple-black solution was allowed to cool to room temperature*, whereupon 250 cm^3 of acetone was added. The sealed flask was left overnight at 0 °C. A black microcrystalline solid was recovered, and washed with water (6 * 50 cm^3) and diethyl ether (6 * 50 cm^3) (2.7 g ~49% based on ruthenium trichloride trihydrate).

Anal. Calcd for $C_{24}H_{16}Cl_2N_4Ru.H_2O$: C, 52.37; H, 2.93; N, 10.18. Found: C, 52.58; H, 2.95; N, 10.48.

* on occasion, a black crystalline material has separated on cooling of the reaction mixture. In all cases this has been characterised by IR to be the required product.

Preparation of tris(1,10-phenanthroline) ruthenium(II) salts (C1)

To a refluxing solution of 1,10-phenanthroline (720 mg, 4.0 mmol) in DMF, was added ruthenium(III) chloride, anhydrous (250 mg, 1.2 mmol). After heating for 1 hr. (bright red, clear solution) the solvent was removed under reduced pressure, and the residue dissolved in water (20 cm^3), heated to boiling and concentrated hydrochloric acid (40 cm^3) added. The volume was reduced to 40 cm^3 and the solution filtered and allowed to cool. Bright red needle crystals separated

(**C1-Cl**, 680 mg, 80%). An analytical sample was recrystallised from water.

The hexafluorophosphate salt was prepared by dissolving 100 mg of the dichloro in methanol and adding this dropwise to a hot solution of ammonium hexafluorophosphate. The precipitate was collected and purified on alumina (acetonitrile). Yield 90 mg.

C1-Cl Anal. Calcd for $C_{36}H_{24}N_6Ru.Cl_2.6H_2O$: C, 52.69; H, 4.42; N, 10.24. Found: C, 52.80; H, 4.35; N, 10.38.

ν_{max}: 3409, 3039, 1628, 1500, 1424*, 1338, 1203, 1140, 1093, 845*, 776, 736-722* and 528 cm^{-1}

C1 Anal. Calcd for $C_{36}H_{24}N_6Ru.P_2F_{12}.2H_2O$: C, 44.68; H, 2.92; N, 8.68. Found: C, 44.50; H, 3.00; N, 8.60.

ν_{max}: 3437, 2922, 1628, 1519, 1427*-1411, 1340, 1206, 1148, 1096, 838*, 775, 724* and 558 cm^{-1}

<u>Also prepared by this proceedure were:</u>

i) <u>Tris(4,7-dichloro-1,10-phenanthroline)ruthenium(II) bis(hexafluorophosphate)</u> **C25**

Anal. Calcd for $C_{36}H_{18}Cl_6N_6Ru.P_2F_{12}.2H_2O$: C, 36.82; H, 1.89; N, 7.16. Found: C, 36.70; H, 1.90; N, 7.20.

ν_{max}: 3433, 3100, 1619*-1599-1559*, 1500, 1413*, 1400, 1337, 1299, 1218, 1189, 1150, 1120, 1089, 1038, 841*-797 and 558* cm^{-1}

ii) Tris(4,7-dibromo-1,10-phenanthroline)ruthenium(II) bis(hexafluorophosphate) **C26**

Anal. Calcd for $C_{36}H_{16}Br_6N_6Ru.4H_2O.P_2F_{12}$: C, 29.27; H, 1.77; N, 5.69.

Found: C, 29.15; H, 1.80; N, 5.50.

ν_{max}: 3431, 1612, 1538, 1481, 1405*, 1341*, 1263, 1184*, 1135, 1068, 842*-800-785, 713 and 558* cm^{-1}

Preparation of tetrakis(1,10-phenanthroline)[μ-3,6-bis(2'-pyridyl)-1,2,4,5-tetrazine) diruthenium(II) tetrakis(hexafluorophosphate) **(C28)**

The complex **(L17)** (0.5 g, 0.0009 mol) was refluxed with **(CDC)** (0.125 g, 0.0005 mol) in 25 cm^3 of 95% ethanol for 72 hours. The mixture was allowed to cool, and then poured into 25 cm^3 of water. To this was added an excess solution of ammonium hexafluorophosphate. The dark green precipitate so formed was isolated and washed with a small amount of 1:1::water:ethanol mixture [0.6 g ~40% based on **(L17)**]

TLC of the product on silica plates using 0.5 M ethanol solution of TEAB as eluent, gave a single, front running green spot.

TLC of, the complex in 2:1::benzene:ACN gave only a green baseline spot.

Separation on a Sephadex LH20 column using ACN (spectroscopic grade) as eluent gave i) baseline of pinkish material, ii) penultimate band of olive component, iii) front running band of deep green colour (product).

Anal. Calcd for $C_{60}H_{40}N_{14}Ru_2.P_4F_{24}.4H_2O$: C, 39.79; H, 2.67;

N, 10.82. Found: C, 39.67; H, 2.34; N, 10.66

^{1}H n.m.r.-to impure to resolve!

ν_{max}: 3441, 1630-1604, 1429*-1414*, 1321, 1252-1227, 1164*, 1110, 1033*, 839*, 721* and 558* cm^{-1}

Preparation of bis(1,10-phenanthroline)(4,5-diazafluoren-9-one) ruthenium(II) dihexafluorophosphate (C14)

Obtained in a way similar to that given above from:

(CDC) (0.5 g, 0.0009 mol)

[L20] (0.1584 g, 0.0009 mol)

[0.52 g ~59% based on (CDC)].

A sample of product was recrystallised from ACN with the aid of toluene.

Anal. Calcd for $C_{35}H_{28}N_6O_3Ru.P_2F_{12}.2H_2O$: C, 43.27; H, 2.90; N, 8.65. Found: C, 43.15; H, 3.16; N, 8.56

Preparation of bis(1,10-phenanthroline)bis(trifluoromethane-sulphonato) ruthenate(II) (CTf)

To (CDC) (2.0 g, 0.003 mol) was quickly added anhydrous trifluoromethanesulphonic acid (10 cm^3). The solution was warmed, with stirring, to and maintained at 90 ~ 100 °C. After the evolution of HCl had ceased (~three hours, monitored by passing the effluent gas through a solution of $AgNO_3$), the flask was cooled in an ice bath to 0 °C. Diethyl ether (30 cm^3) was added dropwise with vigorous mechanical stirring. The solution was poured into 50 cm^3 of ether, and the solid filtered and triturated on the frit with ether (50 cm^3).

The air dried product was ground in a mortar, boiled in chloroform (50 cm^3) for ten minutes "to remove traces of CF_3SO_3H", filtered, washed with ether and dried *in vacuo* over P_2O_5 to give a reddish brown solid [2.5 g ~94% based on **(CDC)**].

Anal. Calcd for $C_{26}H_{16}F_6N_4O_6S_2Ru$: C, 41.11; H, 2.12; N, 7.38. Found: C, 40.87; H, 2.07; N, 7.53.

Preparation of bis(1,10-phenanthroline)(1,10-phenanthroline-5,6-quinone) ruthenium(II) dihexafluorophosphate **(C15)**

To a solution of **(L21)** (0.05 g, 0.000238 mol) in 20 cm^3 HPLC grade acetone, was added **(CTf)** (0.167 g, 0.000220 mol). The reaction mixture was refluxed for three hours, filtered while hot and allowed to cool.

To an ice cold solution of ammonium hexafluorophosphate was added the reaction mixture with stirring, to afford a deep red crystalline product [0.105 g ~47% based on **(CTf)**]

Anal. Calcd for $C_{36}H_{22}N_6O_2Ru.P_2F_{12}.2H_2O$: C, 43.34; H, 2.63; N, 8.42. Found: C, 43.38; H, 2.77; N, 8.24.

The following complexes were all synthesised by the methodology for the foregoing compound. In all cases, isolated yields were greater than 85%.

1) C1N (CTf + L2)

Anal. Calcd for $C_{36}H_{23}N_7O_2Ru.P_2F_{12}.2H_2O$: C, 42.70; H, 2.69; N, 9.68. Found: C, 42.72; H, 2.60; N,9.71.

d (ACN-d_3) 9.60d (1 H, s, 6f-H), 9.54d (1 H, d, J = 9.0 Hz, 7f-H), 9.22d (1 H, d, J = 9.0 Hz, 4f-H), 9.06d (4 H, d, J = 9.0 Hz, 4*-H; 7*-H), 8.64d (4 H, s, 5*-H; 6*-H), 8.50d (6 H, m, 2f-H; 9f-H; 2*-H; 9*-H), 8.10d (6 H, m, 3f-H; 8f-H; 3*-H; 8*-H)

ii) C2 (CTf + L3)

Anal. Calcd for $C_{36}H_{28}N_7Ru.P_2F_{12}.3H_2O$: C, 43.21; H, 3.12; N, 9.80. Found: C, 43.20; H, 3.08; N, 9.71.

d (ACN-d_3) 8.90d (1 H, d, J = 9.0 Hz, 4f-H), 8.54d (4 H, d, J = 9.0 Hz, 4*-H; 7*-H), 8.16d (4 H, s, 5*-H; 6*-H), 8.00d (6 H, m, 7f-H; 2f-H; 9*-H; 2*-H), 7.60d (6 H, m, 9f-H; 3f-H; 8*-H; 3*-H), 7.36d (1 H, dd, $J_{8,7}$ = 8.3 Hz; $J_{8,9}$ = 5.3 Hz, 8f-H), 7.17d (1 H, s, 6f-H)

ν_{max}: 3639-3398*-3088-2853, 1639*-1593, 1510-1491, 1461-1427*, 1340, 1255, 1186, 1120, 839*, 722* and 556* cm^{-1}

iii) C5M (CTf + L8)

Anal. Calcd for $C_{38}H_{28}N_6Ru.P_2F_{12}$: C, 47.56; H, 2.94; N, 7.51. Found: C, 47.40; H, 3.11; N, 7.30.

d (acetone-d_6) 8.58d (4 H, d, J = 7.5 Hz, 4*-H; 7*-H), 8.33d (2 H, s, 5f-H; 6f-H), 8.22d (8 H, m, 5*-H; 6*-H; 2*-H; 9*-H), 8.06d (2 H, d, J = 5.3 Hz, 2f-H; 9f-H), 7.64d (4 H, m, 3*-H; 8*-H), 7.50d (2 H, d, J = 5.3 Hz, 3f-H; 8f-H), 2.88d (6 H, split s, $-CH_3$)

iv) C6 (CTf + L7)

ν_{max}: 3412, 3070, 1602*-1576*-1549*, 1498, 1425-1411-1382, 1306, 1222-1205, 1055, 972, 841*, 742-721, 690 and 558* cm^{-1}

v) **C13B** (CTf + L17)

Anal. Calcd for $C_{36}H_{24}N_{10}Ru.P_2F_{12}$: C, 43.78; H, 2.45; N, 14.18. Found: C, 43.80; H, 2.31; N, 14.27.

(KBr, cm^{-1}) 3437*, 1629, 1520, 1494, 1430*, 1390*, 1287, 1256-1226, 1148, 974, 840*, 721, 559*

vi) **C13C** (CTf + L18)

ν_{max}: 3437, 1631-1588*-1567, 1526, 1467, 1402*, 1314-1280-1246, 1154-1119-1098, 1039, 993, 843*-790-755, 711, 670, 622, 601, 558* and 397 cm^{-1}

vii) **C18** (CTf + L28)

Anal. Calcd for $C_{35}H_{23}N_7ORu.P_2F_{12}.3H_2O$: C, 41.93; H, 2.92; N, 9.78. Found: 41.74; H, 3.04; N, 9.69.

viii) **C19** (CTf + L30)

Anal. Calcd for $C_{42}H_{26}N_8Ru.P_2F_{12}.2H_2O$: C, 47.16; H, 2.83; N, 10.47. Found: C, 47.03; H, 2.80; N, 10.35.

ix) **C20** (CTf + L31)

Anal. Calcd for $C_{42}H_{25}N_7O_2Ru.P_2F_{12}.3H_2O$: C, 44.53; H, 2.76; N, 11.13. Found: C, 44.67; H, 2.50; N, 11.20.

x) **C21A** (CTf + L32)

Anal. Calcd for $C_{42}H_{26}N_6Ru.P_2F_{12}.2H_2O$: C, 48.33; H, 3.09; N, 8.05. Found: C, 48.30; H, 3.13; N, 7.90.

xi) C23 (CTf + $2KNO_2$)

Anal. calcd for $C_{24}H_{16}N_6O_4Ru$: C, 52.08; H, 2.91; N, 15.18. Found: C, 51.87; H, 3.10; N, 15.00.

NMR- Too insoluble.

ν_{max}: cis 3441*, 3062, 1628, 1429*, 1326*-1287-1255, 847*, 819 and 722* cm^{-1}

ν_{max}:-rx water- trans 3434, 3046, 1625, 1425*, 1358*-1332*-1311-1280*, 1203, 855*, 818, 723* and 605 cm^{-1}

xii) C29 (2CTf + L37)

Anal. Calcd for $C_{42}H_{28}N_8Ru_2.P_4F_{24}.H_2O$: C, 34.92; H, 2.09; N, 7.76. Found: C, 34.66; H, 2.16; N, 7.73.

Preparation of bis(1,10-phenanthroline)[3,6-bis(2'-pyridyl)-4,5-dihydro-1,2,4,5-*t*erazine]ruthenium(II) dihexafluoro-phosphate (C13).

Achieved in a way similar to that for C15.

but using:

(CTf)	(0.50 g, 0.000659 mol)
(L18)	(0.20 g, excess)
HPLC grade acetone	20 cm^3

Reflux was discontinued after only one hour. The cooled filtered reaction mixture was added dropwise to a boiling solution of ammonium hexafluorophosphate. The mixture was filtered at 60 °C, to yield a green compound, and again at 0 °C to yield a red-purple crystalline product (0.33 g (C13) ~60% based on (CTf)).

Anal. Calcd for $C_{36}H_{26}N_{10}Ru.P_2F_{12}$: C, 43.78; H, 2.45; N, 14.18. Found: C, 43.80; H, 2.31; N, 14.27.

Preparation of bis(1,10-phenanthroline)(5,6-Diaza-1,10-phenanthroline)ruthenium(II) bis(hexafluorophosphate) **C12**

As above, but using:

CTf	(344 mg, 0.45 mmol)
L14	(83 mg, 0.45 mmol)

Yield: 370 mg (88%)

Anal. Calcd for $C_{34}H_{22}N_8Ru.P_2F_{12}$: C, 43.74; H, 2.38; N, 12.00. Found: C, 43.90; H, 2.40; N, 11.88.

ν_{max}: 3437*, 2360, 1631, 1429*, 839*, 722* and 559* cm^{-1}

Preparation of **(C28)** from **(CTf)**

Prepared as described for **(C15)** but using:

(CTf)	(0.50 g, 0.000659 mol)
(L17)	(0.070 g, 0.000297 mol)
HPLC grade acetone	20 cm^3

The filtrate was added dropwise to a boiling vigorously stirred solution of ammonium hexafluorophosphate. This was filtered at room temperature to yield a deep green microcrystalline product [0.47 g ~90% based on (L17)]

Anal. Calcd for $C_{60}H_{40}N_{14}Ru_2.P_4F_{24}.H_2O$: C, 41.01; H, 2.40; N 11.16. Found: C, 40.96; H, 2.29; N, 10.93.

Preparation of bis(1,10-phenanthroline)(3,8-dicarboxy-4,7-dihydroxy-1,10-phenantroline) ruthenium(II) dihexafluorophosphate **(C10)**

Obtained in a way similar to **(C15)** but using a different solvent, thus:

(CTf)	(0.30 g, 0.000395 mol)
(L11)	(0.1313 g, 0.000437 mol)
glycerol	25 cm^3

The glycerol and **(L11)** were heated together at 140 °C for forty minutes and then **(CTf)** added. The mixture was maintained at 140 °C for three hours. Isolation was as above Anal. Calcd for $C_{36}H_{24}N_6O_6Ru.P_2F_{12}.3H_2O$: C, 41.27; H, 2.73; N, 7.60. Found: C, 41.10 H, 2.80; N, 7.50.

Preparation of bis(1,10-phenanthroline)(4,7-dichloro-1,10-phenanthroline) ruthenium(II) dihexafluorophosphate **(C4)**

Obtained in a similar way to that given above, but using:

(CTf)	(0.30 g, 0.000395 mol)
(L5)	(0.10 g, 0.000402 mol)
glycerol	25 cm^3

The mixture was heated at 140 °C for thirty mins. It was then cooled and poured into 200 cm^3 dilute hexafluorophsphoric acid (ice cold) with vigorous stirring. The suspension was then allowed to stand at 0 °C for two hours. The solid was isolated and dried at reduced pressure.

Anal. Calcd for $C_{36}H_{22}N_6Cl_2Ru.P_2F_{12}.3H_2O$: C, 41.00; H, 2.67; N, 7.96. Found: C, 41.08 H, 2.35; N, 7.78.

ν_{max}: 3386*, 2936, 1619-1599-1581-1560, 1428*-1412*, 1337, 1310, 1219-1189, 1149-1086-1043*-993, 842*, 723 and 559* cm^{-1}

Also prepared by this method:

Bis(1,10-phenanthroline)(4,7-dibromo-1,10-phenanthroline) ruthenium(II) dihexafluorophosphate (C5) (CTf + L6)

Anal. Calcd for $C_{36}H_{22}N_6Br_2Ru.P_2F_{12}.H_2O$: C, 42.97; H, 2.40; N, 8.35. Found: C, 43.10; H, 2.55; N, 8.17

ν_{max}: 3431, 3089, 1615, 1576, 1538, 1428*-1410*-1376, 840*, 722* and 558* cm^{-1}

Bis(1,10-phenanthroline)(4,7-dihydroxy-1,10-phenanthroline) ruthenium(II) dihexafluorophosphate C3

Anal. Calcd. for $C_{36}H_{24}N_6O_2Ru.P_2F_{12}.3H_2O$: C, 42.48; H, 2.97; N, 8.26. Found: C, 42.40; H, 2.90; N, 8.00.

Preparation of bis(1,10-phenanthroline)[bathophenanthroline-disulphonate (bpds)] ruthenate(II) (C7)

Prepared as described for (C4) but using:

(CTf)	(0.70 g, 0.000922 mol)
Na_2bpda	(0.50 g, 0.000932 mol)
glycerol	25 cm^3

The reaction mixture was quenched in acetone (200 cm^3) with vigorous stirring, and a bright red solid was isolated [0.47 g ~49% based on (CTf)]

Anal. Calcd for $C_{48}H_{30}N_6O_6S_2Ru.7H_2O$: C, 53.48; H, 4.11; N, 7.80. Found: C, 53.22 H, 4.38; N, 7.72.

Preparation of bis(1,10-phenanthroline)[bathophenanthroline-disulphonylchloride (bpdscl)] ruthenium(II) dihexafluoro-phosphate (C8)

A mixture of phosphorous oxychloride (2 cm^3) and phosphorous pentachloride (~1 g, 0.005 mol) was heated to 90 °C. To this mixture was added (C7) (0.0919 g, 0.0000896 mol, and the mixture heated at 120 °C for seventeen hours. The cooled reaction mixture was poured into 200 cm^3 dilute hexafluorophosporic acid (iced) and stirred vigorously until an orange solid formed. This was isolated and dried at reduced pressure [0.10 g ~87% based on (C7)].

Anal. Calcd for $C_{48}H_{30}Cl_2N_6O_4S_2Ru.P_2F_6.3H_2O$. C, 43.19; H, 2.71; N, 6.30. Found: C, 43.32 H, 2.60; N, 6.56.

Preparation of bis(1,10-phenanthroline)[4-(4-sulphonylchloro) phenyl-1,10-phenanthroline ruthenium(II) bishexafluorophos-phate (C27)

To chlorosulphonic acid (10 cm^3) was added C21A (300 mg, 0.29 mmol). The mixture was refluxed for 1 hr. and then the liquid removed *in vacuo* . The residue was dissolved in THF and added to a hexafluorophosphoric acid solution. The resulting precipitate was collected. Yield 300 mg, 90%.

Anal. Calcd for $C_{42}H_{27}ClN_6O_2SRu.P_2F_{12}.3H_2O$: C, 43.48; H, 2.35; N, 7.24. Found: C, 43.50; H, 2.46; N, 7.10.

ν_{max}: 3646, 3442, 3089, 1628, 1594, 1428*-1413*, 1373*, 1085, 1171*, 839*, 739, 722, 600 and 557* cm^{-1}

The dichloro salt was isolated by dissolving the above compound in a 1:1 dichloromethane/THF mixture and bubbling with hydrogen chloride.

Preparation of N-{[5-(1,10-phenanthroline)bis(1,10-phenanthroline)ruthenium(II)bis(hexafluorophosphate)]}-acetamide (C2A)

To a solution of C2 (100 mg, 0.1 mmol) in dichloromethane was added trimethylamine (100 mg, 1.0 mmol) and acetyl chloride (79 mg, 0.1 mmol). The solution was stirred at room temperature overnight and then the solvent removed. The residue was dissolved in water and added to a solution of ammonium hexafluorophosphate.

The precipitate was washed with a large volume of water and chromatographed on alumina (acetonitrile). Yield 95 mg. Anal. Calcd for $C_{38}H_{27}N_7ORu.P_2F_{12}.H_2O$: C, 45.34; H,2.90; N, 9.74. Found: C, 45.30; H, 2.80; N, 9.70.

d (ACN-d_3) 9.35d (1 H, d, -NH-), 9.20d (4 H, d, J = 7.5 Hz, 4*-H; 7*-H), 9.11d (1 H, d, J = 7.5 Hz, 4f-H), 8.98d (1 H, d, J = 7.5 Hz, 7f-H), 8.66d (5 H, s, 5*-H; 6*-H; 6f-H), 8.47d (6 H, m, 2*-H; 9*-H; 2f-H; 9f-H), 8.08d (6 H, m, 3*-H; 8*-H; 3f-H; 3f-H), 2.37d (3 H, split s, $-CH_3$)

The above reaction conditions were employed in the synthesis of the following complexes:

i) **C21** (C27 + p-ethylphenol)

d (acetone-d_6) 8.56d (4 H, d, J = 7.5 Hz, 4*-H; 7*-H), 8.20d (9 H, m, 5f-H; 5*-H; 6*-H; 2*-H; 9*-H), 8.00-7.50d (10 H, m, 6f-H; 7f-H; 2f-H; 9f-H; 3f-H; 8f-H; 3*-H; 8*-H), 7.10d (2 H, d, J = 7.5 hz, Ar-H), 6.90 (2 H, d, J = 7.5 Hz, Ar-H), 2.56d (2 H, m, $-CH_2-$), 1.14d (3 H, m, $-CH_3$)

ii) **C22** (C27 + phenylalanine methyl ester)

Anal. Calcd. for $C_{32}H_{29}N_7O_4SRu.P_2F_{12}.3H_2O$: C, 47.93; H, 3.48; N, 7.52. Found: C, 48.00; H, 3.65; N, 7.50.

ν_{max}: 3351, 3086, 1742*, 1627, 1599, 1428*, 1413, 1340, 1161, 1095, 839*, 795*, 722* and 558* cm^{-1}

iii) **C24** (C27 + phenylalanine chloromethyl ketone using THF as solvent)

Anal. Calcd for $C_{32}H_{28}ClN_7O_3SRu.P_2F_{12}$: C, 48.59 ; H, 3.14; N, 7.63. Found: C, 48.45; H, 3.20; N, 7.74.

The dichloro salt was prepared as for **C27**.

Preparation of N-([5-(1,10-phenanthroline)bis(1,10-phenanthroline)ruthenium(II)bis(hexafluorophosphate)])-4-carboxybutanamide (C2B)

To a solution of glutaric anhydride (114 mg, 1.0 mmol) in glacial acetic acid (5 cm^3) was added C2 (100 mg, 0.1 mmol). The solution was brought to reflux, and a small amount of zinc powder added. After refluxing for 1 hr., the reaction was worked up as C27. Yield 95 mg ~90%.

Anal. Calcd for $C_{41}H_{31}N_7O_3Ru.P_2F_{12}.4H_2O$: C, 43.47; H, 2.76; 8.65. Found: C, 43.50; H, 2.84; N, 8.80

ν_{max}: 3428*, 3091, 1729, 1685*, 1629, 1428, 1358, 1249, 1175, 1143, 841*, 722* and 559* cm^{-1}

Preparation of N-{[5-(1,10-phenanthroline)bis(1,10-phenanthroline)ruthenium(II)bis(hexafluorophosphate)]}-1-aminocyclohexanamide **C2C**

To a stirred suspension of 1-aminocyclohexane carboxylic acid (1.0 g, 7 mmol) in THF (30 cm^3) was added triethylamine (4 cm^3). The mixture was heated to 55 °C and triphosgene (0.65 g, 2.3 mmol) added. Stirring was maintained until the mixture went clear (6 hours). The solvent was removed at reduced pressure and residue triturated with dichloromethane. To the combined washings triethylamine (0.5 cm^3) was added, followed by **C2** (0.10 g, 0.1 mmol). The mixture was refluxed overnight. Precipitation in ammonium hexafluorophosphoric solution, followed by isolation from alumina (acetonitrile) gave **C2C** (70 mg, 63%).

Anal. Calcd for $C_{43}H_{36}N_8ORu.P_2F_{12}.2H_2O$: C, 46.62; H, 3.28; N, 10.11. Found: C, 46.80; H, 3.06; N 9.99.

ν_{max}: 3500-3440, 3420, 1670*, 1610, 1428*, 840*, 722*, 558*.

Functionalisation of **C2B**; formation of phenylalanine chloromethyl ketone derivative

To oxalyl chloride (30 cm^3), **C2B** (300 mg, 0.27 mmol) was added and the mixture refluxed for 2 hrs. The liquid was removed under reduced pressure, and the residue dissolved in

dichloromethane (5 cm^3) and triethylamine (1 cm^3). To this was added L-phenylalanine chloromethyl ketone, hydrochloride (100 mg) suspended in THF (10 cm^3) and mixture stirred for 2 days. To the solvent stripped residue was added methanol (10 cm^3) and dilute sodium hydroxide (4 cm^3, 3M), and the mixture shaken for 20 minutes. Methanol was removed, and the reaction mixture acidified (hexafluorophosphoric acid) and extracted with dichloromethane. After stripping the extracts of solvent, the dried residue was refluxed in oxalyl chloride for 2 hr. After removing the liquid *in vacuo*, the residue was dissolved in dry THF (20 cm^3) and added to excess diazomethane over 15 mins (cool in ice bath). After allowing to stand for 2 hr, the reaction mixture was bubbled with hydrogen chloride gas. The chloride salt was converted to the hexafluorophosphate in the usual way, and product purified on alumina (20% ACN/dichloromethane). Yield 52 mg.

δ(ACN-d_3) 8.77d (5 H, d, J = 7.5 Hz, 4*-H; 7*-H; 4f-H), 8.51d (1 H, d, J = 9.0 Hz, 7-H), 8.38d (4 H, s, 5*-H; 6*-H), 8.24d (7 H, m, 2f-H; 9f-H; 6f-H; 2*-H; 9*-H), 7.80d (6 H, m, 3f-H; 8f-H; 3*-H; 8*-H), 7.40d (5 H, s, Ph-H), 5.02d (2 H, s, -CH_2-Cl), 4.32d (1 H, m, -CH<), 3.26d (2 H, m, -CH_2-Ph), 2.98d (4 H, m, -CO-CH_2-), 2.28d (2 H, m, -CH_2-)

Alkylation of C3: reaction with allyl bromide

Allyl bromide (50 mg, 0.41 mmol) and C3 (100 mg, 0.10 mmol) were combined with crushed potassium carbonate in acetone and the mixture refluxed for 3 hr. The reaction mixture (bright orange) was filtered and the hexafluorophosphate salt

isolated in usual way.

d (ACN-d_3) 8.95d (4 H, d, J = 7.5 Hz, 4*-H; 7*-H), 8.67d (2 H, s, 5f-H; 6f-H), 8.57d (4 H, s, 5*-H; 6*-H), 8.51d (2 H, d, J = 4.5 Hz, 2*-H; 9*-H), 8.38d (2 H, d, J = 7.5 Hz, 2*-H; 9*-H), 8.00d (6 H, m, 3*-H; 8*-H; 2f-H; 9f-H), 7.39d (2 H, d, J = 6.0 Hz, 3f-H; 8f-H), 6.38d (2 H, m, -CH-), 5.69d (4 H, unsym. t, O-CH_2-), 5.08d (4 H, d, =CH_2)

Preparation of bis(1,10-phenanthroline)(3,3-diaminobipyridine)ruthenium(II) bis(hexafluorophosphate) **C17**

Complex **C12** was reduced as for **L16**, but using:

C12 (40 mg, 0.04 mmol)

Yield: 36 mg (96%)

Calcd for $C_{54}H_{36}N_8Ru.P_2F_{12}.H_2O$: C, 42.73; H, 2.95; N, 11.73.

Found: C, 42.66; H, 3.01; N, 11.70.

ν_{max}: 3423, 2919, 1630*-1588*, 1466*-1428* 841*, 722* and 559* cm^{-1}.

APPENDIX I

Electrochemistry of some ruthenium(II) diimine complexes (*vs* SCE)

Complex	E(3+/2+)/V	E(2+/1+)/V
[Ru(bipy)$_3$]$^{2+}$	+1.354	-1.332
[Ru(phen)$_3$]$^{2+}$	+1.40	-1.41
[Ru(4,7-Me$_2$phen)$_3$]$^{2+}$		-1.52
[Ru(5-Clphen)$_3$]$^{2+}$		-1.22
[Ru(terpy)$_2$]$^{2+}$	+1.28	-1.43

Thermodynamic parameters for the reduction of the Heme site in Native sperm whale myoglobin Mb (pH 7.0)

thermodynamic parameter	native Mb ($Fe^{3+/2+}$)
E°, mV vs. SHE (25 °C)	~ 58
ΔG°, kcal mol^{-1} (25 °C)	-1.2
ΔS°, e.u.	-39
ΔH°, kcal mol^{-1} (25 °C)	-13

Sperm whale myoglobin is very stable and forms excellent crystals from 3 M ammonium sulphate (concentrated solution of protein, pH 7). Its tertiary structure and amino acid sequence are all known. It is an extremely compact (45 x 35 x 25 Å) small protein (M.W. 17,600).

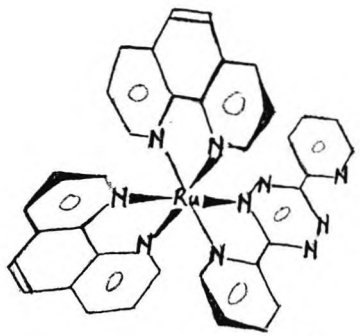

The proton nmr (200 MHz) of complex **C13B.**

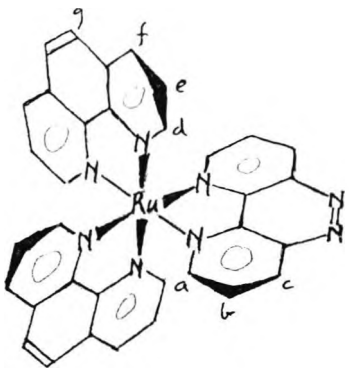

The proton nmr (200 MHz) of complex C12.

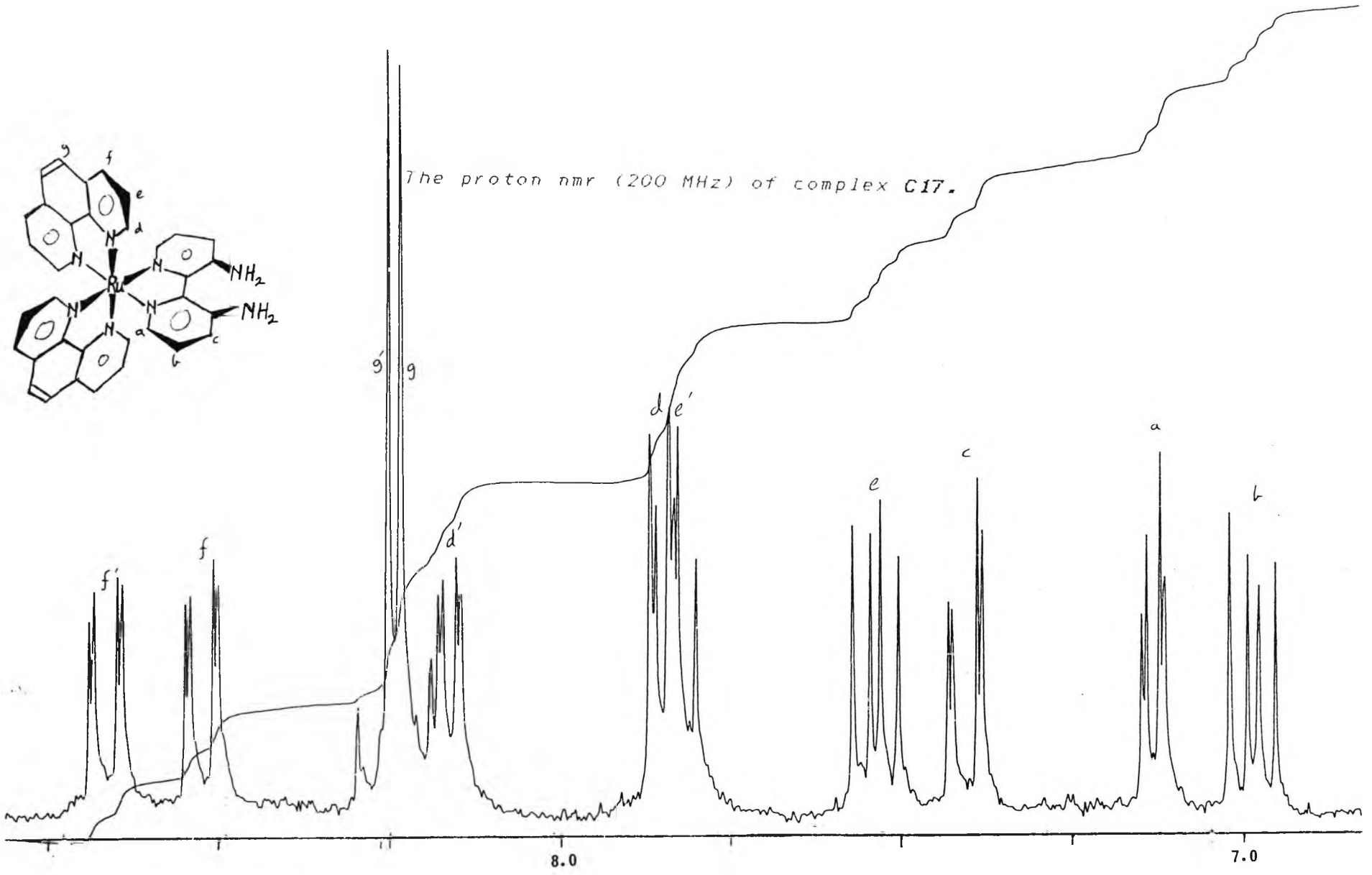
The proton nmr (200 MHz) of complex C17.
g
f
e
d
NH2
NH2
a
c
b
g'
g
d'
d
e'
e
c
a
b
f'
f
8.0
7.0

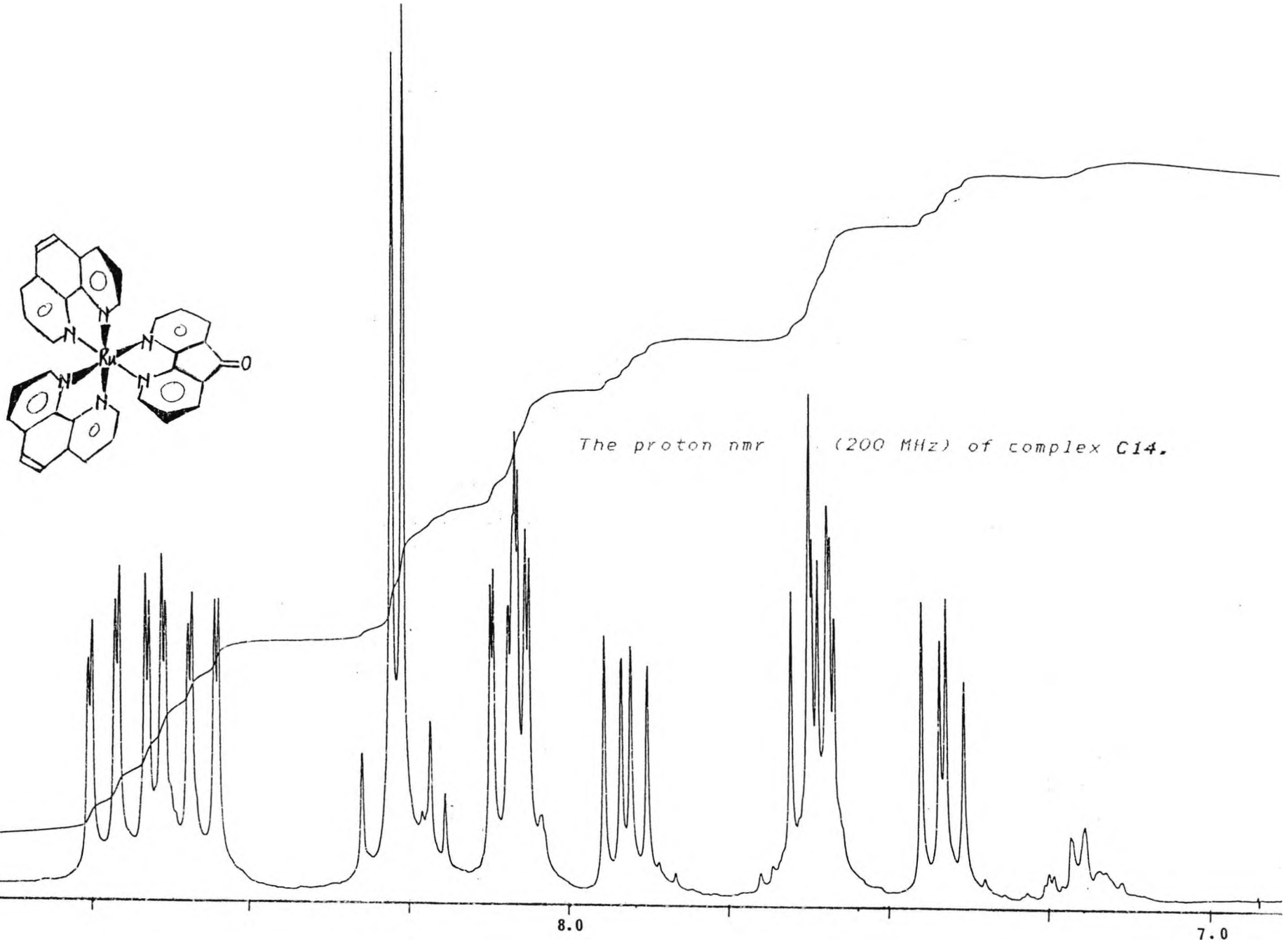

The proton nmr (200 MHz) of complex **C14.**

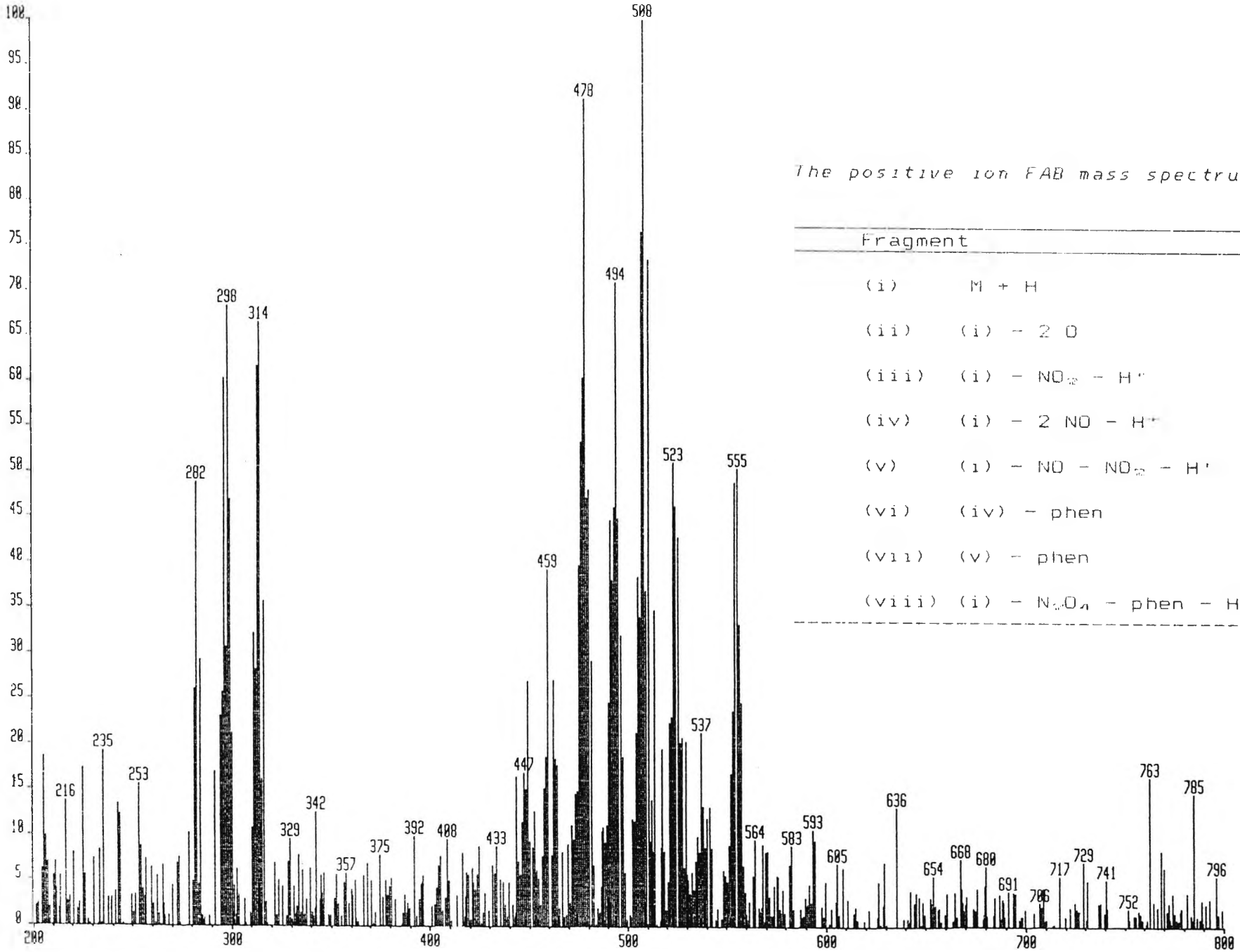

The positive ion FAB mass spectrum of complex ***C23.***

Fragment		Mass
(i)	M + H	555
(ii)	(i) − 2 O	523
(iii)	(i) − NO_2 − H'	508
(iv)	(i) − 2 NO − H'	494
(v)	(i) − NO − NO_2 − H'	478
(vi)	(iv) − phen	314
(vii)	(v) − phen	298
(viii)	(i) − N_2O_4 − phen − H'	282

Structural formulae of the ligands

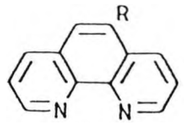

1. R = H
2. R = NO_2
3. R = NH_2

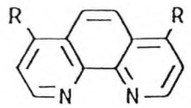

4. R = OH
5. R = Cl
6. R = Br
7. R = S-Ph

BPDS. R = $C_6H_4-SO_3^-$

BPDSCL. R = $C_6H_4-SO_2Cl$

9. R = CH=CHArCHO

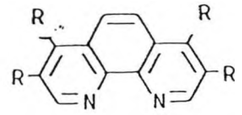

10. R1 = OH : R2 = CO_2Et
11. R1 = OH : R2 = CO_2H
12. R1 = Cl : R2 = CO_2Et
13. R1 = OCH_2ArCN : R2 = CO_2Et

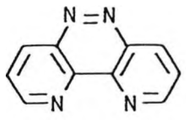

14.

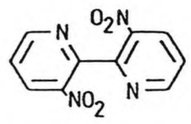

15.

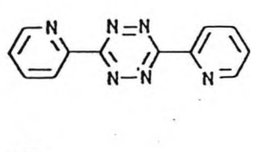

17.

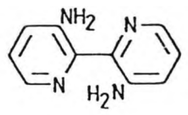

16.

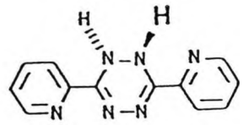

18.

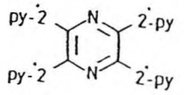

19.

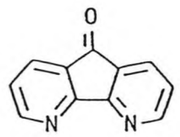

20.

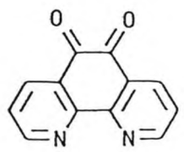

21.

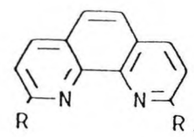

22. R = CHO
23. R = CH_2OH
24. R = $CHNOCH_2CO_2H$
25. R = CH_2Br
26. R = CBr_3
27. R = CO_2H

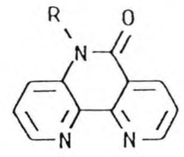

28. R = H
29. R = CH_2OH

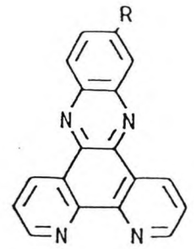

30. R = H
31. R = NO_2

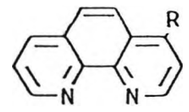

32. R = Ph
34. R = $C_6H_4-SO_3-C_6H_4-C_2H_5$
35. R = $C_6H_4-SO_2$-Phe-OMe
36. R = $C_6H_4-SO_2$-Phe-CH_2Cl

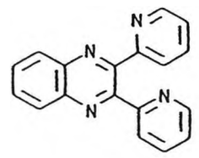

33.

APPENDIX III

THE TERTIARY STRUCTURE OF α-CHYMOTRYPSIN. CATALYTICALLY IMPORTANT RESIDUES ARE MARKED IN COLOUR.

PLATE 1.0 Molecular model of sperm whale myoglobin: highlighted are uncoordinated histidines (cf. page 22).

PLATE 1.1 Molecular model of the three-dimensional structure of sperm whale myoglobin: amino termini of lysine residues and terminal glycine are highlighted.